The Role of the Retinoblastoma Protein Family in Skeletal Myogenesis

by

Giovanni Ciavarra

A thesis submitted in conformity with the requirements

for the degree of Doctor of Philosophy

Graduate Department of Laboratory Medicine and Pathobiology

University of Toronto

The Role of the Retinoblastoma Protein Family in Skeletal Myogenesis

Giovanni Ciavarra

Doctor of Philosophy

Laboratory Medicine and Pathobiology, University of Toronto

2011

ABSTRACT

The retinoblastoma tumor suppressor (pRb) is thought to orchestrate terminal differentiation by inhibiting cell proliferation and apoptosis and stimulating lineage-specific transcription factors. In this thesis I have shown that in the absence of pRb, differentiating primary myoblasts fused to form short myotubes that never twitched and degenerated via a non-apoptotic mechanism. The shortened myotubes exhibited an impaired mitochondrial network, mitochondrial perinuclear aggregation, autophagic degradation and reduced ATP production. Bcl-2 and autophagy inhibitors restored mitochondrial function and rescued muscle degeneration, leading to twitching myotubes that expressed normal levels of muscle-specific proteins and eventually exited the cell-cycle. A hypoxia-induced glycolytic switch also rescued the myogenic defect after chronic or acute inactivation of Rb in a HIF-1-dependent manner. These results demonstrate that pRb is required to inhibit apoptosis in myoblasts and autophagy in myotubes but not to activate the differentiation program.

I next tested the effect of retinoblastoma protein family members – p107 and p130 – on skeletal myogenesis in the absence of Rb. Chronic or acute inactivation of Rb plus p130 or Rb plus p107 increased myoblast cell death and reduced myotube formation, yet expression of Bcl-2, treatment with autophagy antagonist or exposure to hypoxia extended myotube survival, leading to long, contracting myotubes that appeared indistinguishable from control myotubes. Triple mutations in Rb family genes further accelerated cell death and led to elongated myocytes or myotubes containing two nuclei, some of which survived and twitched under hypoxia. Whereas nuclei in $Rb^{-/-}$ myotubes were unable to stably exit the cell-cycle, myotubes lacking both p107/p130 became permanently post-mitotic, suggesting that pRb, but not p107 or p130 may be lost in cancer because of the unique requirement for cell-cycle exit during terminal

differentiation. This thesis demonstrates that pRb is required to inhibit apoptosis in myoblasts and autophagy in myotubes but not to activate the differentiation program, and reveal a novel link between pRb and cell metabolism.

ACKNOWLEDGEMENTS

To my mentor, Dr. Eldad Zacksenhaus, for his patience, support, great ideas, enthusiasm and belief in this project. Thank you. To my many colleagues and friends from the 4th floor of the Canadian Blood Services building and beyond, especially - Andrew T. Ho, Rajwinder Lehal, Zhe Jiang, Jeffrey Liu, Tao Deng, Hui Qin Li - for all of your help, countless discussions, encouragement and most important of all, friendship during my time at the Zacksenhaus laboratory. To my committee members, Dr. Rod Bremner and Dr. Mansoor Husain, I am grateful for your guidance and support during the length of this project.

To my wife, Vivienne C. Tedesco-Ciavarra, for her understanding, endless support, patience and encouragement when it was most needed. To my family, and in particular to my parents Michele and Anna Ciavarra, for all of their sacrifices, and who most likely shoved aside their own dreams to give their family a better opportunity in Canada.

Looking back over seven years, I feel blessed to have had so many great people in my life who have supported me and helped me grow during my journey – thanks to each and every one of you!

TABLE OF CONTENTS

LIST OF TABLES

LIST OF FIGURES

LIST OF APPENDICES

LIST OF PUBLICATIONS

Ciavarra G and Zacksenhaus E. Rescue of myogenic defects in Rb-deficient cells by inhibition of autophagy or by hypoxia-induced glycolytic shift. *The Journal of Cell Biology*. 2010 Oct 18;191(2):291-301. (Permission to reproduce)

Ciavarra G, Ho AT, Cobrinik D and Zacksenhaus E. Unique and redundant functions of Retinoblastoma protein family during skeletal myogenesis. 2010. (*Submitted for publication*)

Ciavarra G and Zacksenhaus E. Role of Rb in differentiation: re-visited (Invited Review in Cell Cycle) (*In preparation)*

Ciavarra G and Zacksenhaus E. Direct and indirect induction of autophagy by Rb. (Invited Review in Autophagy) *(In preparation)*

ABBREVIATIONS

3-MA	3-methyladenine
Ad	Adenovirus
AMPK	5'- AMP-activated protein kinase
ATG	Autophagy-related gene
ATP	Adenosine 5'-triphosphate
bFGF	Basic fibroblast growth factor
bHLH	Basic helix-loop-helix
BL	Basal lamina
BM	Basement membrane
BrdU	Bromodeoxyuridine (5-bromo-2-deoxyuridine)
BSA	Bovine serum albumin
C/EBPα	CCAAT/enhancer-binding protein alpha
CDKI	Cyclin-dependent kinase inhibitor
CDK	Cyclin-dependent kinase
cDNA	Complementary deoxyribonucleic acid
CMA	Chaperone-mediated autophagy
Cre	Cre recombinase
DHPR	Dihydroxypyridine receptor
DM	Differentiation Medium
DMEM	Dulbecco's modified Eagle medium
DMSO	Dimethyl sulfoxide
DNA	Deoxyribonucleic acid
EV	Empty vector
FACS	Fluorescent activated cell sorting
FAO	Fatty acid β-oxidation
FBS	Fetal Bovine Serum
FITC	Fluorescein isothiocyanate
FoxO	Forkhead box transcription factor class O
GFP	Green fluorescent protein
GM	Growth Medium
GSK-3β	Glycogen synthase kinase-3β
H&E	Haemotoxylin and eosin
HAT	Histone acetyl transferase
HDAC	Histone deacetylase
HIF	Hypoxia inducible factor
HRP	Horse radish peroxidase
HS	Horse Serum
IMM	Inner mitochondrial membrane
kDa	Kilodalton
LiCl	Lithium Chloride
LC3	Microtubule-associated protein-1 light chain
MCK	Muscle creatine kinase
MEF	Mouse embryonic fibroblast
MEF2	Myocyte enhancer factor-2

MRF	Myogenic Regulatory Factor
MEM	Mouse embryonic myoblast
MHC	Myosin heavy chain
MOI	Multiplicity of infection
MOMP	Mitochondrial outer membrane permeability
mPTP	Mitochondrial permeability transition
MRF	Myogenic regulatory factor
mtDNA	Mitochondrial DNA
mTOR	Mammalian target of Rapamycin
nuDNA	Nuclear DNA
OMM	Outer mitochondrial membrane
OXPHOS	Oxidative phosphorylation
PARP	Poly(ADP-ribose) polymerase
PBS	Phophate buffered saline
PCR	Polymerase chain reaction
PE	Phosphatidylethanolamine
PGC-1α	Peroxisome proliferator-activated receptor-γ coactivator 1α
PPAR	Peroxisome proliferator-activated receptor
PtdIns3K	Class III phosphatidylinositol 3-kinase
RFP	Red fluorescent protein
RyR	Ryanodine receptor
SR	Sarcoplasmic reticulum
S6K	40S ribosomal protein S6 kinase
SDS-PAGE	Sodium dodecyl sulfate polyacrylamide gel electrophoresis
SV40	Simian virus 40
Tag	Large tumor antigen
TBST	Tris-buffered saline containing 0.1% Tween 20
TCA	Tricarboxylic acid cycle
TUNEL	Terminal deoxynucleotydyl transferase-mediated dUTP nick end-labeling
XIAP	X-linked inhibitor of apoptosis

CHAPTER 1: INTRODUCTION

1.1 THE *RB* TUMOR SUPPRESSOR & CELL CYCLE REGULATION

1.1.1 The Rb Tumor Suppressor

The retinoblastoma tumor suppressor gene *RB* was initially identified as the cause for retinoblastoma - a malignant tumor of the eye – after deletions and subsequent missense mutations were identified in the gene in retinoblastoma tumors [1, 2]. Retinoblastoma, which occurs almost exclusively in children under five years of age, presents as either hereditary or non-hereditary cancer [1]. In the hereditary form, both eyes (bilateral retinoblastoma) are affected with nearly 100% penetrance; whereas non-hereditary retinoblastoma is due to somatic *RB* mutations in the developing retina, often leading to sporadic retinoblastoma [1]. In 1971, Knudson proposed a model to explain the genetics behind hereditary and non-hereditary retinoblastoma; whereby tumor onset - in both heritable and non-heritable retinoblastoma - is the result of two mutational events [2]. Knudson's hypothesis was later validated when it was established that the two mutations required for retinoblastoma to occur, target one gene locus on chromosome 13q14 [3, 4]. In 1986, the cDNA of the first identified tumor suppressor gene, *RB*, was identified [3] and later found to be deleted or mutated in a variety of human cancers [4-6]. Molecular analyses showed that the *RB* gene product, pRb, is widely expressed, regulated by phosphorylation in a manner consistent with a role in cell cycle control [4, 5] and its over-expression was capable of suppressing cell proliferation at the G1-restriction point [4]. Further clues of pRb function in growth suppression came from discoveries that DNA tumor viruses encode oncoproteins such as adenovirus E1A, SV40 large T antigen (Tag) and human papilloma virus E7 that bind and inhibit pRb as a prerequisite for neoplastic transformation [4-7]. Subsequent studies revealed that loss of *RB* function – in

human and mouse models - contributes to the initiation and progression of a variety of malignancies [4-9]. In addition, it was shown that pRb controls the G1 checkpoint through inhibition of the E2F family of transcription factors by acting as a co-repressor that recruits chromatin remodeling enzymes to suppress target genes required for cell cycle progression and cell death. Rb is also thought to control differentiation and chromosomal stability [4-10]. In mammalian cells, pRb and two-related proteins - p107 and p130 - make up the Rb family where each member has distinct and overlapping roles [4, 5].

1.1.2 Role of Rb in Cell Cycle Regulation

RB is a transcriptional repressor that regulates cell cycle progression by inhibiting the activity of E2F transcription factors [4-11]. This family of transcription factors is comprised of eight members, E2F1 - E2F8, which are sequence-specific DNA-binding factors that regulate expression of genes required for S-phase entry and DNA synthesis [4-7]. The activating E2Fs (E2F1, E2F2 and E2F3a), which are capable of advancing quiescent fibroblasts into G1, are repressed when bound by pRb [4-10]. Indeed, by eliminating E2F1, E2F2 or E2F3, the ectopic division detected in the lens, retina and central nervous system (CNS) of Rb-null embryos can be rescued to various extents [9, 11-14]. In addition to the activator E2Fs, the family includes transcriptional repressors – E2F3b, E2F4, E2F5, E2F6, E2F7 and E2F8 [8, 15, 16]. E2F1 - E2F6 bind DNA as a heterodimer, interacting with one of three dimerization partner (DP) proteins, whereas E2F7-E2F8 lack a DP-binding domain but contain a DNA binding domain [17-21]. pRb suppresses expression of E2F-regulated genes by binding and blocking the activation domain of E2F proteins [22] and by recruiting histone deacetylases (HDACs) [23-25] and

the SWI/SNF factor BRG1 [26], both of which influence the nearby nucleosome structure to regulate access of transcription factors to their binding sites [27, 28]. The seminal finding that E2F1 could prompt quiescent cells to enter G1 phase in the absence of mitogens, first demonstrated a functional link between E2Fs and cell cycle control [29]. Since then, E2Fs have been shown to regulate expression of many G1/S genes including DNA polymerase-α, proliferating cell nuclear antigen (PCNA), cyclin E, cyclin A, dihydrofolate reductase (DHFR) and others [30-33]. E2Fs also regulate expression of genes associated with the G2/M phase of the cell cycle as well as apoptosis and cellular differentiation [34-37]. As for E2F expression during myogenic differentiation, E2F2 is highly expressed during embryogenesis in mouse skeletal muscle, whereas E2F1 was not detectable and E2F3 - E2F5 were detected at very low levels by *in situ* hybridization [38]. It was also shown that E2F3b, and not E2F3a or other E2F family members, is uniquely able to promote myogenic differentiation and that this requirement for E2F3b does not depend on pRb [39].

Although the total level of pRb protein remains relatively constant through the cell cycle - G1, S, G2 and M-phase [40-42] - its phosphorylation state is highly regulated [43, 44]. In quiescent cells, pRb is hypo-phosphorylated, and as cells progress through G1, pRb is sequentially phosphorylated by cyclin/cyclin dependent kinase (Cdk) complexes and maintained in a hyper-phosphorylated state from late G1 (the restriction point) to mitosis, where it is dephosphorylated [45]. During the mammalian cell cycle, mitogenic signals are detected by D-type cyclins – D1, D2 and D3 – which bind and activate Cdk4 and Cdk6 during G1 [46]. In late G1, cyclin D-Cdk4/6 complexes phosphorylate pRb on specific amino acids [47, 48] and subsequently, expression and

activity of E-type cyclins – E1 and E2 – is induced, forming complexes with Cdk2 [47-50]. Cyclin E-Cdk2 further phosphorylates pRb, resulting in its inactivation and release from E2Fs [47, 49-53]. E2Fs induce cyclin E expression, hence creating a positive feedback-loop that generates an increase in E2F-dependent transcription and S-phase entry. During the late stage of DNA replication, Cdk1 and Cdk2 are activated by cyclin A, maintaining pRb phosphorylation and driving the transition through G2 to mitosis [54-57]. Mitosis begins when Cdk1 associates with its regulatory subunit, cyclin B1, whose cytoplasmic levels increase during G2 and peak in M [58-60]. Immediately before mitosis, cyclin B1/Cdk1 complexes translocate to the nucleus to promote completion of chromosome condensation and spindle assembly [61].

The activity of the Cdks is controlled by Cdk inhibitors (Ckis), which are divided into two groups based on their structure and specificities [62]. The first category includes the INK4 proteins - $p16^{INK4a}$ [63], $p15^{INK4b}$ [64], $p18^{INK4c}$ [65, 66] and $p19^{INK4d}$ [66, 67] - which inhibit kinase activity of Cdk4 and Cdk6 by preventing association with D-type cyclins [62, 68]. The second class of inhibitors, known as the Cip/Kip family, binds to both cyclin and Cdk subunits [69-71] and includes $p21^{Cip1}$ [72-74], $p27^{Kip1}$ [75, 76] and $p57^{Kip2}$ [77, 78] and inhibit E- and A-type dependent kinases. Interestingly, although $p21^{Cip1}$and $p27^{Kip}$ are potent inhibitors of cyclin E- and A-dependent Cdk2, they are positive regulators of cyclin D-dependent kinases [62, 79]. Overall, D-type cyclins are thought to serve three functions: 1) cyclin D-Cdk4/6 complexes phosphorylate pRb, leading to its inactivation (a catalytic function); 2) cyclin D-Cdk4/6 complexes sequester Cip/Kip proteins, releasing cyclin E-Cdk2 in late G1 (a non-catalytic function); 3) cyclin

D1 acts as a transcriptional cofactor to modulate gene expression (a cdk-independent function) [62, 79, 80].

1.1.3 Role of Rb in Apoptotic Cell Death

In addition to S phase gene activation, E2Fs also induce expression of pro-apoptotic factors and the tumor suppressor *ARF* ($p19^{ARF}$ in mice and $p14^{ARF}$ in humans), which stabilizes p53 by inhibiting Mdm2 [81, 82], and thus, connecting Rb to the p53 pathway [83, 84]. As a result, p53 stabilization can induce cell cycle arrest by transcriptional activation of $p21^{Cip1}$ [85], or apoptosis, by inducing pro-apoptotic factors such as *Bax* [86-90]. E2F1 also transactivates pro-apoptotic genes including *Apaf1*, *caspases-3*, *-7*, *-8* and *-9* [89, 91] and members of the Bcl-2 homology 3 (BH3)-only group of genes such as *Bax, Bnip3, Noxa and Puma* (detailed in section 1.4.2) [92]. Indeed, some Rb-deficient tissues, such as lens, central nervous system (CNS) and liver, display massive apoptosis that is E2F1 and p53-dependent, whereas in other tissues, such as the peripheral nervous system (PNS) and skeletal muscle, the cell death is p53-independent [12, 93-95]. E2Fs are not required for normal mammalian cell division, but have an unexpected pro-survival role in development as described in two recent reports: 1) E2F1-3-null retinal progenitor cells retain the ability to divide, however, their absence causes downregulation of the p53 deacetylase Sirt1, p53 hyperacetylation and elevated apoptosis [96] and 2) in the absence of the activator E2Fs, dividing progenitors of the small intestine undergo p53-independent apoptosis [97] and in the early stages of differentiation, pRb forms a repressive complex with activator E2Fs, an action necessary to downregulate E2F targets [97].

1.1.4 Role of Rb in Terminal Cellular Differentiation

During terminal cellular differentiation, pRb is thought to not only maintain the post-mitotic state, but also cooperate with tissue-specific transcription factors to alter gene expression. During adipocyte differentiation, pRb was shown to directly bind to two CCAAT/enhancer-binding protein (C/EBP) family members - C/EBPβ and NF-IL6 - and enhance their sequence-specific DNA binding and transactivation abilities [98, 99]. pRb was also shown to promote osteoblast differentiation by acting as a transcriptional coactivator to the osteoblast-specific transcription factor CBFA1 (also referred to as RUNX2) [100, 101]. During skeletal muscle differentiation, the muscle-specific transcription factors MyoD and myogenin were shown to directly bind to unphosphorylated pRb and this interaction is thought to mediate myoblast cell commitment and differentiation [102] and overexpression of MyoD in Rb-null MEFs does not induce myogenic conversion as it does in Rb-positive MEFs [102]. pRb also stimulates the transcriptional activation domain of myocyte enhancer factor-2C (MEF2C) (detailed in section 1.3) [103]. Although a direct interaction between pRb and MyoD/myogenin is appealing, some studies have been unable to reproduce this interaction *in vitro* or *in vivo* [104, 105] while a recent report detected a pRb-MyoD interaction in human but not mouse [106].

1.1.5 Rb relatives: p107 and p130

Two Rb related family members - p107 [107] and p130 [108] – perform unique and overlapping roles during development [109-111]. Four properties distinguishing the proteins are: 1) their expression profiles through the cell cycle and development; 2) their interaction with members of the E2F family and other factors; 3) the number and location

of phosphorylation sites (Figure 1.1); and 4) presence of cyclin and cdk inhibitory domains in p107 and p130 but not pRb (Figure 1.1) [112-118]. As described earlier, the level of pRb remains relatively constant throughout the cell cycle; however, expression of p107 and p130 is altered: in quiescent cells, p107 levels are low but sharply increase as cells move through the cell cycle, whereas p130 is highly expressed in quiescent or differentiated cells and is down-regulated as cells enter the cell cycle [109, 113, 119].

A defining characteristic of all three family members is the highly conserved pocket domain, comprised of A- and B-domains with an intervening spacer domain (Figure 1.1) [109, 111, 120, 121]. Within the B-domain is a region responsible for binding of factors containing an LxCxE motif, such as HDAC1, as well as E1A, Tag and E7 [111, 120, 122, 123]. The pocket region is also a target of non-LxCxE containing proteins, such as the E2F family, which bind the pocket domain and C-terminus (Figure 1.1) [111, 120, 124]. A unique spacer region between the A and B-domains of p107 and p130, but not pRb, binds to and inhibits Cyclin E/Cdk2 and Cyclin A/Cdk2 complexes [111, 125, 126].

1.1.6 Phenotypes of Rb knockout mice

Homozygous *Rb*-deficient mice die by embryonic day (E) 13.5 with extensive apoptosis, ectopic proliferation and developmental defects - precluding studies of processes such as skeletal muscle differentiation, that occur mostly after E13.5 [127-130]. To circumvent this lethality, two mouse models were previously constructed - both of which were used in this thesis. In the first model, a transgenic mouse was generated to carry an *Rb* minigene (mgRb) [93]. The mgRb - which directs pRb expression in mgRb:$Rb^{-/-}$ embryos exclusively to the CNS and placenta - consists of a genomic fragment spanning

the 1.3kb mouse *Rb* promoter region, followed by the first exon and intron fused to exons 2 to 27 of the mouse *Rb* cDNA [93, 131]. In the second model, conditional inactivation of *Rb* was achieved by flanking exon 19 of the *Rb* gene with LoxP sites (herein referred to as Rb^{f}) [132-134]. The $Rb^{f/f}$ mice, in conjunction with tissue-restricted cre recombinase expression, has allowed for analysis of pRb function in tissues such as skeletal muscle, heart, epidermis, retina, forebrain and mammary gland [133-138].

mgRb:$Rb^{-/-}$ embryos survive to birth, but die thereafter with specific defects in tissues that normally express Rb during embryogenesis such as skeletal muscle, liver and lens [93, 116, 131]. Beyond E13.5, mgRb:$Rb^{-/-}$ embryos display a pronounced skeletal muscle defect characterized by massive cell death, reduced muscle fiber density, endoreduplication within residual myotubes and reduced expression of a subset of late muscle-specific genes, including muscle creatine kinase (MCK) and MRF4 [93, 95]. Thus, the mgRb:$Rb^{-/-}$ model represents a scenario where pRb is chronically inactivated during skeletal myogenesis. Interestingly, a subset of defects associated with *Rb* loss during development have been rescued in $Rb^{-/-}$:$Id2^{-/-}$, $Rb^{-/-}$:$E2F1^{-/-}$,$Rb^{-/-}$:$E2F3^{-/-}$,$Rb^{-/-}$:$p53^{-/-}$, $Rb^{-/-}$:$Apaf1^{-/-}$ double-mutant mice or by supplying a wild-type placenta, but none have fully rescued the associated skeletal muscle defect [13, 95, 129, 139, 140]. The skeletal muscle defect appears to be cell-autonomous and the death of skeletal muscle in the context of Rb-loss may occur by a non-apoptotic death pathway.

1.1.7 Functional redundancy and antagonism between Rb family members

Sensitivity to Rb loss is cell-type dependent due to differing degrees of functional compensation among Rb family members in different tissues. During murine development, combined loss of Rb and either p107 or p130 in the retina, heart,

cerebellum and epidermis results in more severe defects [133-135, 141-143], whereas in other tissues, such as the mammary gland, combined inactivation of *Rb* and *p107* does not exacerbate the defect relative to Rb-deficient mammary gland [138].

Mice deficient for p107 or p130 are viable and fertile in a mixed 129Sv:C57BL6 genetic background, alluding to the redundant roles of these proteins in murine development [142, 144-146]. In a Balb/cJ background, $p107^{-/-}$ mice are also viable and fertile but are impaired in growth and exhibit myeloid hyperplasia in the spleen and liver [145]. When Rb/p107 chimeric mice were generated, $Rb^{-/-}$:$p107^{-/-}$ retinoblasts gave rise to retinoblastoma, indicating that p107 can function as a tumor suppressor *in vivo* [142, 147]. Compound $Rb^{-/-}$:$p107^{-/-}$ mutant mice die *in utero* at E11.5, two days earlier than embryos deficient for Rb alone, suggesting pRb and p107 perform overlapping functions in some tissues [142]. Furthermore, p107 is responsible for the G0/G1 arrest of $Rb^{-/-}$ MEFs when Rb is chronically inactivated [148]. A similar compensatory mechanism is thought to occur during differentiation of Rb-deficient muscle; normally, p107 is highly expressed in proliferating myoblasts and down-regulated as the cells terminally differentiate [149], but in Rb-deficient muscle, p107 levels remain high during differentiation [149-151]. Interestingly, one study suggested pRb was not necessary for differentiation of a teratoma-derived $Rb^{-/-}$ myoblast cell line, but was required to maintain the terminally differentiated state (a function for which p107 could not compensate) [149]. In contrary, a different study reported that pRb is required for differentiation, but not to maintain the terminally differentiated state [150]. This discrepancy may be a result of differences in the origin of myogenic cells (teratoma-derived vs. satellite cells) or in experimental assay differences.

Although mice deficient for p130 in a C57BL6 background are viable and fertile, in an enriched Balb/cJ genetic background, p130 null mice die *in utero* between E11.5 and E13.5 with a reduced number of neurons in the spinal cord, and extensive apoptosis in the CNS and dermomyotome but not the heart [146]. Using heart-restricted Rb- and Rb:p130-deficient mice, a functional redundancy between p130 and pRb was uncovered in the heart [134]. Although Rb-deficient cardiac myocytes differentiate normally, concomitant loss of p130 leads to ectopic myocyte division and death due to heart failure in approximately 40% of the mice [134]. The tumor suppressor function of p130 was revealed by generating chimeric $Rb^{-/-}$:$p130^{-/-}$ mice [152], whereby these mice formed a broad spectrum of tumors – in comparison to $Rb^{+/-}$ and $Rb^{-/-}$ chimeric mice [152, 153]. Simultaneous inactivation of p107 and p130 in a C57BL6 genetic background led to deregulated chondrocyte growth, shortened limbs and neonatal lethality [144]. Thus, in some instances, p107 and p130 perform unique functions that pRb cannot perform.

The effect of inactivating all three Rb family genes has been studied in mouse embryonic fibroblasts (MEFs) obtained from chimeric embryos [28, 154, 155]. Triple knockout (TKO) MEFs fail to arrest in G0/G1 following exposure to growth-restricting conditions whereas MEFs lacking pRb, p107 or p130 maintain this ability when constitutively inactivated [28, 154, 155]. Acute inactivation of Rb in quiescent fibroblasts is sufficient for cell-cycle entry and is phenotypically different from germ line loss of Rb partly due to functional compensation by p107 [148]. Interestingly, Rb loss in mature hepatocytes also results in cell cycle re-entry [156]; however, it was suggested that inactivation of Rb or the entire Rb family in neurons and differentiated muscle does not allow for cell cycle re-entry [150, 157, 158].

Antagonism between Rb family members has been demonstrated *in vitro*. For example, over-expression of p107 inhibits adipocyte differentiation, whereas pRb over-expression enhances differentiation [159]. In the C2C12 myoblast cell line, it was suggested that p130 over-expression antagonizes myogenic differentiation [160]. Thus, one would expect enhanced differentiation capacity of $p130^{-/-}$ MEMs, but in this thesis it is demonstrated that primary $p130^{-/-}$ MEMs do not exhibit enhanced differentiation potential (Chapter 4).

1.2 SKELETAL MYOGENESIS

1.2.1 Skeletal Muscle Development

Skeletal muscles maintain body posture, temperature and help perform a range of movements [161]. Muscles of the trunk and limbs of vertebrate embryos are derived from somites - a series of transient repeating epithelial structures that derive from the paraxial mesoderm and lie on either side of the neural tube [162]. Somites eventually differentiate into five major cell types: cartilage, bone and tendons of the trunk, skeletal muscles of the body and the dermis of the back [162-165]. This process is regulated by sonic hedgehog (Shh) and Wnt signals that emanate from tissues surrounding the somites (Figure 1.2A) [166, 167]; leading to patterning of the epithelial structures into distinct compartments that give rise to diverse cell lineages [164, 165, 167, 168]. The compartments formed are the mesenchymal sclerotome - which contributes to cartilage and bone of the vertebral column and ribs - and the dorsally located epithelial dermomyotome - where myogenic precursors are localized and ultimately give rise to epaxial (back) and hypaxial (muscles of the ventral body wall, limbs, diaphragm and tongue) muscles (Figure 1.2A-B) [168, 169]. All cells of the dermomyotome, including

the epaxial and hypaxial extremities, are initially positive for the Pax3 transcription factor, whereas Pax3/Pax7-double positive cells are located in the central domain only [170]. Myogenesis is initiated by the translocation of myogenic progenitors that migrate as Pax3-positive cells from the extremities of the dermomyotome to the myotomal layer below or as Pax3/7-double positive cells from the central dermomyotome to the myotome [162, 167, 171-176]. These cells enter the myogenic program after activating Myf5 and Mrf4 (section 1.2.2 for a complete description of the myogenic regulatory factors (MRFs)); MRFs that regulate entry of cells into the myogenic program [177, 178]. Double-mutant Pax3/Pax7 mouse embryos suffer from a major skeletal muscle deficit where only the early myotome is formed, but these cells do not activate Myf5 or MyoD and consequently fail to enter the myogenic program and die or assume a non-myogenic fate [179, 180]. For myogenesis at distant sites, Pax3-positive myogenic progenitors delaminate and migrate from the hypaxial dermomyotome to establish the muscles of the ventral body wall, limbs, diaphragm and tongue [167, 168, 174, 181-183]. The activation of Pax3 in these cells promotes their migration by altering the expression of the tyrosine kinase c-Met [184, 185], which is required for these cells to migrate toward the limb buds where the ligand for c-Met, hepatocyte growth factor, is expressed at high levels [185, 186]. Once these Pax3-positive cells reach their distant sites, Pax3 directly activates Myf5 by binding a regulatory sequence required for Myf5 transcription [171, 172, 187]. Notably, $Pax3^{-/-}$ mice have no limb muscles because muscle precursors fail to delaminate from the hypaxial dermomyotome [174, 178], whereas $Pax7^{-/-}$ mice fail to renew and propagate their myogenic satellite cells and the animals are ~33% smaller than wild-type control and die by two weeks of age [188-190]. Overall, Pax3 and Myf5/Mrf4 control the

activation of MyoD, another MRF family member (detailed in section 1.2.2), whereby MyoD-positive myogenic precursors differentiate into myofibers or remain as a proliferating population - referred to as the satellite cell population - within the muscle mass [183, 191]. Satellite cells, which are Pax7-positive [192-194], lie mitotically quiescent until activated, for example by muscle injury, at which point they mediate postnatal growth, hypertrophy and regeneration of muscle [179, 183, 191, 195-199]. Progeny of activated satellite cells, termed myogenic precursor cells, undergo multiple rounds of division before either fusing with existing myofibers [198, 200] or self-renewing the satellite cell pool [191, 200-203]. Once satellite cells are activated, MyoD and Myf5 expression is induced [193, 204-207], and following the initial proliferative phase of myogenic precursor cells, myogenin and MRF4 mark the onset of myogenic differentiation [204-206, 208].

1.2.2 MRF Family of Transcription Factors

Skeletal muscle-specific gene expression and differentiation is regulated by the MRF transcription factors - MyoD, Myf5, Mrf4 and myogenin [209-214] - which share a homologous basic helix-loop-helix (bHLH) domain required for binding to control regions of muscle-specific genes [210-212, 214-217]. The MRFs heterodimerize with E proteins, such as E47 and HEB, to transactivate muscle-specific genes via consensus E-box (CANNTG) sequences [217]. Two of the MRFs, MyoD and Myf5, can individually specify the skeletal muscle lineage in mice. The muscle of *MyoD*$^{-/-}$ mice displays no obvious abnormalities, but expresses elevated levels of Myf5 and has a reduced capacity to regenerate after injury [218, 219]. *Myf5*$^{-/-}$ mice are also viable and have no detectable skeletal muscle defects [171, 220, 221]. Whether myogenesis can proceed in the absence

of both *MyoD* and *Myf5* remains a matter of debate. Initially, *MyoD:Myf5* double-mutant mice were reportedly devoid of skeletal muscle and myoblasts [222]. However, subsequent work showed that *Myf5:MyoD* double-mutant mice also harbored a compromised *Mrf4* gene. By restoring *Mrf4* in *MyoD:Myf5* double-mutants, embryonic myogenesis was partially rescued [223] and potentially identified Mrf4 as a myogenic *determination* factor in the somite [223]. Myogenin and Mrf4 are required for terminal muscle differentiation, have distinct differentiation functions [224-226] and both myogenin$^{-/-}$ and Mrf4$^{-/-}$ mouse embryos contain myoblasts but are deficient in differentiated skeletal muscles [227-230]. Overall, the MRFs are functionally classified into two groups: Myf5, MyoD and Mrf4 (determination factors) and MyoD, myogenin and Mrf4 (differentiation factors). Notably, MyoD is both a determination and differentiation factor and the role of Mrf4 as a determination factor remains to be fully defined. A second class of transcription factors controlling myogenesis is the MEF2 family - consisting of the MEF2A, -B, -C and -D proteins - which is highly expressed in developing mouse skeletal muscle [231-233]. The MRFs induce the expression of the MEF2 family which act as co-regulators to the MRFs to potentiate their myogenic transcriptional activity during differentiation [231, 234-240]; but unlike the MRFs, MEF2 proteins are also expressed in other cell types [233, 241].

The Id family of proteins, consisting of Id1- Id4, function as dominant-negative regulators of bHLH factors by forming inactive heterodimers [242-246]. Id proteins also bind other factors such as Rb family members [247, 248]. Deletion of Id2 rescues some Rb mutant embryo phenotypes [140], but the concomitant inactivation of Id2 and Rb does not rescue the Rb mutant myogenic defect (see section 1.3) [140].

1.2.3 Classes of Myogenic Cells

Three classes of myogenic cells have been identified – embryonic myoblasts, fetal myoblasts and satellite cells – each characterized by specific features but most likely sharing a common origin [183, 249]. As described earlier, embryonic myogenesis in the mouse begins with the migration of muscle progenitor cells from the dermomyotome to the underlying myotome layer at E10.5 - E12.5 [162, 175, 249, 250]. Fetal myogenesis occurs between E14.5 - E17.5 in the mouse and is characterized by the fusion of fetal myoblasts with each other [251] or with existing myofibers [249, 252, 253]. Following this phase of myogenesis, basal lamina begins to surround individual myofibers and satellite cells become juxtaposed between the plasma membrane of myofibers and the basal lamina [254, 255].

1.2.4 Structure and Function of Skeletal Muscle

Structurally, skeletal muscles are composed of fascicles, which are bundles of individual myofibers, each of which has a structure related to its specialized contractile and metabolic functions [161, 231]. Each myofiber consists of contractile units, referred to as myofibrils [161, 256], which contain repeating units known as the sarcomere; the fundamental contractile unit of striated muscle [161, 256]. During muscle contraction – according to the generally accepted *sliding filament model* [257, 258] – myosin filaments remain constant in length while contacting actin filaments through molecular cross-bridges and slide opposing actin filaments towards each other within the sarcomere [259]. The movement of actin filaments is controlled by two regulatory proteins, tropomyosin and troponin, which form a complex that regulates contraction in response to Ca^{2+} [256, 259, 260].

Skeletal muscle myofibers are generally classified as type I (oxidative/slow) or type II (glycolytic/fast) and differ with respect to contraction, metabolism and susceptibility to fatigue [261]. Type I fibers are rich in mitochondria and mainly use oxidative metabolism for energy production [231, 262, 263]. Type II fibers comprise three subtypes, IIa, IIx, and IIb. Type IIb fibers have the fewest mitochondria and rely on glycolytic metabolism as a major energy source, while the oxidative and contraction functions of type IIa and IIx lie between type I and IIb [264, 265].

The primary regulatory and signaling molecule in skeletal muscle is Ca^{2+} [259, 264] and its concentration is regulated by a system composed of the sarcoplasmic reticulum (SR), which is an intracellular Ca^{2+}ion storage depot, the ryanodine receptor (RyR), which is the major channel for Ca^{2+}release from the SR [266] and the transverse (T)-tubule membrane, which is part of the sarcolemma and contains the voltage-sensor dihydroxypyridine receptor (DHPR) [267] [268]. Interaction of DHPR with RyR connects the SR and T-tubule membranes and this connection is responsible for the excitation-contraction (EC) coupling that triggers muscle contraction [264, 268]. The Ca^{2+} cycle starts when an action potential is propagated along the surface of the sarcolemma and T-tubules [267, 268]. Once depolarization of the T-tubules occurs, the signal is transduced by the DHPR and transmitted to the RyR in the closely apposed SR membrane [267-269] [270]. Once the RyR Ca^{2+}release channels are opened, Ca^{2+}ions flow from the SR lumen to the cytosol, increasing the intracellular Ca^{2+}concentration about 100-fold [264]. Ca^{2+} then binds to the troponin complex, inducing a contraction [264]. When the contraction stimulus ends, a Ca^{2+}-ATPase pumps Ca^{2+}ions back into the

lumen of the SR, lowering the Ca^{2+}ion concentration to a level insufficient to induce myofiber contraction [271, 272].

1.2.5 Regulation of Cell Cycle Exit & Terminal Myogenic Differentiation

In transition from proliferation to differentiation, myoblasts irreversibly withdraw from the cell cycle and fuse to form multinucleated myotubes [273, 274]. During this process, cell cycle activators such as cyclin D1 and Cdks are down-regulated [275, 276] and cell cycle inhibitors such as $p18^{INK4c}$ [277], $p21^{Cip1}$ [278, 279] and $p57^{Kip2}$ [280] are induced. However, withdrawal from the cell cycle is not an obligatory event for myotube formation since $Rb^{-/-}$ myoblasts do transiently differentiate despite the failure of Rb-deficient myonuclei to permanently exit the cell cycle [93, 149]. This is in contrast to the post-mitotic nuclei of wild-type skeletal muscle which are unable to reinitiate DNA synthesis even in the presence of mitogens [281]. As described earlier, pRb is thought to participate in both processes (cell cycle exit & differentiation) during myogenesis.

The observation that muscle differentiation correlates with high levels of hypophosphorylated pRb was the first clue implicating pRb in this process [102, 282]. In addition, expression of simian virus 40 (SV40) large tumor antigen (TAg) - which sequesters and functionally inhibits pRb [283, 284], p107 [285], p130 [285] p53 [286], p300 [287] and other factors [288] - induces DNA synthesis in terminally differentiated myotubes [289, 290]. Similarly, expression of adenovirus E1A protein, which binds the pRb family and other factors, but not p53 [291-293], reactivates the cell cycle in terminally differentiated muscle [294] and over-expression of E1A in myoblasts blocks differentiation [295, 296]. Furthermore, using myotubes harbouring a $Rb^{f/f}$ allele, it was suggested that once the post-mitotic state is established, maintenance is pRb independent

[150, 158]. Recently, it was demonstrated that post-mitotic myonuclei can re-enter the cell cycle by eliminating Rb and ARF [297]. In other work, p130 was shown to block rather than induce myogenic differentiation [160]. Presently, it remains unclear to what extent p107 and p130 collaborate with pRb during skeletal myogenesis.

A role for other Rb-pathway proteins in skeletal myogenesis has also been described. For example, Cyclin D3 may promote differentiation since it is induced and possibly stabilized in a pRb-dependent manner during myogenesis [298-301]. In contrast, Cyclin D1 and its associated Cdk activity are down-regulated during myogenic differentiation, and ectopic expression of Cyclin D1 blocks differentiation and the transcription of MRF-regulated genes [300, 302, 303]. However, whether this function of Cyclin D1 is via pRb or through its direct interaction with transcription factors remains unknown [80]. The induction of $p21^{Cip1}$ during muscle differentiation - which is MyoD dependent [278, 304-306] - has been well characterized both *in vivo* and *in vitro* [278, 279, 307] and its suppression is sufficient for differentiated C2C12 myotubes to re-enter the cell cycle [308]. Although the skeletal muscle of $p21^{Cip1-/-}$ and $p57^{Kip2-/-}$ mice is mostly normal [309, 310], simultaneous inactivation of $p21^{Cip1}$ and $p57^{Kip2}$ results in severe muscle defects similar to mgRb:$Rb^{-/-}$ embryos [280]. Mice deficient for $p27^{Kip1}$, which is expressed at low levels in differentiated skeletal muscle, or $p16^{INK4a}$, display no obvious skeletal muscle defects [311-314].

Two potent inhibitors of myoblast differentiation, the fibroblast growth factor (FGF) and transforming growth factor type-β (TGF-β) families [274, 315-317], repress muscle gene expression and myogenic bHLH factors without stimulating cell

proliferation [274, 315, 318, 319]. Within the MRF family, myogenin and Mrf4 are most sensitive to growth factor repression, whereas MyoD and myf5 are not [320-324].

1.3 RB IN SKELETAL MYOGENESIS

1.3.1 Current Models

Although Rb transcripts are detectable by *in situ* hybridization at all stages of murine skeletal myogenesis [93], the role of pRb during myogenic differentiation remains unsolved. To date, three models have been proposed describing an active role for pRb during terminal muscle differentiation [102, 103, 149, 151, 325].

The first model asserts that by interacting directly with MyoD and myogenin, pRb participates in the differentiation and maintenance of the terminally differentiated state [102]. Moreover, using MyoD-converted $Rb^{-/-}$ MEFs, it was shown that Rb-deficient myotubes inappropriately accumulate in S and G2 in response to mitogens and fail to express late muscle differentiation markers; suggesting MyoD activity requires the presence of pRb [151]. The major limitation to these studies is the use of MyoD-converted non-myogenic cell lines (U2OS, Saos-2, MEFs) [102, 151], which may not accurately represent myoblasts. Furthermore, a direct interaction between pRb and MyoD/myogenin has not been reproduced in mice [104, 105] and this model is further challenged by the observation that Rb-deficient mouse embryos, such as the mgRb:Rb-/- model, do form skeletal muscle [93].

The second model states that in addition to cell cycle arrest during muscle differentiation, pRb is required to cooperate with MyoD to stimulate the transactivation domain of MEF2C [103]. Thus, although MyoD-converted $Rb^{-/-}$ MEFs can proceed through the early stages of muscle differentiation, late-muscle gene expression is

compromised due to transcriptionally inert MEF2C. Again, a major limitation of this study was the use of MyoD-converted $Rb^{-/-}$ MEFs to study muscle differentiation.

The third model proposes that pRb sequesters inhibitors of differentiation to indirectly stimulate the transcriptional activity of MyoD. It was suggested that during myogenic differentiation pRb titrates HDAC1 from MyoD, facilitating the association of MyoD with the acetyltransferases p300/CBP and PCAF to promote activation of muscle-specific gene transcription [325-328]. This model couples cell-cycle exit and differentiation but has yet to be substantiated further. Other work proposed that during myogenic differentiation, pRb sequesters Id2, a member of the inhibitor of DNA binding (Id) protein family, which can inhibit differentiation of various cell lineages by inactivating target proteins, including the MRFs *in vitro* [244, 246]. However, $Rb^{-/-}$:$Id2^{-/-}$ mutant embryos exhibit myogenic defects similar to those observed in mgRb:$Rb^{-/-}$ embryos, suggesting that the myogenic defect is unlikely caused by deregulated Id2 [140]. It was also shown that the E1A-like inhibitor of differentiation (EID-1), which binds pRb and p300, functions as a repressor of MyoD function by binding p300, which is required for MyoD transcriptional activity [329]. It has also been reported that pRb binds to Retinoblastoma binding protein 2 (RBP2) to prevent RBP2 from repressing genes required for differentiation [330].

1.4 REGULATION OF CELL DEATH: APOPTOSIS & AUTOPHAGY

1.4.1 Modes of Cell Death

Based on the morphology of dying cells in prenatal tissues, *Schweichel and Merker* originally classified cell death into three categories (which have since been renamed): apoptosis (type I), autophagy (type II) and necrosis (type III) [331]. Their main features

are summarized in Table 1.1 (Adapted from [332]). Apoptosis and autophagy are described in detail in sections 1.4.2 and 1.4.3, respectively. Notably, although autophagy is often a morphological feature of dying cells, it has recently become clear that one major function of autophagy is to help preserve cell viability in unfavorable conditions [333, 334].

1.4.2 Apoptosis

The term 'apoptosis' was coined by *Kerr et al.* in 1972 to describe specific morphological aspects of cell death [335]. Apoptosis, or programmed cell death, is an energy-dependent mode of cell death, that is accompanied by rounding-up of the cell, retraction of pseudopodes, reduction of cellular and nuclear volume (pyknosis), nuclear fragmentation (karyorrhexis), plasma membrane blebbing (maintained intact) and engulfment by phagocytes [332, 335]. The executioners of apoptosis are the caspases; a conserved family of cysteine proteases that cleave after an aspartate residue in their substrates [336, 337]. Two routes of caspase-dependent apoptosis have been characterized in mammalian cells: extrinsic (extracellular signal-mediated) and intrinsic (intracellular signal-mediated) [338].

In the extrinsic apoptotic pathway, transmembrane death receptors belonging to the tumor necrosis factor (TNF) receptor gene super family engage death ligands [338, 339]. Examples of death ligands and their corresponding receptors include TNFα/TNFR1, FasL/FasR and Apo3L/DR3 [338, 339]. Once engaged, the receptors form a death-inducing signalling complex (DISC) by recruiting adaptor proteins and procaspase-8 and -10. Upon activation, these caspases cleave and activate downstream effector caspases such as caspase-3 or the cytosolic protein Bid [338-340]. Active

(truncated) tBid then translocates to the outer mitochondrial membrane and induces mitochondrial outer membrane permeabilization (MOMP) and cytochrome c release [338-340].

The intrinsic apoptotic pathway can be activated by stimuli such as DNA damage, chemotherapeutic agents and serum starvation [338, 339, 341]. By impinging on the mitochondria, these stimuli cause MOMP and release of pro-apoptogenic proteins - including cytochrome c, Smac/DIABLO, Omi and AIF - from the intermembrane mitochondrial space into the cytosol [336, 338, 339, 341]. After release, cytochrome c binds Apaf-1 to form the apoptosome; a complex that facilitates clustering of procaspase-9 leading to its auto-activation [338, 339, 342]. Smac/DIABLO and Omi both bind to inhibitors of apoptosis (IAPs) and relieve their inhibitory effects on caspase activity [338, 339, 341]. For example, X-linked IAP (XIAP) mediates inhibition of apoptosis by blocking caspase-3, -7 and -9 [343-345] and tumor cells with high XIAP levels resist apoptosis in response to different apoptotic stimuli and become chemotherapeutic resistant [346, 347]. Upon release from the mitochondria, AIF translocates to the nucleus and causes nuclear chromatin condensation and DNA fragmentation leading to caspase-independent apoptosis [338, 339, 341, 348]. MOMP is controlled by members of the Bcl-2 family of proteins which can be divided into three groups: 1) inhibitors of apoptosis (such as Bcl-2, Bcl-XL, Bcl-w); 2) promoters of apoptosis (such as Bax and Bak) and 3) a divergent group of factors - including Bim, Bid, Puma, Noxa and Bad - that have a conserved BH3 domain that can bind and antagonize the anti-apoptotic Bcl-2 proteins to stimulate apoptosis [341, 349, 350]. A major function of the anti-apoptotic Bcl-2 family is to prevent release of cytochrome c from mitochondria, mostly by antagonizing pro-

apoptotic Bak and Bax [351-354] which induce apoptosis by permeabilizing the mitochondrial outer membrane [354-356]. During apoptosis, Bak and Bax oligomerize to form pores that result in MOMP and release of pro-apoptotic factors [338, 339, 341, 354]. Activation of BH3-only proteins seems to depend on stress signals; for example Puma [88] and Noxa [90] are induced by p53 in response to DNA damage and Bim responds to endoplasmic reticulum stress [357]. In addition, as described in section 1.1.3, Rb loss leads to an E2F1-mediated induction of BH3-only pro-apoptotic factors, Apaf-1, and most caspases.

After the release of pro-apoptogenic factors and the apoptosome forms, procaspase-9 is cleaved and activated, followed by downstream activation of the executioner caspases-3 and -7 which cleave a plethora of cellular proteins leading to cell demise [350]. Although apoptosome formation is critical to activate caspase-9 in most cases, there are cell-types such as myoblasts and thymocytes, which can bypass the apoptosome to undergo apoptosis [358-360].

1.4.3 Autophagy

Currently, three forms of autophagy are recognized in mammalian cells: macroautophagy, microautophagy and chaperone-mediated autophagy (CMA) [334, 361]. Macroautophagy, is the process by which bulk cellular material, including large organelles such as mitochondria [362], is sequestered within a double membrane vesicle called an autophagosome [334, 361]. Through a fusion event, autophagosomes deliver their cargo to hydrolase-rich lysosomes, forming autolysosomes (Figure 1.3) where macromolecules are degraded into their constituents and shuttled out of the lysosome for reutilization [334, 363]. Microautophagy occurs when the lysosome membrane

invaginates and sequesters cytoplasm and organelles directly without a transport intermediate [364-366]. Although microautophagy has been well documented in yeast, little is known regarding the molecular details and functional importance of this pathway in mammalian cells [364-366]. CMA mediates the selective degradation of proteins containing a KFERQ amino acid sequence; this sequence is represented in about 30% of cytosolic proteins [367, 368]. Targeted proteins are translocated directly across the lysosomal membrane with the help of a molecular chaperone complex consisting of heat shock protein of 70kDa (hsc70), LAMP-2A and a cohort of co-chaperones [369-372]. For the purpose of this thesis, macroautophagy (referred to as autophagy herein) was studied in the context of Rb loss since autophagosomes were detected using various autophagosome-specific biomarkers.

Autophagy is regulated by a series of conserved autophagy-specific proteins, the Atg family [373], which is divided into four groups based on function: 1) protein kinases are part of the regulatory complex that responds to upstream signals (such as Atg1, Atg13, Atg17); 2) lipid kinases that mediate vesicle nucleation (such as Atg6, Vps34); 3) proteins forming a ubiquitin-like protein conjugation system required for vesicle expansion and completion (such as Atg8/LC3, Atg12); 4) a series of proteins required for the disassembly of Atg protein complexes from mature autophagosomes (such as Atg2, Atg9, Atg18) [334, 374].

From yeast to humans, the serine/threonine kinase mammalian target of rapamycin (mTOR) regulates two major processes: translation of selected mRNAs in the cell and autophagy [375]. Under nutrient-rich conditions, mTOR activates cap-dependent initiation of translation and ribosomal biogenesis to promote cell growth [376] and

phosphorylates and inactivates Atg1 and Atg13 to block autophagy [377-379]. During nutrient-deprivation, mTOR controlled protein translation is down-regulated and Atg1 is activated and phosphorylates Atg13 and Atg17, and together with Atg10, localize to the phagophore; the initial sequestering compartment that expands into an autophagosome [363, 373, 377, 380, 381]. mTOR is regulated by multiple signalling pathways including Wnt [382], downstream effectors of receptor tyrosine kinases (RTKs) such as Ras and phosphatidylinositol 3-kinase (PI3K) [383] and the intracellular energy sensor, 5'- AMP-activated protein kinase (AMPK) [384, 385]. In response to a drop in ATP and a rise in AMP, activated AMPK suppresses mTOR activity, through the TSC1/TSC2 complex, to activate autophagy [384-388]. In addition, AMPK phosphorylates and stabilizes $p27^{Kip1}$, which permits cells to survive metabolic stress by promoting cell cycle arrest and autophagy rather than apoptosis [389]. Other, mTOR-independent, autophagy pathways have been identified: 1) inhibition of inositol monophosphatase leads to reduced levels of free inositol and inositol-1,4,5-triphosphate (IP_3) - a second messenger that controls many cellular processes by regulating intracellular calcium levels [390-395]; and 2) during starvation, the Forkhead box class O3 (FoxO3) transcription factor regulates autophaghic genes such as LC3, Atg12, Vps34 (vacuolar protein sorting 34), Beclin-1 and Bnip3 [396, 397].

The nucleation of the initial phagophore membrane requires the class III phosphatidylinositol 3-kinase (PtdIns3K) complex composed of the PtdIns3K Vps34, Vps15, Atg14 and Atg6/Beclin-1[363, 398, 399]. Bcl-2 negatively regulates the formation of the phagophore by binding and sequestering Beclin-1 in nutrient-rich conditions, and dissociation of these proteins is required for autophagy induction (Figure

1.3) [398, 400]. The PtdIns3K complex, together with other Atg proteins like Atg20 and Atg24, further recruits two conjugation systems, Atg12-Atg5-Atg16 and LC3–PE (phosphatidylethanolamine), which regulate membrane elongation and expansion of the phagosome [401]. Through a series of conjugations, an Atg12-Atg5-Atg16 complex is formed and attached to the phagophore [402]. Subsequently, unconjugated LC3-I is conjugated to PE and becomes localized to both sides of the phagophore as the PE-conjugated form, LC3-II [403, 404]. Experimentally, the lipidation of LC3-I is widely used to monitor the induction of autophagy [405]. For example, as the autophagosome-associated LC3-II accumulates, it can be detected as characteristic punctate staining by immunocytochemistry using fluorescently tagged LC3-I or an anti-LC3 antibody. LC3-II can also be detected by SDS-PAGE since LC3-II migrates faster than the unconjugated, LC3-I form [405, 406]. Once autophagosome formation is complete, LC3-II attached to the outer membrane is cleaved from PE and released to the cytosol [407]. The nucleotide derivative 3-methyladenine (3-MA) inhibits class III PI3K activity and effectively blocks autophagy [408] although it has been reported to have other putative functions [409].

The fusion of the autophagosome and lysosome - to form an autolysosome - requires at least one isoform of the LAMP-2 lysosomal membrane proteins [410] as well as the small GTPase Rab7 [411] but the molecular details remain to be fully uncovered. The fusion of these vesicles is inhibited by the lysosomotropic drug chloroquine, allowing autophagic flux to be measured, since static images of untreated cells with increased autophagosomes could reflect either an increase in autophagy or a defect in autophagosome-lysosome fusion [412]. Once fusion is complete, the inner vesicle is degraded by a series of lysosomal hydrolases including proteinases A and B and

cathepsins B, D and L [413]. The constituents of the degraded macromolecules are transported back to the cytosol to replenish energy reserves, and during a period of starvation, preventing bioenergetic catastrophe that would lead to cell death [404]. Amino acids generated by this process contribute to adaptive protein synthesis and are shuttled to the tricarboxylic acid (TCA) cycle to generate ATP, nucleotides and acetyl CoA [361, 363].

In addition to responding to nutrient deprivation, autophagy also clears superfluous and damaged organelles such as the specific elimination of mitochondria in a process termed *mitophagy* [362, 414]. For example, aging mitochondria, which normally turnover with a half-life of 10-25 days, are selectively removed by mitophagy [415, 416] as are mitochondria from differentiating erythroid cells [417]. Furthermore, in some cell-types, a blockade in the apoptotic pathway redirects cell death to proceed by autophagy (and possibly mitophagy) and vice versa (Figure 1.4) [418-424]. Whether mitophagy is a stochastic or selective process has long been controversial. However, recent work has identified a mitophagy receptor, Atg32 in yeast [425, 426] and a defined mitophagic mechanism is emerging in mammalian cells [427, 428]. For instance, in response to inner mitochondrial membrane depolarization, the ubiquitin ligase Parkin translocates from the cytosol to mitochondria, triggering mitochondrial elimination by mitophagy [427], a process that is dependent on VDAC (a mitochondrial outer membrane protein) [428].

1.4.4 Links between Rb and Autophagy

Based on numerous studies, the Rb pathway has been linked to autophagy in two ways: 1) E2F1 was shown to regulate the expression of certain autophagy genes including *Bnip3, LC3, Atg1 and Beclin-1* [429, 430], and notably Bnip3 and a related protein

Bnip3L are BH3-only proteins capable of inducing cell death as well as autophagy [431-434]. Both proteins were shown to increase autophagosome formation in atrophying skeletal muscle [396] and Bnip3L was shown to specifically induce mitophagy during erythroid differentiation [417]. 2) The E2F1-regulated $p19^{ARF}$ as well as a short mitochondrial form (smARF) translocate to mitochondria and cause dissipation of the inner mitochondrial membrane, resulting in massive autophagy and caspase-independent cell death [83, 417, 435, 436]. Some mouse tumors, such as lymphomas with silenced $p19^{ARF}$, show impaired progression, suggesting $p19^{ARF}$ may enhance tumor progression under some circumstances [437].

1.5 CELLULAR METABOLISM

1.5.1 Cellular Metabolism

Multiple metabolic pathways converge at the mitochondria, including oxidative phosphorylation (OXPHOS), single carbon and fatty acid (FA) metabolism [438-440].

1.5.2 The Mitochondrion

Functionally, mitochondria serve to maintain energy stores, thermogenesis and multiple biosynthetic processes [438-441]. Given their vital role in these processes, the regulation of mitochondrial mass and function is essential and dynamically regulated in response to physiological cues such as nutrient availability, temperature and physical activity [438-441]. Furthermore, disruption of mitochondrial integrity elicits mitochondrial-dependent apoptosis as described earlier [341]. Mitochondria are double-membrane structures containing an autonomously replicating circular mitochondrial DNA genome (mtDNA) [441-443], which encodes the requisite enzymes for mtDNA transcription and replication

and protein synthesis components [443, 444]. The nuclear genome encodes the remainder of the approximately one-thousand proteins in the mitochondria, which are imported from the cytosol [441, 442, 445, 446]. The inner mitochondrial membrane (IMM), which is freely permeable only to O_2, CO_2 and H_2O, is where the complexes of the electron transport chain are localized (detailed in section 1.5.6) [447, 448]. The outer mitochondrial membrane (OMM) is the permeability barrier between the energy-transducing IMM and the cytosol [447, 448]. The OMM contains the pore-forming voltage-dependent anion channel (VDAC) [447-450]. VDAC interacts with several other proteins including adenine nucleotide translocase (ANT located in the IMM) and cylophilin D (CypD located in the matrix) [451] to form a permeability transition pore complex (PTPC) [452]. The PTPC, formed in response to multiple signals including high levels of Ca^{2+} and elevated levels of reactive oxygen species (ROS), increases the permeability of the mitochondrial membranes to molecules of less than 1.5kDa [452, 453]. As a consequence, the free entry of solutes into the mitochondrial matrix leads to depolarization of the IMM leading to bioenergetic failure and matrix swelling followed by necrotic or apoptotic cell death [452, 453]. Factors such as Bnip3L and $p19^{ARF}$ can cause mitochondrial depolarization followed by a massive induction of autophagy/mitophagy [83, 417, 435, 436]. Enclosed in the intermembrane space are respiratory chain substrates, numerous metabolic proteins as well as apoptogenic factors such as Smac, Omi and AIF [447, 448, 454, 455], whereas the matrix contains enzymes for oxidative reactions involved in the citric acid cycle and fatty acid oxidation [456].

1.5.3 Mitochondrial Biogenesis

The PGC-1 coactivators - PGC-1α and PGC-1β - have various biological activities, most of which have been linked to oxidative metabolism in tissues such as the heart and skeletal muscle [457-460]. When overexpressed in skeletal muscle, both PGC-1α and PGC-1β induce mitochondrial biogenesis, whereas in their absence there is abnormal skeletal muscle energetics and a reduced endurance capacity [460-462]. PGC-1 coactivators interact with the peroxisome proliferator-activated receptors (PPARs); a family of nuclear receptors that regulate gene expression in response to ligand-binding [463, 464]. To date, three PPARs have been identified [465-469]: 1) PPAR-α - regulates fatty acid metabolism and is primarily expressed in tissues with elevated mitochondrial fatty β-oxidation rates such as heart and skeletal muscle [463, 465, 470]; 2) PPAR-γ - is expressed largely in white and brown adipose tissue where it regulates the number and size of adipocytes as well as lipid metabolism [471]; and 3) PPAR-δ - is expressed in highly metabolic tissues such as liver, heart and skeletal muscle [472, 473] and treatment of rodents with synthetic PPAR-δ agonists increases the expression of genes involved in fatty β-oxidation oxidation, mitochondrial respiration and oxidative metabolism [474, 475]. Induction of PPARs using synthetic agonists, such as the pan-PPAR agonist bezafibrate, stimulates mitochondrial biogenesis in skeletal muscle and OXPHOS capacity was shown to be enhanced *in vitro* and *in vivo* [476-479].

1.5.4 Glycolysis

Glycolysis, which occurs in the cytosol and does not require O_2, produces ATP faster but less efficiently than OXPHOS by converting glucose into two molecules of ATP and two molecules each of pyruvate and NADH [480]. Under aerobic conditions, pyruvate and NADH are shuttled and used in the mitochondria to generate more ATP [40, 480-483].

In normal cells, glycolysis is greatly inhibited by O_2, a phenomenon termed the *Pasteur effect* [484]. As noted previously, under aerobic conditions, pyruvate (in the form of acetyl-CoA) is oxidized in the mitochondria by the citric acid cycle (CAC) [40, 483]. Under anaerobic conditions, pyruvate is converted to lactate by lactate dehydrogenase (LDH) and the lactate diffuses out of the cell and is transported to highly aerobic tissues such as cardiac muscle and liver [40, 483, 485]. By converting pyruvate to lactate, regeneration of NAD^+ from NADH can occur, and thus, allowing glycolysis and ATP production to continue [40, 483]. Notably, not all the carbon entering the pathway is converted to pyruvate since intermediate compounds are also shuttled to anabolic pathways [483].

1.5.5 Citric Acid Cycle

Pyruvate generated during glycolysis is transported from the cytosol to mitochondria where it is decarboxylated to acetyl-CoA by the pyruvate dehydrogenase complex, yielding one molecule of NADH in the process [40, 483, 486, 487]. Acetyl-CoA then enters the eight-step CAC, which generates three NADH and one $FADH_2$ [40, 483, 486]. Therefore, the net products of the CAC from one molecule of glucose (two molecules of pyruvate) are: eight NADH, two $FADH_2$ and two ATP (the reduced substrates yield 30 molecules of ATP per glucose) [40, 483, 486].

1.5.6 Oxidative Phosphorylation

Under aerobic conditions, cells generate ATP primarily through OXPHOS [40, 483, 488-490]. The OXPHOS system, which is embedded in the IMM, consists of two electron acceptors - coenzyme Q and cytochrome c - and five multi-subunit protein

complexes (complexes I-V) [40, 483, 488-490]. The passage of electrons, donated from reduced substrates such as NADH and $FADH_2$, between these complexes releases energy stored in the form of a proton gradient across the membrane [40, 483, 488-490]. Three of these complexes pump protons across the membrane creating a transmembrane electrochemical potential, and in the presence of ADP, protons flow from the intermembrane space back into the mitochondrial matrix. This process is facilitated by a proton carrier known as ATP synthase which is coupled to ATP synthesis as it pumps protons back into the mitochondrial matrix [40, 483, 488-490]. The last electron acceptor is O_2, which is reduced to H_2O [40, 483, 488-490].

1.5.7 Cancer Cell Metabolism

In the 1920s Otto Warburg discovered that in contrast to most normal tissues, tumors use glycolysis as the major form of ATP production even in the presence of oxygen [484, 491-494]. This phenomenon has become known as aerobic glycolysis or the *Warburg effect* [484, 491]. The underlying mechanism by which this metabolic alteration evolves during tumorigenesis is emerging. These mechanisms include mitochondrial malfunction and defects, oncogenic signaling, abnormal expression of metabolic enzymes and adaptation to hypoxic tumor microenvironment [495, 496]. The advantages of aerobic glycolysis to tumor cells is three-fold: 1) as tumors grow and oxygen becomes limiting, tumor cell survival is extended since anaerobic glycolysis can proceed; 2) glycolysis and the related pentose phosphate pathway are sources of precursors required for the biosynthesis of nucleic acids, phospholipids and FAs; and 3) lactate acidifies the tumor environment, which is destructive to normal cells. This may also protect tumor cells

from the immune system as well as destroy nearby cells and matrix, allowing tumor cells to invade distant sites [483, 484, 491, 497-499].

One well-characterized response to aerobic glycolysis is the stabilization of the hypoxia-inducible factor (HIF) transcription factor [497, 498, 500]. Under normal oxygen tension, HIF is targeted for proteosomal degradation by the sequential action of oxygen-dependent prolyl hydroxylases and the Von Hippel-Lindau (VHL) tumor suppressor, an E3 ubiquitin ligase [501-504]. HIF is stabilized not only under hypoxic stress but also by oncogenic and metabolic stress [496, 505, 506] whereby it coordinates a transcriptional program that shifts metabolism towards glycolysis by inducing glycolytic enzyme genes [497-499, 507]. Furthermore, numerous HIF-independent oncogenic events - such as activation of *RAS*, *MYC*, *AKT* and loss of *P53* - have been linked to metabolic reprogramming [508-515].

Recent work has shown that tumor growth is dependent on aerobic glycolysis. For example, knock-down of the NADH-dependent enzyme *lactate dehydrogenase A* (LDH-A), which catalyzes the conversion of pyruvate to lactate, restricted the growth of tumor cells under hypoxic conditions [516]. In another study, it was shown that many tumor types express the M2 splice isoform of pyruvate kinase, which is necessary for the shift in metabolism to aerobic glycolysis, and that shifting M2 to M1 expression suppressed tumor growth [517]. These studies suggest that the glycolytic-shift, even in the presence of a functional OXPHOS system, may be required to support tumor cell growth, especially under oxygen-limited conditions.

1.6 SYNOPSIS

It is commonly thought that the Rb tumor suppressor protein influences terminal differentiation by inhibiting cell cycle progression and apoptosis while actively stimulating tissue-specific transcription factors. For example, during skeletal muscle differentiation, pRb was shown to interact with and enhance the activity of MyoD, myogenin and Mef2c. However, since $Rb^{-/-}$ mice die by E14.5, which precludes studies of muscle development, many investigators have relied on MyoD-converted $Rb^{-/-}$ fibroblasts as a surrogate for $Rb^{-/-}$ myoblasts; which may be more prone to inconsistencies. Furthermore, pRb and the other Rb family members, p107 and p130, play overlapping and unique functions during development, but their contributions to skeletal muscle differentiation remain ill-defined. The **first objective** of this thesis was to investigate the role of pRb during skeletal myogenesis in a cell autonomous manner. This was accomplished using $Rb^{-/-}$ myoblasts derived from E16.5 partially rescued mgRb:Rb-/- fetuses. By uncoupling differentiation from cell cycle exit and survival, analyses in chapter 3 demonstrate that pRb is not required for differentiation *per se*, but to enforce cell cycle exit and promote survival of the differentiated state. The **second objective** of this work was to determine the contributions of p107 and p130 to the skeletal muscle differentiation defect observed in the absence of Rb. This was done using myoblasts with mutations in Rb alone or combined inactivation of Rb:p107, Rb:p130 and Rb:p107:p130. Data from chapter 4 reveal that Rb plays a unique function in maintaining myotube survival and cell cycle exit of differentiated muscle whereas p107 and p130 help suppress myoblast cell death during the early stages of differentiation. Further, combined inactivation of three Rb family proteins severely compromised myoblast fusion and led to polyploid myocytes.

Table 1. 1. Modes of cellular death

Cell Death Mode	Features
Apoptosis	• Intact plasma membrane • Rounding-up of the cell • Reduction of cellular and nuclear volume (pyknosis) • Retraction of pseudopodes • Nuclear fragmentation (karyorrhexis) • Plasma membrane blebbing • Engulfed by resident phagocytes • Bioenergetic dependent
Autophagy	• Intact plasma membrane • Lack of chromatin condensation • Massive vacuolization of the cytoplasm • Accumulation of double-membraned autophagic vesicles • Little or no uptake by phagocytes • Bioenergetic dependent
Necrosis	• Rupture of the plasma membrane • Cytoplasmic swelling • Swelling of cytoplasmic organelles • Moderate chromatin condensation • Bioenergetic independent

Adapted from Kroemer et al. Cell Death and Differentiation, (2009) 16, 3-11

Figure 1. 1. Schematic representation of Rb family proteins

Schematic representing the mouse Rb family proteins. p107 and p130 are more highly related to each other than to pRb based on sequence homology and their shared cyclin binding and cdk inhibitory domains. Many of the phosphorylation sites in mouse Rb family proteins are predicted by similarity based on human Rb family protein data. Phosphorylation sites are represented by ↑. Human Rb has an additional 7 amino acids for a total size of 928aa and is 91% identical to mouse Rb. Human p107 is 1068aa in length. Human p130 is 1139aa in length. Regions known to bind other proteins are indicated [117, 118, 120, 121, 518].

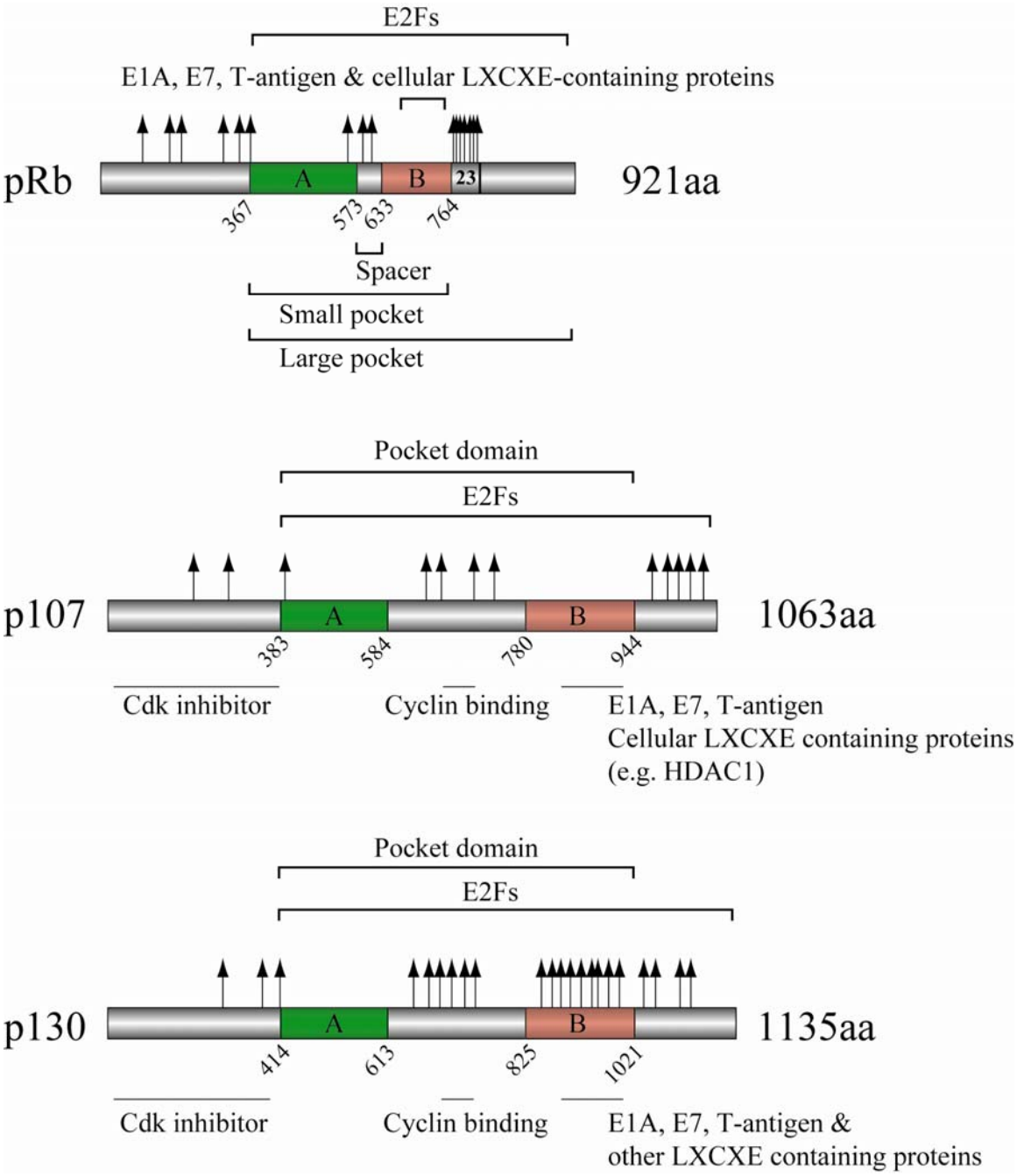
E2Fs
E1A, E7, T-antigen & cellular LXCXE-containing proteins
pRb
A
B
23
921aa
367
573
633
764
Spacer
Small pocket
Large pocket
Pocket domain
E2Fs
p107
A
B
1063aa
383
584
780
944
Cdk inhibitor
Cyclin binding
E1A, E7, T-antigen
Cellular LXCXE containing proteins
(e.g. HDAC1)
Pocket domain
E2Fs
p130
A
B
1135aa
414
613
825
1021
Cdk inhibitor
Cyclin binding
E1A, E7, T-antigen &
other LXCXE containing proteins

Figure 1. 2. The embryonic origin of limb and trunk skeletal muscles

(A) Vertebrate myogenesis initiates from the paraxial mesoderm, which segments into blocks of epithelial cells known as somites. In response to Shh and Wnt signals from the notochord and neural tube, somites delaminate to form the sclerotome and dermomyotome. **(B)** The dermomyotome is further subdivided into hypaxial and epaxial regions, which migrate to form the hypaxial and epaxial myotome. Pax3-positive cells from the hypaxial lips of the myotome delaminate and migrate to distant regions, such as the limb buds, for muscle development. The epaxial myotome will eventually form the musculature of the trunk and back muscles. Figure courtesy of Dr. Andrew T. Ho.

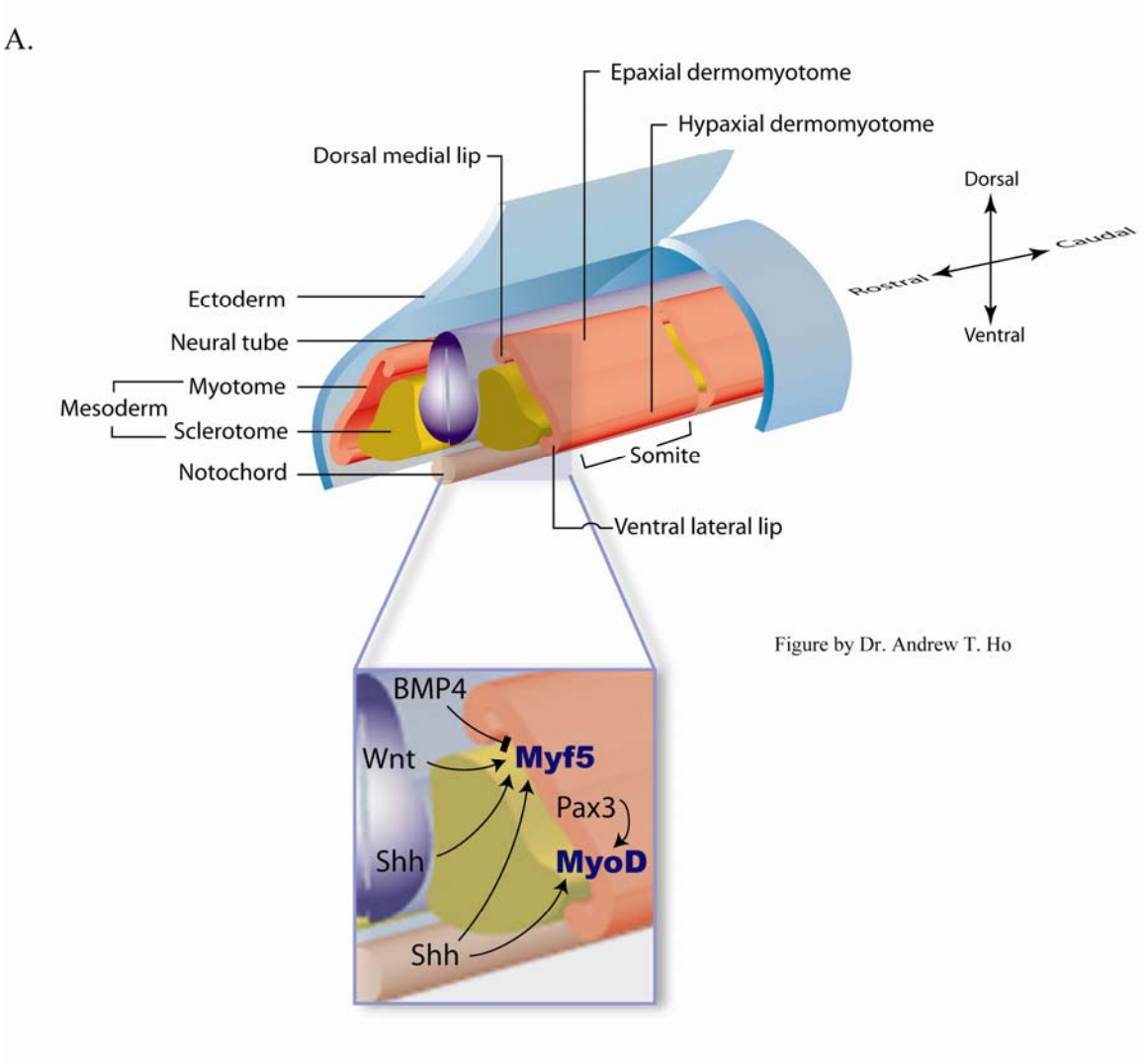

Figure by Dr. Andrew T. Ho

B.

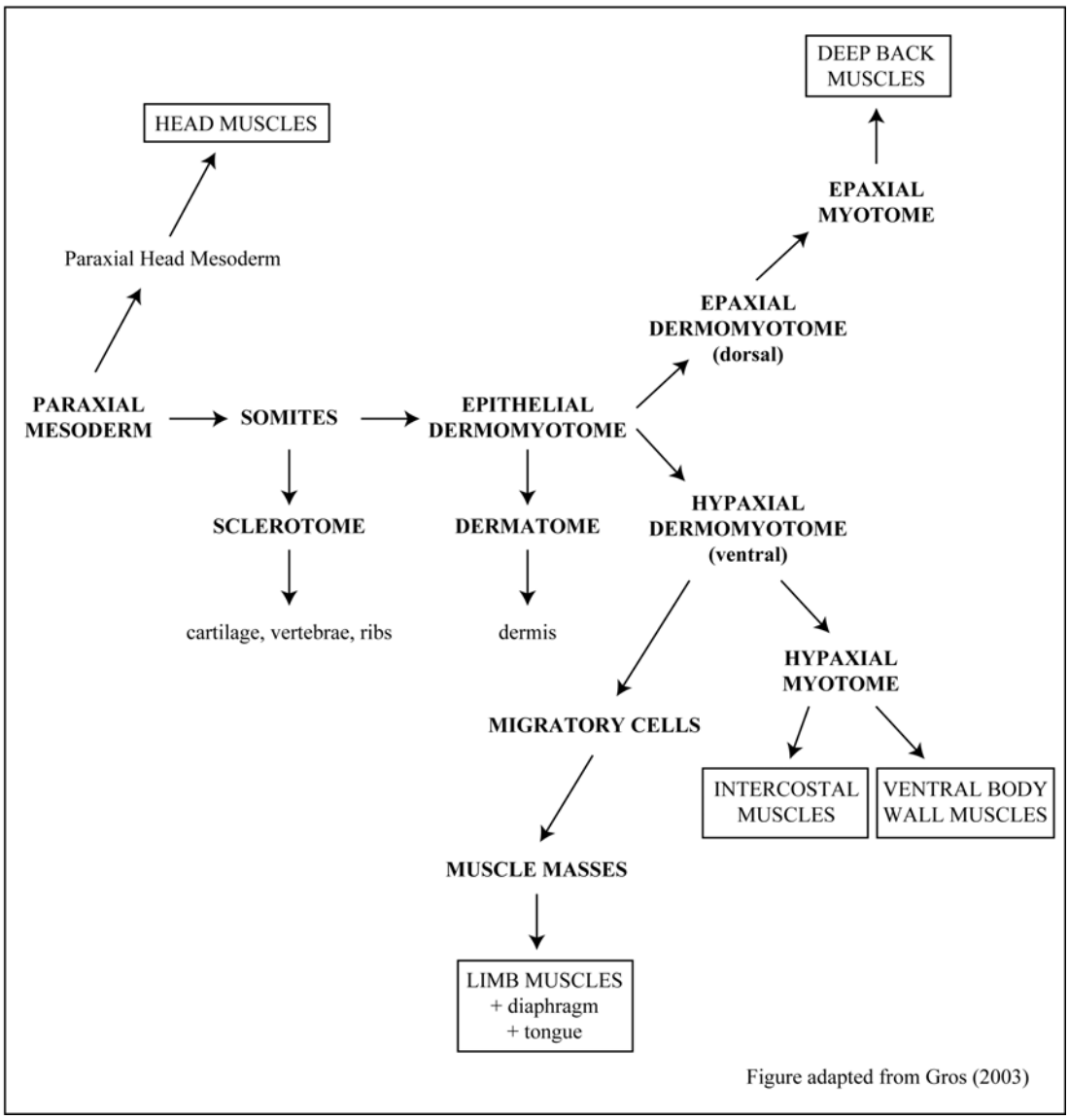
DEEP BACK MUSCLES
HEAD MUSCLES
EPAXIAL MYOTOME
Paraxial Head Mesoderm
EPAXIAL DERMOMYOTOME (dorsal)
PARAXIAL MESODERM
SOMITES
EPITHELIAL DERMOMYOTOME
SCLEROTOME
DERMATOME
HYPAXIAL DERMOMYOTOME (ventral)
cartilage, vertebrae, ribs
dermis
HYPAXIAL MYOTOME
MIGRATORY CELLS
INTERCOSTAL MUSCLES
VENTRAL BODY WALL MUSCLES
MUSCLE MASSES
LIMB MUSCLES + diaphragm + tongue
Figure adapted from Gros (2003)

Figure 1. 3. Schematic model of autophagy

The beclin-1/Vps34 complex mediates nucleation of the phagophore membrane, sequestering cytosolic proteins, protein aggregates and organelles. This process can be blocked by Bcl-2 and 3-MA as indicated. Recruitment of Atg16-Atg5-Atg12 and Atg8-PE (LC3-II) together with Atg9 assist in phagophore elongation. Once vesicle formation is complete, referred to as an autophagosome, Atg proteins dissociate allowing for fusion to lysosomes forming autolysosomes. Cargo is degraded by lysosomal proteases and shuttled back to the cytosol for reutilization. Figure adapted from [363].

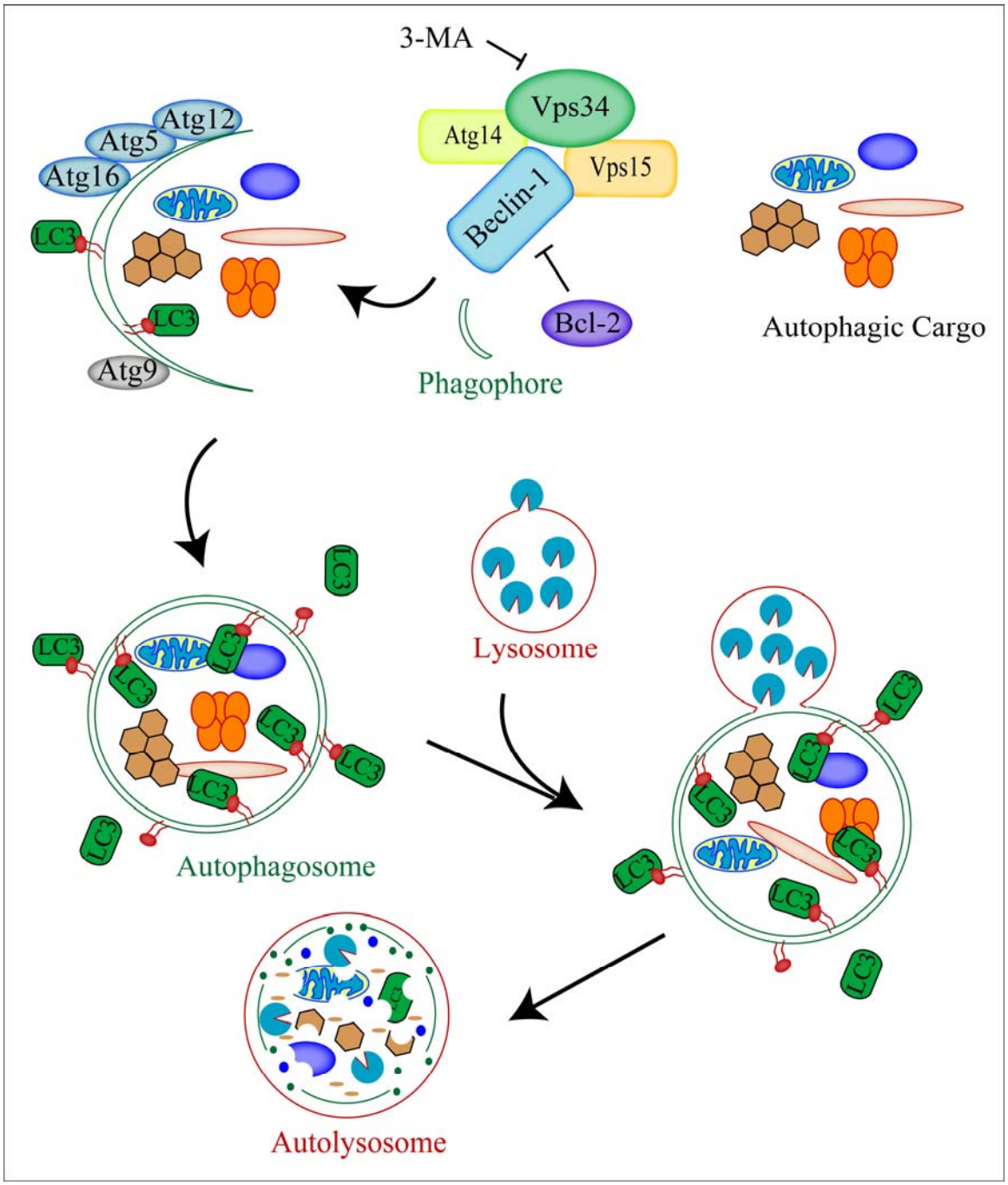
3-MA
Vps34
Atg14
Vps15
Beclin-1
Bcl-2
Atg12
Atg5
Atg16
LC3
Atg9
Phagophore
Autophagic Cargo
Lysosome
Autophagosome
Autolysosome

Figure 1. 4. Relationship between autophagy and apoptosis

Common stressors can induce either autophagy or apoptosis in a context-dependent manner. Whether autophagy or apoptosis leads to cell death may depend on cell-type sensitivity thresholds. Although autophagy is primarily regarded as an adaptive survival response, excessive autophagy can also lead to non-apoptotic cell death.

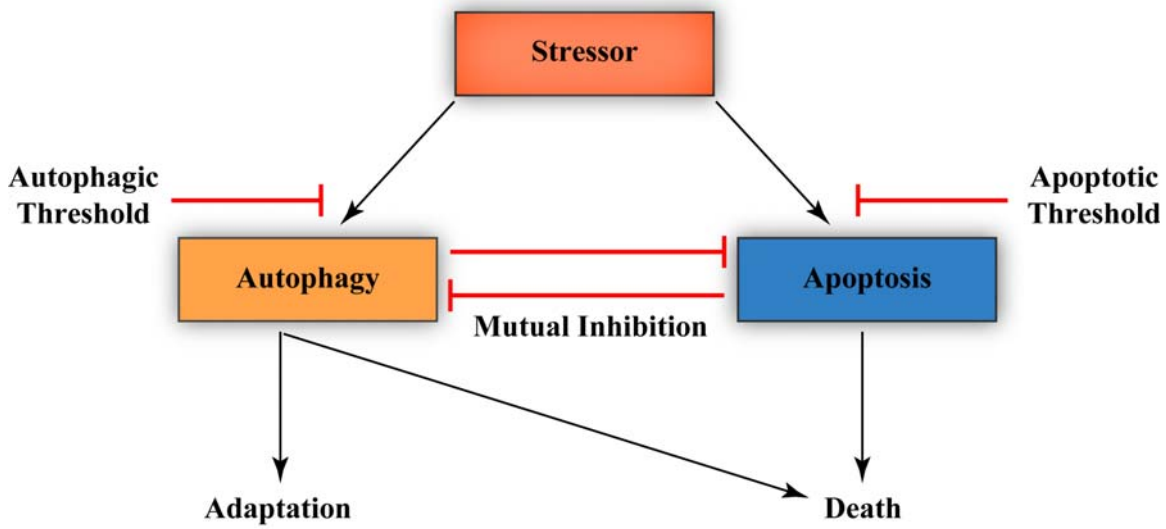

Adapted from *Maiuri et al.* Nat. Rev. Mol. Cell Biology 8 (September 2007)

CHAPTER 2: METHODS

2.1 Mouse maintenance, genotyping & timed-pregnancy

All experimental protocols were in accordance with the guidelines of the Animal Ethics Committee of the University Health Network (UHN), Toronto, Ontario. Mice were genotyped using DNA extracted from tail biopsies and the indicated primers (Table 1.2). Tails were treated overnight in DNA Lysis Buffer (0.1M Tris-HCl (pH 8.5), 5mM EDTA (pH 8.0), 0.2% SDS, 200mM NaCl) containing proteinase K (400 mg/ml) at 55°C. DNA was extracted once with phenol:chloroform (1:1) by shaking for 1hr followed by centrifugation at room temperature for 10min. DNA was then isopropanol precipitated, washed once with 70% ethanol and resuspended in 50µl ddH_2O. PCR reactions were conducted using 2.5µl DNA, 1x PCR buffer (100mM Tris-HCl (pH 8.3), 500mM KCl), 0.2mM dNTPs, 0.1mg/ml gelatin and 0.5µM of each primer in 50µl reactions made to volume with ddH_2O. PCR cycling conditions included 30 cycles of 50sec each at 94°C, 58°C, and 72°C. For timed-pregnancies, mice were mated overnight and the observation of a vaginal plug on the next morning was considered E0.5. On the day of harvest, pregnant females were sacrificed and embryos removed from the womb by dissection.

Table 1. 2 Genotyping primer sequences

Allele	**Forward (5' → 3')**	**Reverse (5' → 3')**
mgRb:Rblox	(EZ99) ATTTCAGAAGGTCTGCCAAC	(EZ163) AGAGCAGGCCAAAAGCCAGGA
Rb mutant	(EZ118) AATTGCGGCCGCATCTGCATCTTTATCGC	(EZ119) GAAGAACGAGATCAGCAG
Rb wt	(EZ118) AATTGCGGCCGCATCTGCATCTTTATCGC	(EZ162) CCCATGTTCGGTCCCTAG
p130 mutant	(EZ225) ACGGATGTCAGTGTCACG	(EZ226) GAAGAACGAGATCAGCAG
p130 wt	(EZ225) ACGGATGTCAGTGTCACG	(EZ227) TACATGGTTTCCTTCAGCGG
p107 mutant	(EZ402) TCGTGAGCGGATAGAAAG	(EZ403) CCGCTTCCATTGCTCAGCGG
p107 wt	(EZ402) TCGTGAGCGGATAGAAAG	(EZ401) GTGTCCAGCAGAAGTTA
Rb^{floxed}	(EZ404) GGCGTGTGCCATCAATG	(EZ405) CTCAAGAGCTCAGACTCATGG

2.2 Isolation of myoblasts and cell culture

Primary mouse embryonic myoblasts (MEMs) were derived from the skeletal muscle of the four limbs from E.16.5 – E.17.5 embryos. After decapitating embryos, limbs were removed with scissors and the muscle was separated from the skin and bone under a dissecting microscope. The muscle tissue was digested for 20min at 37°C in 80µl of a solution containing 1.5 U/ml collagenase IV (Sigma), 2.4U/ml Dispase (Roche) and 5mM $CaCl_2$. Once during this incubation, the tissue was gently triturated using a glass pasteur pipette to break apart large chunks of muscle tissue. After the 20min incubation, the tissue was again triturated & plated onto a 60mm collagen-I coated culture dish. Primary myoblasts were maintained in Growth Medium (GM) consisting of HAM's-F10 (Sigma) supplemented with 20% FBS (PAA) and 2.5ng/ml basic fibroblast growth factor (bFgf) (Sigma) in a humidified incubator at 5.5% CO_2 and 37°C. To induce myoblast differentiation, cells were rinsed once in 1x Phosphate Buffered Saline (PBS) and fed with Differentiation Medium (DM) - consisting of Dulbecco's modified Eagle's medium (DMEM, high-glucose and sodium pyruvate) (Sigma) supplemented with 3% Horse Serum (PAA). To maintain consistency between experiments, primary myoblasts were cultured in high growth-factor medium and induced to differentiate at passage two by shifting confluent cultures to low serum differentiation media (DM). Over 1000 independent myoblast cultures were isolated and analyzed for these studies. All other cell-types were maintained in DMEM supplemented with 10% FBS and Penicillin/Streptomycin (Sigma).

2.3 Drug treatments

Drugs were added to myoblasts when medium was changed from GM to DM. Bezafibrate (500μM) and minocycline (200μM) were refreshed every other day. 3-MA (5mM) and LiCl (5mM) were not refreshed. Chloroquine (10μM) was added for 24hr before harvesting protein lysate. Aphidicolin was used at 2.5μg/ml.

2.4 Hypoxia

Myoblasts were induced to differentiate with DM and cultures were immediately transferred to hypoxic conditions (1% O_2, 5% CO_2 and 37°C) (HERA Cell 150 – Kendro Laboratory Products). Lonidamine (Sigma) was added to DM-1 cultures at a concentration of 50μM and refreshed every other day.

2.5 BrdU DNA synthesis assay

DM-1 myotube cultures were restimulated in GM or maintained in DM supplemented with 20μM BrdU for 16h before fixation with 3.7% formaldehyde (10min). For BrdU/aphidicolin experiments, 2.5μg/ml aphidicolin was added to cultures 5hrs before addition of BrdU for 16hr. For Myosin/BrdU double immunostaining, cultures were permeabilized using 0.3% Triton X-100 for 10min and treated with 2N HCl for 25min. This was followed by two neutralization washes with 0.5M sodium borate, pH 8.5 for 5min. The cells were then blocked in 1.0% BSA for 20min and incubated with the primary anti-MHC antibody; 1:50 (Sigma) for 1hr, followed by three washes of three minutes each with PBS. MHC was detected using a fluorescein-conjugated secondary antibody (Alexa Fluor 563 - Invitrogen). BrdU was detected using an anti-BrdU antibody directly conjugated to FITC (BD Biosciences) (as per manufacturer's suggested protocol, 20μl anti-BrdU was added to 50μl of 0.5% Tween 20/PBS per 22mm coverslip). Nuclei were counterstained with DAPI (Invitrogen) for 5min, followed by three washes of three

minutes each with PBS and mounted in fluorescent mounting media (Dako). Fluorescent images were viewed and captured using an Axioskop2 fluorescent microscope (Carl Zeiss Inc.) or a Zeiss LSM510 confocal microscope (Carl Zeiss Inc.). Confocal images were captured at room temperature using a 40x or 63x c-apochromat objective lens (water)/1.2NA using a Zeiss LSM510 META confocal microscope (Carl Zeiss Inc.) and Zeiss AIM 3.2 acquisition software. Adobe Photoshop CS2 was used to overlay images.

2.6 Immunofluorescence & Electron Microscopy

500,000 primary myoblasts were seeded on 22mm round Collagen-I coated coverslips (BD Biosciences) and induced to differentiate by changing GM to DM 24hr later. At this time, treatments were added to DM when required, and depending on the experiment – differentiated for the desired number of days. Cells were subsequently fixed with 3.7% formaldehyde, permeabilized with 0.3% Triton X-100 and blocked for 20min using 1% BSA in PBS at room temperature. The following primary antibodies were used to stain the cells for 1hr at room temperature: Bnip3, 1:50 (38621; Abcam); LC3, 1:50 (2775; Cell Signaling); myogenin, 1:10 (F5D; Santa Cruz); MHC, 1:50 (MY-32; Sigma); MCK, 1:50 (sc-15161; Santa Cruz); cyclin D3, 1:50 (clone c-16, Santa Cruz); cytochrome c, 1:50 (clone A-8, Santa Cruz) and Rb (14001A, BD Biosciences). Secondary antibodies were fluorescein-conjugated (Alexa Fluor 563 or Alexa Fluor 488 - Invitrogen) and incubated for 1hr to detect the primary antibody. Nuclei were counterstained with DAPI (Invitrogen) for 5min and mounted in fluorescent mounting media (Dako). Mitochondrial-LC3 (Red:Green) colocalization was conducted with Colocalization Plug-in for ImageJ (http://www.uhnres.utoronto.ca/facilities/wcif/imagej/colour_analysis.htm). Fluorescent images were viewed and captured as

described in previous section. For electron microscopy, myoblasts were grown and differentiated in 24-well plates and fixed at DM-2 using Karnovsky fixative (4% paraformaldehyde, 2.6% glutaraldehyde in 0.1M phosphate buffer, pH 7.2) for 30min at room temperature. Post-fixation epoxy embedding, extraction and counter-staining were performed by personnel at the electron microscopy facility at the University of Toronto. Electron micrographs were captured at 80kV using a Hitachi H-7000 transmission electron microscope equipped with an AMT digital camera (Hitachi). Image contrast and clarity were enhanced using Adobe Photoshop CS2.

2.7 Embryo Histology and Immunofluorescence

Embryos were fixed in 4% paraformaldehyde at 4°C overnight. Next day, embryos were washed in PBS for 30min, dehydrated sequentially to 100% ethanol, paraffin embedded and sectioned at 5µm. Sections were then rehydrated sequentially to PBS. Antigen retrieval was performed by immersing sections in boiling sodium citrate buffer (0.21% w/v) for 10min. Slides were cooled to room temperature and washed with PBS and blocked with 1% BSA/PBS. Sections were stained for immunofluorescence and captured as described in the immunofluorescence section.

2.8 Western Blot Analysis

Cells were lysed on ice in K4IP buffer (50 mM HEPES, pH 7.5, 0.1% Tween-20, 1mM EDTA, 2.5mM EGTA, 150 mM NaCl, 1.0mM DTT, 10% Glycerol) containing protease inhibitors (Sigma). Lysates were incubated on ice for 30min followed by centrifugation at 4°C for 25min at max speed to remove cellular debris. The extracts were normalized for protein concentration using the BioRad protein dye. 30µg - 50µg of lysate was resolved using sodium dodecyl sulfate-polyacrylamide gel electrophoresis (SDS-PAGE)

and transferred to a nitrocellulose membrane at 45V overnight at 4°C. After transfer, membranes were blocked in 5% non-fat dry milk (1x PBS, 0.1% Tween-20) for 1.5hr at room temperature on a rotating platform. Subsequently, the following antibodies were used to probe the blots for 3hr at room temperature or overnight at 4°C: α/β-tubulin, 1:4000 (Cell Signaling); MHC, 1:200 (MY-32; Sigma); LC3, 1:500 (2775; Cell Signaling); MCK, 1:200 (sc-15161; Santa Cruz), Rb, 1:1000 (14001A; BD Biosciences); Troponin T-FS, 1:200 (clone c-18; Santa Cruz); PARP, 1:500 (9542; Cell Signaling); cleaved caspase-3, 1:500 (9661L; Cell Signaling); Bcl-2 (14-6700-81; eBioscience); p107 (SD9; Santa Cruz); p130 (c-20; Santa Cruz); Xiap (gift from Dr. Robert G. Korneluk). Membranes were subsequently washed three times for 5min each in immunoblot buffer (1x PBS, 0.1% Tween-20) and incubated with secondary HRP-linked anti-IgG, 1:2000 (Cell Signaling) for 1.5hr in blocking buffer. The membrane was washed three times for 5min each, and HRP activity was detected using SuperSignal West Dura chemiluminescent substrate (Pierce) and captured using X-ray film. Films were digitized using a Canon scanner and images processed using Adobe Photoshop CS2. Quantification of western blots was conducted using Dr. Luke Miller's method fully outlined here: www.lukemiller.org/journal/2007/08/quantifying-western-blots-without.html. For LC3 quantification, the ratio of LC3-II to tubulin was calculated for each sample. Control samples were arbitrarily set to 1. Rb-deficient samples were plotted relative to control and expressed as fold-change. All Statistical analyses were conducted using Microsoft Excel's Analysis ToolPak.

2.9 Mitochondrial and Nuclear DNA Quantitative PCR

mtDNA copy number was quantified using the abundance of an 80bp fragment of the mouse mitochondrial genome (Forward Primer 5'- GCAAATCCATATTCATCCTTCTCAAC-3' and Reverse Primer 5' – GAGAGATTTTATGGGTGTAATGCGGTG-3') relative to the NADH dehydrogenase (ubiquinone) flavoprotein 1 (NDUFV1) single copy nuclear gene (GenBank accession # NM_133666) (Forward Primer 5'- CTTCCCCACTGGCCTCAAG-3' and Reverse Primer 5' - CCAAAACCCAGTGATCCAGC-3'). DNA from skeletal muscle tissue (from four limbs of E.16.5 – E.17.5 embryos) or cells was extracted using phenol:chloroform (see Total DNA isolation protocol). Quantification of the 80bp fragment and NDUFV1 copy number was assessed using quantitative PCR (Applied Biosystems – 7900T lightcycler). The qPCR reaction contained 5µl DNA (40ng/ml), 0.25µl sense primer (100µM), 0.25µl antisense primer (100µM), 12.5µl Sybr Green 2x Mix (Applied Biosystems) and sterile distilled water to 25µl. Cycling parameters were as follows: Reaction was heated at 50°C for 2min, followed by denaturation at 95°C for 10min. Amplification was carried out for 40 cycles of PCR using an annealing temperature of 60°C for 1min and extension temperature of 72°C for 15sec. Product melt analysis was conducted at the end of each reaction to characterize the amplified product(s). Results were acquired using the SDS 2.0 software (Applied Biosystems) and exported to Microsoft Excel where statistical analyses were performed. The change in the 80bp fragment/NDUFV1 ratio between mgRb:$Rb^{-/-}$ and control represents fold-change in mtDNA copy number.

2.10 ATP Assay

ATP quantification was conducted using the ATPlite™ Luminescence Detection System (6016943; Perkin Elmer) according to the manufacturer's suggested protocol. Briefly,

ATP assay from skeletal muscle tissue was performed using the four limbs from E.16.5 – E.17.5 embryos. After decapitating embryos, limbs were removed with scissors and the muscle was separated from the skin and bone under a dissecting microscope. Tissue was then snap-frozen in liquid nitrogen. When all samples were collected, tissue was thawed on ice, weighed and resuspended in 200µl ice-cold PBS. Immediately following, 100µl of mammalian cell lysis solution was added to each sample. Samples were shaken for 10min using an orbital shaker at 900rpm and then lysed completely by dounce homogenization. Subsequently, 100µl fresh substrate solution was added to each sample and shaken for 10min at 700rpm using an orbital shaker. For ATP assay from DM-2 cultures, myoblasts were differentiated in 100µl DM for the indicated number of days in wells of a 96-well microplate. On the day of harvest, 50µl of mammalian cell lysis solution was added to the 100µl of DM. Microplate was shaken for 5 min on an orbital shaker at 700rpm. Subsequently, 50µl substrate solution was added to the wells and shaken again for 5 min at 700rpm on an orbital shaker. For both *in vivo* and *in vitro* assays, final volume from each sample was divided into two and transferred to a white OptiPlate-96 (96-well) (Perkin Elmer) and dark adapted for ten minutes. Luminescence was measured using a Victor X3 Multilabel Plate Reader (Perkin Elmer) and the data exported to Microsoft Excel for analysis.

2.11Mitotracker® Red CMXRos Assay

To detect mitochondria with intact membrane potential, DM-2 myotube cultures grown on 22mm round collagen-I coated coverslips (BD Biosciences) were incubated in DM containing Mitotracker® Red CMXRos (400nM) according to manufacturer's protocol (M7512; Invitrogen) for 1hr at 37°C and 5% CO_2. Subsequently, cells were washed

twice in DM for 5min each at 37°C and 5% CO_2. Cells were fixed in 3.7% formaldehyde for 10min at room temperature in the dark. Fixed cells were then rinsed three times in PBS and mounted in fluorescent mounting medium (DAKO). Images were viewed and captured as previously described in immunofluorescence section.

2.12 TUNEL Assay

500,000 primary myoblasts were grown and differentiated for 2 days on 22mm round collagen-I coated coverslips (BD Biosciences). Cells were fixed at room temperature using 3.7% formaldehyde for 10min, washed three times in PBS, permeabilized with 0.3% Triton X-100 solution and washed again three times in PBS. Subsequently, 30U Terminal Deoxynucleotidyl Transferase (TdT) (EP0161; Fermentas) was added to 50µl TUNEL-Label Solution (11767291910; Roche). The solution was mixed to equilibrate the components and added to the cells. Samples were incubated 1hr at room-temperature in a humidified chamber in the dark. After the 1hr incubation, samples were rinsed three times in PBS and subsequently (when indicated), stained with anti-MHC (MY-32; Sigma) for 1hr at room temperature, followed by fluorescein-conjugated secondary antibodies for 1hr. Nuclei were counterstained with DAPI (Invitrogen) for 10min and mounted in fluorescent mounting media (Dako). Images were viewed and captured as previously described in immunofluorescence section. TUNEL positive nuclei were detected in the range of 515 – 565nm (green).

2.13 Adenovirus-cre Transductions

For adenovirus-cre (Ad.cre) (1045, Vector Biolabs) and Ad.EV transduction of $Rb^{f/f}$ primary myoblasts, 50,000 cells were seeded in collagen-I coated wells of a 96-well plate and transduced - approximately 8hrs after seeding the cells - using 50µl of GM

containing 1250 multiplicity of infection (MOI) of the respective adenovirus for 16hr. After this incubation, adenovirus containing medium was replaced with fresh GM and the cells were subsequently induced to differentiate by changing GM to DM after another 24hrs. When required, 5mM Lithium Chloride was added to the DM at this point. For hypoxia experiments, cells were transferred to a hypoxia incubator when medium was switched from GM to DM. Myotubes were counted DM-2 and/or DM-5. For immunofluorescence studies, $Rb^{f/f}$ primary myoblasts were seeded at 350,000 cells on 22mm round collagen-I coated coverslips (BD Biosciences) and subsequent steps were as above. The following adenoviruses were graciously provided by: Marco Crescenzi - Ad.Bcl-2 - Dept. of Environment and Primary Prevention, Higher Institute of Health, Viale Regina Elena 299, 00161 Roma, Italy; Aviva M. Tolkovsky - Ad. GFP-LC3 and Ad.RFP-LC3 - Dept Biochemistry, University of Cambridge, Building 0, The Downing Site, Cambridge, CB2 1QW, UK; Karen A. Vincent - Ad. Hif-1α/NFκB and Ad.EV - Genzyme Corporation, 31 New York Ave, P.O. Box 9322, Framingham, MA 01701-9322; Michael Ohh – Ad.VHL-T7-HPACGV - University of Toronto, Medical Sciences Bldg, Rm 6306, 1 King's College Circle, Toronto, Ontario, M5S 1A8; Thomas Force – Ad.β-catenin and Ad.β-cateninΔ - Center for Translational Medicine, Jefferson Medical College, Philadelphia, Pennsylvania; David Murphy -$Ad.Vps34^{DN}$ - Dorothy Hodgkin Building, Whitson Street, Bristol,BS1 3NY; Christopher J. Rhodes – Ad.mTOR, Ad.KD.mTOR and Ad.ca.mTOR - The University of Chicago, KCBD 8130, 900 East 57th Street, Chicago, Illinois 60637; Kenneth Walsh - Ad.FOXO3a and Ad.DN.FOXO3a - Whitaker Cardiovascular Institute, Boston University School of Medicine, Boston, Massachusetts 02118; David S. Park – $Ad.Rb^{\Delta K11}$and Ad.p27 - Department of Cellular

and Molecular Medicine, University of Ottawa, Ottawa, Ontario, Canada K1H 8M5; Robert G. Korneluk - Ad.Xiap - Department of Biochemistry, Microbiology and Immunology, University of Ottawa, 401 Smyth Road, Ottawa, Ontario, K1H 8L1, Canada.

2.14 Brightfield Images and Videos

Brightfield images and videos were captured at room temperature using 20x or 40x air-objective lenses on a Nikon TE200 microscope (Nikon) fitted with a Hamamatsu CCD digital camera. Images were acquired using SimplePCI imaging software (Hamamatsu). Adobe Photoshop CS2 was used to enhance clarity and contrast using same parameters for control and experimental samples.

CHAPTER 3: RESCUE OF MYOGENIC DEFECTS IN RB-DEFICIENT CELLS BY INHIBITION OF AUTOPHAGY OR BY HYPOXIA-INDUCED GLYCOLYTIC SHIFT

Results presented in this chapter (with the exception of some figure panels) have been published:

Ciavarra G and Zacksenhaus E (2010). Rescue of myogenic defects in Rb-deficient cells by inhibition of autophagy or by hypoxia-induced glycolytic shift. *The Journal of Cell Biology*. 2010. Oct 18;191(2):291-301.

3.1 Abstract

The retinoblastoma tumor suppressor (pRb) is thought to orchestrate terminal differentiation by inhibiting cell proliferation and apoptosis and stimulating lineage specific transcription factors. Here it is shown that in the absence of pRb, differentiating primary myoblasts fused to form short myotubes that never twitched and degenerated via a non-apoptotic mechanism. The shortened myotubes exhibited an impaired mitochondrial network, mitochondrial perinuclear aggregation, autophagic degradation and reduced ATP production. Bcl-2 and autophagy inhibitors restored mitochondrial function and rescued muscle degeneration, leading to formation of long, twitching myotubes that expressed normal levels of muscle-specific proteins and stably exited the cell cycle. A hypoxia-induced glycolytic switch also rescued the myogenic defect after either chronic or acute inactivation of Rb in a HIF-1-dependent manner. These results demonstrate that pRb is required to inhibit apoptosis in myoblasts and autophagy in myotubes but not to activate the differentiation program, and reveal a novel link between pRb and cell metabolism.

3.2 Introduction

The retinoblastoma tumor suppressor is lost by mutation or functional inactivation in virtually all human cancer [519, 520]. Its disruption leads to ectopic cell proliferation, apoptotic cell death and incomplete differentiation, and may cause cancer in many cell types [93, 133, 138, 521]. Rb exerts these effects by modulating the activity of transcription factors such as activating E2Fs [8]. These E2Fs activate cell cycle progression and DNA synthesis genes as well as pro-apoptotic, BH3-only factors that induce mitochondrial outer membrane permeabilization (MOMP) and trigger the intrinsic

apoptotic machinery [92, 522]. Activating E2Fs also induce p53 via ARF, various apoptogenic factors as well as autophagic genes [91, 359, 360, 429, 430]. pRb is also thought to stimulate lineage specific transcription factors including MyoD, myogenin and MEF2C [102, 103, 149], and sequester inhibitors of differentiation such as Id2, HDAC1, EID-1 and RBP2 [140, 325, 329, 330]. However, given that ectopic proliferation and apoptosis precludes differentiation, the exact role for pRb in differentiation remains ill-defined. Here, the function of Rb during myogenesis was addressed by uncoupling its effect on cell survival or proliferation from its effect on differentiation.

3.3 Rb-Deficiency During Myogenic Differentiation Induces Autophagy

To identify cell-autonomous functions of pRb during skeletal myogenesis, the differentiation of primary Rb-deficient myoblasts, isolated from limb muscles of E16.5 mgRb:$Rb^{-/-}$ fetuses, was analyzed. These mutant embryos harbor a mini-Rb gene (mgRb) that directs Rb expression to placenta and nervous system but not muscles, thereby extending the life span of $Rb^{-/-}$ embryos, which otherwise die at E13.5-14.5, to birth [93, 131]; Z. Jiang and EZ, unpublished). In mgRb:$Rb^{-/-}$ fetuses, myotubes are initially formed at E14.5-15.5, and express early muscle specific markers, but they continue to synthesize DNA, fail to express late muscle markers and degenerate [93, 95]. As expected, primary myoblasts derived from mgRb:$Rb^{-/-}$ limb muscles were devoid of pRb (Figure 3.1A).

When confluent cultures of control primary myoblasts were incubated in differentiation medium (DM), the cells spontaneously fused to form long multinucleated myotubes that started to twitch by day 3 - 4 and persisted for weeks in culture. Primary Rb-deficient myoblasts also fused to form short myotubes that contained 3 to 6 nuclei

that expressed near-normal levels of MHC (Figure 3. 1B). However, at day 3 post-differentiation, these short myotubes degenerated, and by day 6 virtually all had collapsed (Figure 3. 1B-C). Thus, Rb-deficient myoblasts underwent abortive differentiation *in vitro* that recapitulated defects seen in Rb mutant muscles *in vivo* [93, 95].

Cleaved (activated) caspase 3 and cleaved PARP, markers of intrinsic apoptosis, were elevated in differentiating Rb-deficient cultures relative to control (Figure 3. 1E). However, terminal deoxynucleotidyl transferase biotin-dUTP nick end labeling (TUNEL) positive nuclei were only detected in unfused myoblasts but not within myotubes at 2 and 3 days post-differentiation (Figure 3. 1F and data not shown). Thus, I next asked whether degeneration of Rb-deficient myotubes was accompanied by autophagy, which, depending on the context, can lead to cell death or survival [523]. During autophagy, bulk cytoplasm, including whole organelles, is sequestered in vesicles termed autophagosomes that fuse to lysosomes (forming autolysosomes) for degradation [392, 524, 525]. Importantly, autophagy provides a homeostatic mechanism by which old and damaged mitochondria are destroyed [427]. To detect autophagy, myoblasts were transduced with an adenoviral vector expressing microtubule-associated protein 1A/1B-light chain 3 (LC3) fused to red-fluorescent protein (Ad.LC3-RFP) [526]. LC3 accumulates on autophagosomes as a phosphatidylethanolamine (PE)-conjugated form (LC3-II) and its level serves as a marker for autophagy [406]. At post-differentiation day 2, Ad.LC3 transduced control myotubes exhibited a diffuse red-fluorescent pattern, whereas in Rb-deficient myotubes, LC3 was detected in perinuclear aggregates (Figure 3. 2A), indicative of autophagosome accumulation.

Autophagosome-bound LC3-II migrates faster than unconjugated LC3-I through denaturing protein gels [406]. After 2 days in DM, LC3-II expression was greater than 2 fold higher in Rb-deficient myotube cultures relative to control (n=3; Figure 3. 2B). Chloroquine, an inhibitor of autophagosome-lysosome fusion, enhanced the level of LC3-II in both Rb-deficient and control cultures, demonstrating active autophagic flux. We also detected a 1.5 ± 0.12 (p=0.016) increase in LC3-II expression in skeletal muscle from limbs of E16.5 mgRb:$Rb^{-/-}$ embryos (n=3) relative to control littermates (n=3; Figure 3. 2C-D). Thus, autophagy is elevated in Rb-deficient skeletal muscle both *in vitro* and *in vivo*. In addition, immunostaining for BNip3, an E2F1 regulated BH3-only factor that can induce autophagy by sequestering Bcl-2 [432, 527], was elevated in Rb-deficient myotubes relative to control at day 2 post-differentiation (Figure 3. 2E). This result is consistent with a previous report of increased BNip3 expression in Rb null liver cells, which undergo non-apoptotic, autophagy-associated cell death [429]. To test if re-expression of pRb could suppress autophagy in Rb-deficient cells, myoblasts were transduced with adenovirus vector expressing constitutively active, phospho-mutant pRb ($Ad.Rb^{\Delta K11}$) [528] and induced to differentiate. As expected, expression of pRb prevented collapse of Rb-deficient myotubes (not shown), and concomitantly suppressed the accumulation of LC3-II by ~1.8-fold (n=7; p=0.005; Figure 3. 3A-B).

3.4 Rb Deficiency During Myogenic Differentiation Induces Mitochondrial Loss via Autophagy

To follow mitochondrial fate in Rb-deficient myotubes, we used MitoTracker®, a live-cell probe that accumulates in mitochondria with intact membrane potential. In control myotubes, MitoTracker® staining revealed a uniform, net-like distribution of

mitochondria throughout the cytoplasm (Figure 3.4A, top left). In contrast, at day 2 post-differentiation, Rb-deficient myotubes exhibited strong perinuclear MitoTracker®-positive aggregates and relatively faint cytosolic staining (Figure 3.4A, bottom left). On average, approximately 70% of Rb-deficient myotubes contained perinuclear aggregates compared to less than 10% in control myotubes ($p<0.001$; Figure 3.4B, white bars). Cytochrome c also exhibited differential staining: it was uniformly distributed throughout control myotubes but exhibited irregular punctate/perinuclear staining in Rb-deficient myotubes (Figure 3.4C). To determine whether mitochondria accumulated within autophagosomes in Rb-deficient myotubes, double staining with MitoTracker® and LC3 antibody in the presence of chloroquine was performed. Control myotubes contained very few cytoplasmic aggregates that stained positive for both MitoTracker® and LC3 (Figure 3.4D, left panel). In contrast, 70% of Rb-deficient myotubes exhibited large perinuclear aggregates that stained positive for both markers (Figure 3.4D, middle panel). The level of overlap between LC3 and MitoTracker® was 3.4-fold higher in the entire myotube population and 5-fold higher in the 70% fraction of Rb-deficient myotubes that exhibited perinuclear mitochondrial aggregation (Figure 3.4E). Notably, this level of autophagy is an underestimate, as MitoTracker® stains functional mitochondria only. Electron microscopy (EM) analysis revealed overall reduced mitochondrial content and 2.2-fold increase in perinuclear accumulation of mitochondria in the entire Rb-deficient myotube population relative to control (Figure 3.5A). Some whole or partially degraded mitochondria engulfed by membrane, representing autophagosomes and autolysosomes [392], were observed around the nuclei (Figure 3.5, middle panel (asterisk)) and cytosol (Figure 3.5B-C). Consistent with these results, there was a 20% reduction in

mitochondrial to nuclear DNA ratio, determined by quantitative real-time PCR [529], in Rb-deficient versus control myotube cultures at day 2 post-differentiation ($p<0.001$; Figure 3.6A), and a 50% reduction in E16.5 limb skeletal muscle ($p=0.009$; Figure 3.6B). Moreover, there was a 20% decrease in ATP level in Rb-deficient myotube cultures (not shown), and a 3.2-fold reduction in ATP level in E16.5 skeletal muscle tissue relative to control ($n=3$, $p=0.011$; Figure 3.6C). The observed difference between the *in vitro* and *in vivo* results most likely reflects the fact that *in vitro* cultures contain a smaller ratio of myotubes/unfused cells than skeletal muscle.

3.5 Inhibition of Autophagy Rescues Rb Differentiation Defect

The aforementioned results prompted us to ask whether inhibition of cell death or autophagy would rescue Rb-deficient myotube degeneration. Strikingly, adenovirus-mediated transduction of Bcl-2, a survival factor that inhibits both apoptosis and autophagy [400], efficiently rescued the differentiation defect, leading to long multinucleated myotubes that expressed myosin heavy chain (MHC) and muscle creatine kinase (MCK), and twitched like control myotubes for over 3 weeks in culture (Figure 3.7A-B; videos S1-2). Western blot analysis revealed that myogenin, MHC, MCK and Troponin T were undetectable in Rb-deficient cultures, but expressed at comparable levels in Ad.Bcl-2 transduced Rb-deficient myotubes and control (Figure 3.7C). To test whether specific inhibition of autophagy could rescue the defect, cultures were treated with 3-methyladenine (3-MA), an inhibitor of a class III phosphatidylinositol 3-kinase, Vps34, which is required for nucleation of the autophagic vesicle [363, 524]. Remarkably, a single dose of 3-MA given just prior to the induction of differentiation prevented formation of LC3 positive perinuclear aggregates and perinuclear

mitochondrial accumulation (Figure 3.4D and Figure 3.5A, right panels), and blocked the degeneration of Rb-deficient myotubes, leading to myotubes that twitched for weeks in culture (Figure 3.8A-B; videos S3-4). The number of myotubes formed was 3-fold lower after 3-MA treatment than after Bcl-2 transduction, but the extent of twitching was virtually the same (videos S2 & S4). This is consistent with the observation that Bcl-2 expression increased survival of both myoblasts and myotubes whereas 3-MA rescued myotube degeneration but increased apoptotic death of unfused myoblasts (not shown). The latter observation indicates that different survival pathways operate in myoblasts and myotubes, and importantly, Rb-deficient myotube degeneration is cell-autonomous and not an indirect consequence of high level of death in surrounding, unfused cells. Adenoviral-mediated transduction of a dominant negative Vps34 allele (Ad.Vps34^{dn}) [530], also rescued the Rb myogenic defect leading to twitching myotubes (Figure 3.8C). Collectively, these results indicate that degeneration of Rb-deficient myotubes is associated with autophagy of impaired mitochondria and that inhibition of this process rescues the Rb myogenic defect.

3.6 Rescued Rb-deficient Myonuclei Become Stably Post-mitotic

In addition to increased autophagy, day 2 post-differentiation Rb-deficient myotubes also exhibited ectopic DNA synthesis (Figure 3. 1D) [149, 531]. To determine the cell cycle status of 3-MA-rescued Rb-deficient myotubes, myoblasts were induced to differentiate in the presence or absence of 3-MA and after 1 or 9 days, the cultures were either maintained in DM or shifted to GM and treated with BrdU for 16 hrs. At day 2 post-differentiation, both 3-MA treated and untreated Rb-deficient myotube nuclei, but not control myotube nuclei, labeled positive for BrdU (Figure 3. 8D; left). Strikingly, by day

10 post-differentiation, the 3-MA treated Rb-deficient myotubes ceased to incorporate BrdU under either DM or GM conditions (Figure 3. 8D, right). Thus, rescued Rb-deficient myotubes can eventually enter a stable post-mitotic state.

In contrast to the effect of autophagy inhibitors (Bcl-2, 3-MA, $Vps34^{dn}$), suppression of DNA synthesis with aphidicolin, or cell cycle progression with $p27^{kip1}$, accelerated rather than rescued the differentiation defect of Rb-deficient myoblasts (Figure 3. 9). The effect was specific to Rb-deficient myoblasts and was not observed in control cultures, underscoring the sensitivity of Rb-deficient cells to cell cycle inhibitors under low serum conditions. Transduction of activated mTOR [532] or dominant negative Foxo3a [533], factors known to inhibit autophagy induced by nutrient or insulin/IGF-1 deprivation [396, 397, 534], also failed to prevent Rb-deficient myotube degeneration, though both factors increased the number and size of control myotubes (Figure 3. 10). Thus, Foxo3a and mTOR affect survival-associated autophagy in response to starvation, but not death-associated autophagy that accompanies Rb-deficient myotube degeneration.

3.7 PPAR Agonist and MOMP Antagonist Rescue the Rb Differentiation Defect

If mitochondrial loss underlies myotube degeneration in the absence of pRb, it was proposed that stimulation of mitochondrial biogenesis might also rescue the defect. Mitochondrial biogenesis is regulated by the co-activator PGC-1α and peroxisome proliferator activated receptors (PPARs) which can be activated by bezafibrate, a pan-PPAR agonist [476, 478]. As shown in Figure 3. 8A and E, bezafibrate treatment efficiently blocked degeneration of Rb-deficient myotubes, leading to twitching myotubes that survived for over 8 days. Longer treatment with bezafibrate became

cytotoxic to both control and Rb-deficient myotubes. Treatment of control and Rb-deficient myotubes with bezafibrate also increased overall mitochondrial content as observed by MitoTracker® or cytochrome c staining (Figure 3. 4A, right panels; Figure 3. 8F), and reduced the percentage of myotubes with perinuclear aggregates from ~70% to ~40% ($p<0.001$; Figure 3. 4B). This result is in accord with a report that showed that during erythropoiesis, Rb-deficiency disrupts mitochondrial biogenesis [535]. Next, we assessed the effect of blocking MOMP on Rb-deficient myotube survival using minocycline; a MOMP inhibitor [536]. Minocycline treatment delayed the collapse of mutant myotubes, which survived and twitched for ~8 days (Figure 3. 11A). In contrast, transduction of the X-linked inhibitor of apoptosis, XIAP, which inhibits multiple caspases [360, 537], failed to block myotube degeneration (Figure 3. 11B-C), indicating that collapse of Rb-deficient myotubes can only be effectively inhibited prior to MOMP.

3.8 Hypoxia-Induced Glycolytic Shift Rescues Rb Differentiation Defect Following Chronic or Acute Inactivation of Rb

The aforementioned results indicate that during differentiation, pRb loss leads to mitochondrial dysfunction and autophagy, reduced mitochondrial content and ATP levels, and ultimately myotube degeneration. Inhibition of autophagy and mitochondrial perinuclear aggregation rescued the Rb myogenic defect. An intriguing possibility is that a metabolic shift from oxidative phosphorylation to glycolysis would bypass the requirement for mitochondrial function and rescue the defect as well. To test this notion, we investigated the effect of hypoxia, which induces such a metabolic shift, on myogenic differentiation. Previous reports showed that hypoxia inhibits the differentiation of the immortalized satellite cell line, C2C12 [538]. However, the differentiation of primary

embryonic myoblasts was unaffected in this study. Remarkably, differentiated Rb-deficient myoblasts survived under hypoxic conditions (1% O_2), leading to long MHC-expressing, twitching myotubes (Figure 3.12A). Immunoblotting confirmed high expression of both early (myogenin) and late (MCK) markers in hypoxia-rescued Rb-deficient myotube cultures (Figure 3.12B, left). Densitometry analysis of these factors, normalized for MHC expression (i.e. myotube number), revealed that while expression of MCK was near normal, expression of myogenin was elevated in rescued Rb-deficient myotubes relative to control, though this was not statistically significant (Figure 3.12B, right). Thus, while hypoxia or survival factors rescued the degeneration of mutant myotubes, they did not substitute for pRb functions, such as in preventing ectopic DNA synthesis, and this resulted in subtle changes in progression of the differentiation program. When returned to normoxia after 5 days in hypoxia, the rescued Rb-deficient myotubes continued to twitch, highlighting the transient requirement for Rb function in the first few days post-differentiation. To test whether hypoxia could also rescue the Rb myogenic defect after acute inactivation of this tumor suppressor, embryonic myoblasts from E16.5 $Rb^{f/f}$ embryos were transduced, in which exon 19 of Rb is flanked by loxP sites, with adenovirus encoding Cre recombinase [132, 150]. A relatively high multiplicity of infection was used to ensure $Rb^{f/f}$ was recombined in virtually all cells (Figure 3.12C-D). Remarkably, like after chronic inactivation, hypoxia rescued the differentiation defect following acute inactivation of Rb, leading to long, twitching myotubes that continued to contract even when transferred back to normoxia (Figure 3.12E-F; videos S5-6).

3.9 Hypoxia Rescued Rb Differentiation Defect is Glycolysis and HIF-1 Dependent

Under low oxygen tension, the hypoxia inducible factor-1α (HIF-1α) induces expression of genes responsible for glucose influx and glycolysis [539]. To determine whether hypoxia rescued Rb-deficient myotubes by inducing a glycolytic shift, myoblasts were induced to differentiate in hypoxia in the presence of lonidamine, an antagonist of hexokinase, which catalyzes the conversion of glucose to glucose 6-phosphate [495]. Beginning at day 2 post-differentiation, a relatively low concentration of lonidamine (50μM) had little obvious effect on the survival of control myotubes in hypoxia (Figure 3. 12A,H). Conversely, under hypoxic conditions Rb-deficient myoblasts were highly sensitive to this dose of lonidamine, forming only very short myotubes, most of which ultimately degenerated (Figure 3. 12A,H).

Under normoxia, HIF-1α undergoes ubiquitination via the von Hippel-Lindau tumor suppressor protein (pVHL) leading to its proteosomal degradation [539]. To ask whether HIF-1α was responsible for preventing the degeneration of Rb-deficient myotubes in hypoxia, I first used a VHL allele (Ad.VHL-T7-HPACGV), which is constitutively active in both normoxia and hypoxia [540]. Expression of this allele dramatically reduced survival of Rb-deficient myotubes under hypoxic conditions (Figure 3. 12H, bottom right plot), implicating HIF-1α as required for mediating rescue of Rb-deficient myotubes under low oxygen tension. Next, I tested whether HIF-1α was sufficient to prevent Rb-deficient myotube degeneration, using a constitutively active HIF-1α allele, HIF-1α/NF-κB, in which the N-terminus of HIF-1α (amino acids 1-390) is fused to NF-κB transactivation domain [541]. Transduction of Ad.HIF-1α/NF-κB rescued degeneration of Rb-deficient myotubes in normoxia leading to stable myotubes

for over 10 days (Figure 3. 12I-J). Thus, Rb-deficient myotubes survive in hypoxia due to a HIF-1α-induced glycolytic shift.

These results demonstrate that pRb is required for cell cycle exit and survival during terminal myogenesis - but not for actively stimulating the myogenic differentiation program.

Figure 3. 1. Rb-deficient myoblasts fuse to form short myotubes that degenerate

(A) Western blot analysis for pRb expression in day 2 differentiating control (ctrl) and Rb-deficient myoblast cultures. Tubulin served as the loading control. **(B)** Immunostaining for MHC at day 3 (DM-3) and day 6 (DM-6) differentiating ctrl and Rb-deficient myotubes. Nuclei were counterstained with DAPI (blue). **(C)** Average number of myotubes counted on indicated days post-differentiation. Each time point is an average ± standard deviation of 6 fields at 200X from 6 independent experiments. **(D)** Immunostaining for BrdU in ctrl and Rb-deficient myotubes. Myoblasts were allowed to differentiate for 1 day, exposed to 20μM BrdU for 16 hr in the presence of differentiation (DM) or growth (GM) medium and stained for MHC to detect myotubes (red) and BrdU to detect DNA synthesis (green). Images captured using confocal microscopy at magnification of 630X. Arrowheads label BrdU positive nuclei in Rb-deficient myotubes. **(E)** Western blot analysis for cleaved caspase-3 and PARP/cleaved PARP in ctrl and Rb-deficient cultures at the indicated days post differentiation. Tubulin served as the loading control. **(F)** TUNEL staining of ctrl and Rb-deficient myotubes at day 2 post-differentiation. Arrowheads label TUNEL positive nuclei (green), which are invariably in unfused cells – not within myotubes.

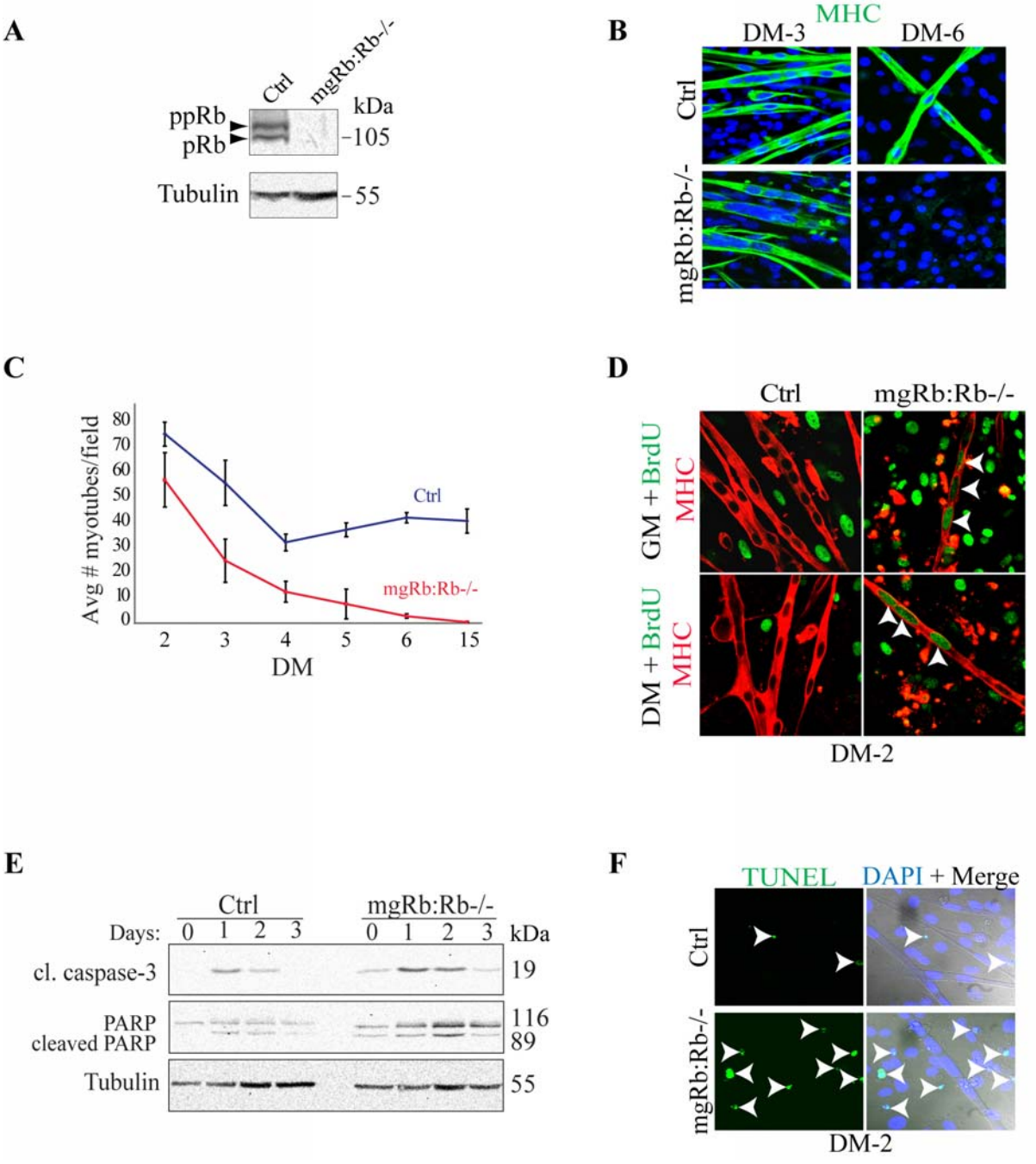
A
Ctrl
mgRb:Rb-/-
kDa
ppRb
pRb
105
Tubulin
55
B
MHC
DM-3
DM-6
Ctrl
mgRb:Rb-/-
C
Avg # myotubes/field
80
70
60
50
40
30
20
10
0
Ctrl
mgRb:Rb-/-
2
3
4
5
6
15
DM
D
Ctrl
mgRb:Rb-/-
GM + BrdU
MHC
DM + BrdU
MHC
DM-2
E
Ctrl
mgRb:Rb-/-
Days:
0 1 2 3
0 1 2 3
kDa
cl. caspase-3
19
PARP
cleaved PARP
116
89
Tubulin
55
F
TUNEL
DAPI + Merge
Ctrl
mgRb:Rb-/-
DM-2

Figure 3. 2. Rb-deficient myotubes express elevated levels of autophagy biomarkers

(A) LC3-RFP expression in ctrl and Rb-deficient myotubes at day 2 post-differentiation. Indicated cultures were transduced with Ad.LC3-red-fluorescent-protein (RFP), induced to differentiate and imaged 2 days later. In this assay, LC3-I and LC3-II appear, respectively, diffuse or punctuate (indicative of autophagosomes). Note LC-II positive perinuclear aggregates. Inlets show nuclear DAPI staining (blue). **(B)** Representative Western blot analysis (n=3) for LC3 expression in post-differentiation day 2 ctrl and Rb-deficient cultures. The lipidated LC3-II form migrates faster than LC3-I in SDS-PAGE protein gels. When indicated, chloroquine was added 12hr prior to cell harvesting. **(C)** Representative Western blot of LC3 in E16.5 ctrl and mgRb:$Rb^{-/-}$ skeletal muscles. **(D)** Quantification of LC3-II to tubulin ratio in E16.5 mgRb:$Rb^{-/-}$ skeletal muscles relative to ctrl as depicted in panel g (mean ± standard deviation, n=3). Asterisk (*) denotes p=0.016 by student's t-test. **(E)** Three independent cultures of Ctrl or Rb-deficient myoblasts were induced to differentiate and immunostained for BNip3 at day 2 post-differentiation (green). Nuclei were counterstained with DAPI (blue). Note the increase in BNip3 expression in Rb-deficient myotubes relative to ctrl.

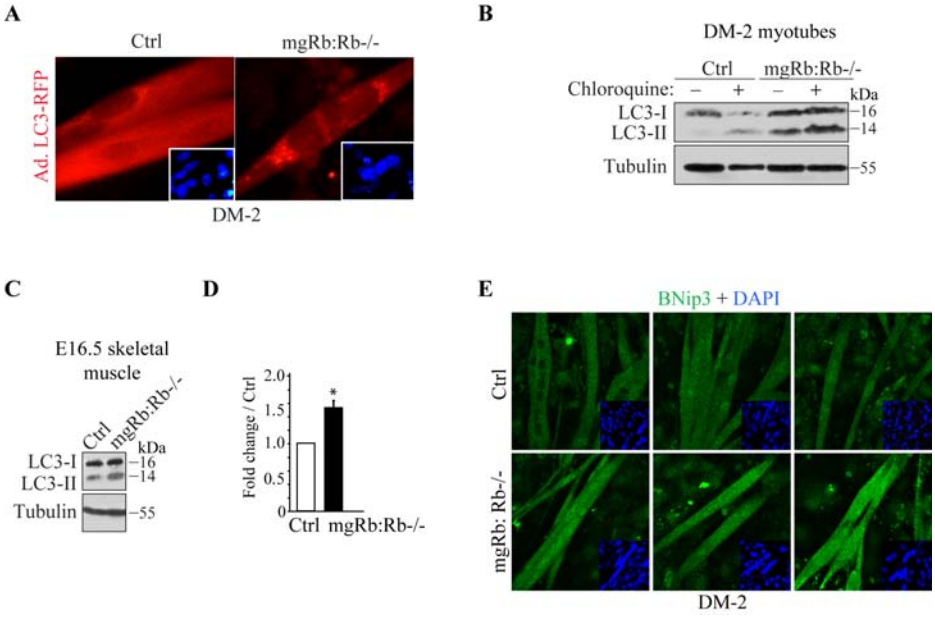
A
Ctrl
mgRb:Rb-/-
Ad. LC3-RFP
DM-2
B
DM-2 myotubes
Ctrl
mgRb:Rb-/-
Chloroquine: – + – +
kDa
LC3-I
LC3-II
16
14
Tubulin
55
C
E16.5 skeletal muscle
Ctrl
mgRb:Rb-/-
kDa
LC3-I
LC3-II
16
14
Tubulin
55
D
Fold change / Ctrl
2.0
1.5
1.0
0.5
0
*
Ctrl
mgRb:Rb-/-
E
BNip3 + DAPI
Ctrl
mgRb: Rb-/-
DM-2

Figure 3. 3. RbΔK11 suppresses accumulation of LC3-II in Rb-deficient myotubes

(A) Representative Western blot analysis for LC3-I and LC3-II expression in whole cell lysates from ctrl or Rb-deficient myotubes transduced with Ad.GFP or Ad.RbΔK11. When indicated, Chloroquine was added 12hr prior to cell harvesting. **(B)** Quantification of LC3-II to tubulin ratio by Western blots as depicted in panel (I) Data represent mean ± standard deviation (n=7). *, p=0.047; ** p=0.005 by ANOVA.

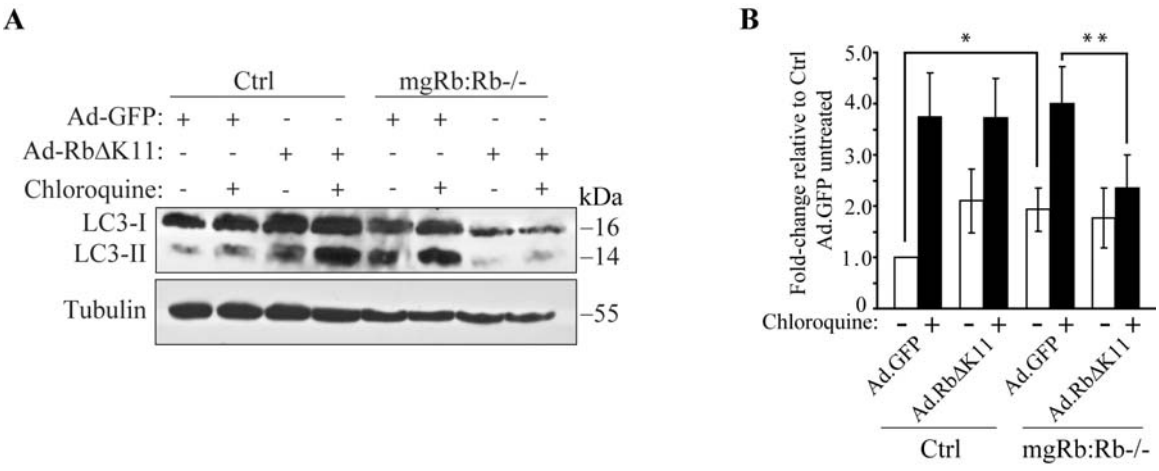
A
Ctrl
mgRb:Rb-/-
Ad-GFP: + + - - + + - -
Ad-RbΔK11: - - + + - - + +
Chloroquine: - + - + - + - +
kDa
LC3-I
LC3-II
–16
–14
Tubulin
–55
B
Fold-change relative to Ctrl Ad.GFP untreated
5.0
4.0
3.0
2.0
1.0
0
*
**
Chloroquine: - + - + - + - +
Ad.GFP
Ad.RbΔK11
Ad.GFP
Ad.RbΔK11
Ctrl
mgRb:Rb-/-

Figure 3. 4. Rb-deficient muscle defect is characterized by perinuclear/autophagosome aggregates.

(A) Left. Mitotracker® staining of ctrl and Rb-deficient myotubes at day 2 post-differentiation. Arrowheads point to large perinuclear aggregates in Rb-deficient myotubes. Right. Mitotracker staining of ctrl and Rb-deficient myotubes treated with bezafibrate for 2 days. Note the increased mitochondrial content and reduced perinuclear aggregates after bezafibrate treatment. **(B)** Quantification of myotubes containing perinuclear Mitotracker®-positive aggregates in untreated (DMSO/vehicle) or bezafibrate treated ctrl and Rb-deficient myotubes 2 days post-differentiation. Data represent mean ± standard deviation (n=3). Both asterisks (*) denote $p<0.001$ by student's t-test. **(C)** Immunostaining for cytochrome c in ctrl and Rb-deficient myotubes at day 2 post-differentiation. Note the smooth network of cytochrome c positive signal in ctrl but irregular and perinuclear aggregation in mutant myotubes. **(D)** Mitotracker® (red) and LC3 immunostaining (green) of ctrl and Rb-deficient myotubes at day 2 post-differentiation. Chloroquine and, where indicated, 3-MA were added 12hr prior to staining/fixation. Note extensive perinuclear overlap of Mitotracker® plus LC3 in Rb-deficient myotubes (yellow), which is inhibited by 3-MA. **(E)** Average percentage of Mitotracker® (red) to LC3 (green) overlap in 25 myotubes from 2 independent cultures, in control versus $Rb^{-/-}$ myotubes (total) or $Rb^{-/-}$ myotubes with perinuclear mitochondrial aggregation (high). Asterisk (*), $p=7.1x10^{-5}$ by student's t-test.

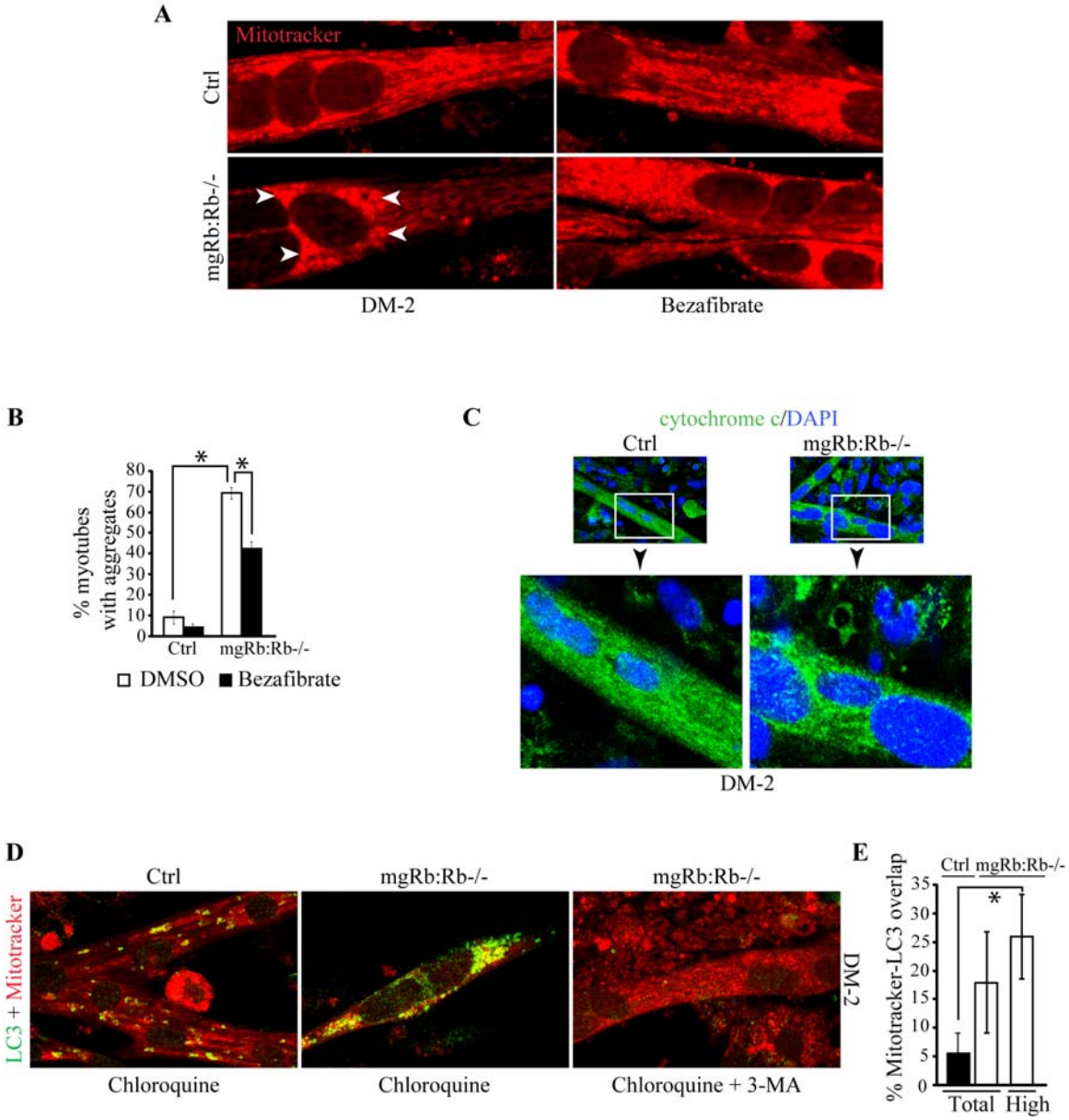
A
Mitotracker
Ctrl
mgRb:Rb-/-
DM-2
Bezafibrate
B
% myotubes with aggregates
80
70
60
50
40
30
20
10
0
*
*
Ctrl
mgRb:Rb-/-
DMSO
Bezafibrate
C
cytochrome c/DAPI
Ctrl
mgRb:Rb-/-
DM-2
D
Ctrl
mgRb:Rb-/-
mgRb:Rb-/-
LC3 + Mitotracker
DM-2
Chloroquine
Chloroquine
Chloroquine + 3-MA
E
Ctrl
mgRb:Rb-/-
% Mitotracker-LC3 overlap
35
30
25
20
15
10
5
0
*
Total
High

Figure 3. 5. Ultrastructural analysis of Rb-deficient myotubes containing autolysosomes.

(A) Ultrastructural analysis of ctrl and Rb-deficient myotubes, treated or not with 3-MA at day 2 post-differentiation. White arrows point to mitochondria. Red asterisk indicates electron dense autolysosome. Note perinuclear mitochondrial accumulation in untreated but not 3-MA treated Rb-deficient myotubes (Magnification 17,000x).
(B) Electron micrographs of Rb-deficient myotubes at day 2 post-differentiation. White arrows point to mitochondria and red asterisks label putative autolysosomes. Top micrograph captured at 9,000x magnification; bottom micrograph, 17,000x. **(C)** Electron micrographs of Rb-deficient myotubes at day 2 post-differentiation. Black arrows point to mitochondria sequestered inside autophagosomes. Top micrograph captured at 20,000x magnification; bottom 60,000x.

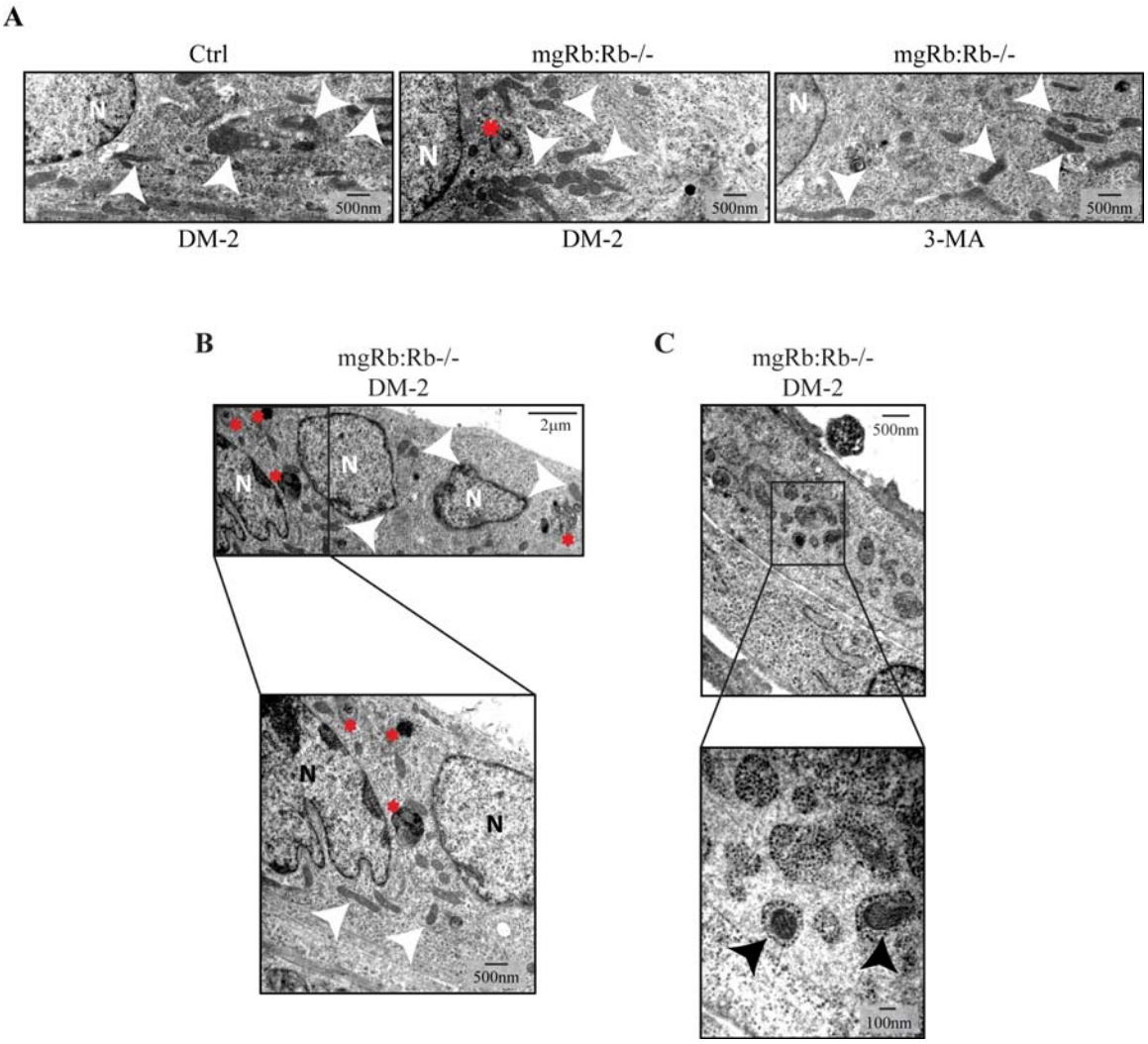
A
Ctrl
mgRb:Rb-/-
mgRb:Rb-/-
N
500nm
DM-2
DM-2
3-MA
B
mgRb:Rb-/-
DM-2
2μm
C
mgRb:Rb-/-
DM-2
500nm
100nm

Figure 3. 6. Rb-deficient muscle has reduced mitochondrial DNA and ATP content

(A) Ratio of mitochondrial/nuclear DNA in ctrl and Rb-deficient myotube culture at post-differentiation day 2, estimated by quantitative real-time PCR using single copy mitochondrial and nuclear DNA (n=3). In e-g, error bars represent standard deviation. *, $p<0.001$. **(B)** Ratio of mitochondrial/nuclear DNA in E16.5 ctrl and mgRb:$Rb^{-/-}$ skeletal muscle tissues, estimated by quantitative real-time PCR (n= 3; *, p=0.009). **(C)** Quantification of ATP in E16.5 ctrl and mgRb:$Rb^{-/-}$ skeletal muscle tissue. Values represent relative light units per mg tissue (n=3; *, p=0.011).

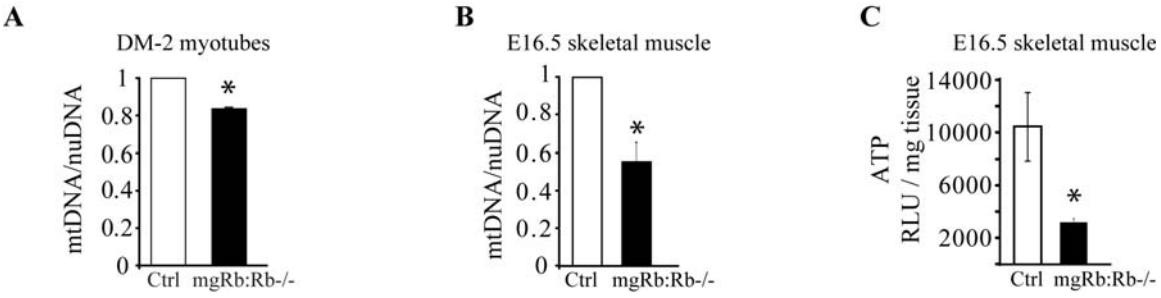
A
DM-2 myotubes
mtDNA/nuDNA
1
0.8
0.6
0.4
0.2
0
*
Ctrl
mgRb:Rb-/-
B
E16.5 skeletal muscle
mtDNA/nuDNA
1
0.8
0.6
0.4
0.2
0
*
Ctrl
mgRb:Rb-/-
C
E16.5 skeletal muscle
ATP
RLU / mg tissue
14000
10000
6000
2000
*
Ctrl
mgRb:Rb-/-

Figure 3. 7. Bcl-2 rescues the degeneration of Rb-deficient myotubes.

(A) Average number of myotubes per field in ctrl and Rb-deficient myoblast cultures induced to differentiate in the presence or absence of LiCl or after transduction with Ad.GFP, Ad.Bcl-2, Ad.β-Catenin or Ad.β-CateninΔN(activated). Each point represents the average ± standard deviation of 6 fields taken at 200X from 6 independent experiments. Note survival of myotubes after Bcl-2 transduction. A video capturing Bcl-2 rescued, twitching Rb-deficient myotubes is shown in Video S2. Inset - Western blot analysis for Bcl-2 in Ad.Bcl2-transduced versus uninfected primary myoblasts. **(B)** Immunostaining for muscle creatine kinase (MCK; green) in Ad.Bcl-2 transduced ctrl and Rb-deficient myotubes at day 6 post-differentiation. **(C)** Western blot analysis for MCK, myogenin, MHC and troponin T expression in ctrl and Rb-deficient myoblast cultures induced to differentiate for 6 days in the presence of LiCl or following transduction with Ad.Bcl-2. Tubulin served as the loading control.

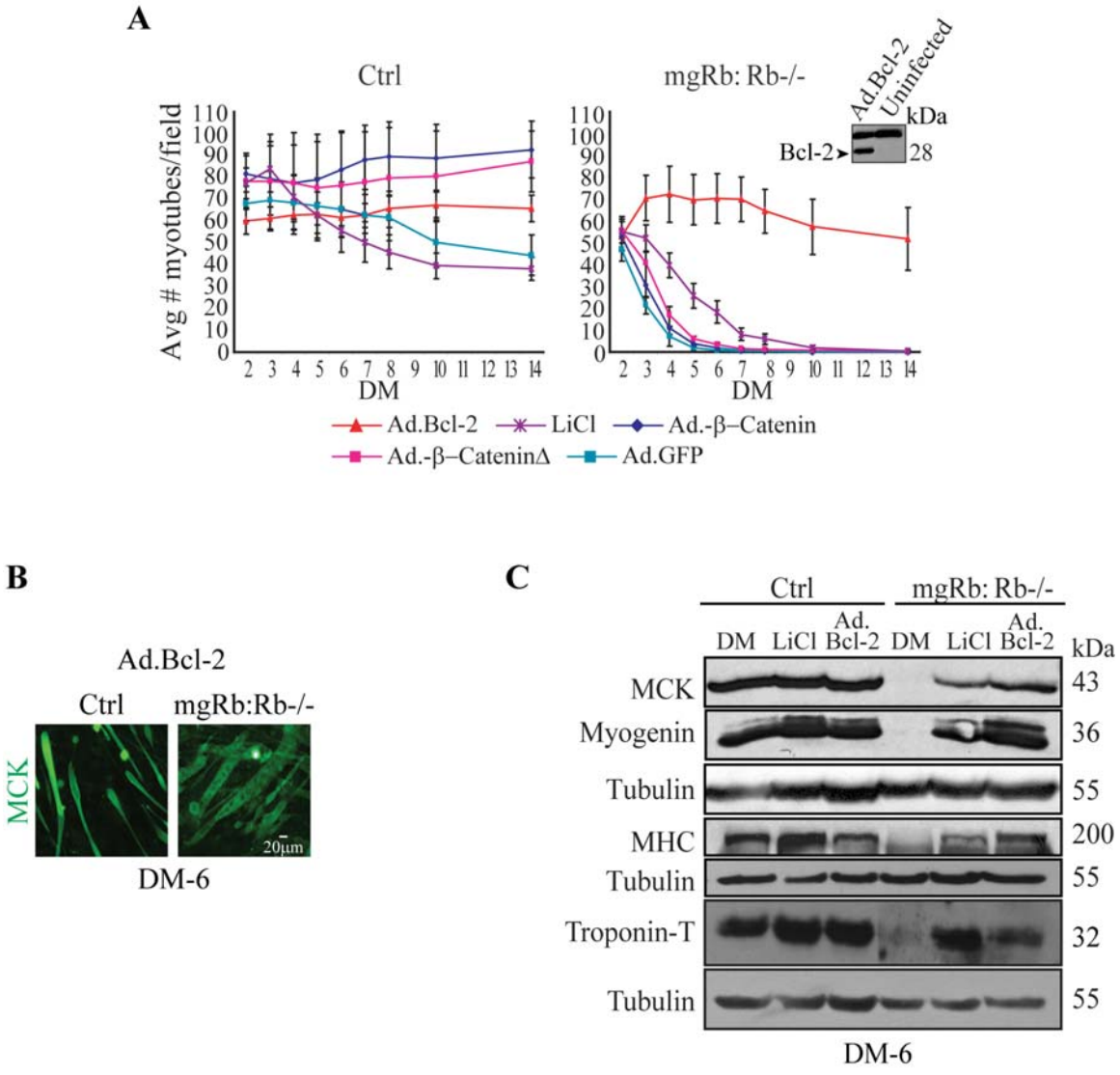
A
Ctrl
mgRb: Rb-/-
Avg # myotubes/field
DM
Ad.Bcl-2
Uninfected
kDa
Bcl-2
28
Ad.Bcl-2
LiCl
Ad.-β–Catenin
Ad.-β–CateninΔ
Ad.GFP
B
Ad.Bcl-2
Ctrl
mgRb:Rb-/-
MCK
20μm
DM-6
C
Ctrl
mgRb: Rb-/-
DM
LiCl
Ad. Bcl-2
kDa
MCK
43
Myogenin
36
Tubulin
55
MHC
200
Tubulin
55
Troponin-T
32
Tubulin
55
DM-6

Figure 3. 8. Inhibition of autophagy rescues the degeneration of Rb-deficient myotubes.

(A) Average number of Rb-deficient myotubes following treatment with 3-MA, bezafibrate or DMSO/vehicle as indicated. Counts are average ± standard deviation of 6 fields at 200X from 4 independent experiments. **(B)** Left and center, brightfield images of ctrl and Rb-deficient myotubes treated or not with 3-MA at day 8 post-differentiation. Right panels show immunostaining for MHC (red) at day 14 post-differentiation in the presence of 3-MA. Nuclei were counterstained with DAPI (blue). Arrowheads label 3-MA-rescued Rb-deficient myotubes at DM-8. A video capturing 3-MA rescued, twitching Rb-deficient myotubes is shown in Video S4. **(C)** Brightfield images of Rb-deficient myoblasts treated with 3-MA or transduced with Ad.Vps34^{dn} at 2 and 6 days post-differentiation. Arrowheads point to myotubes. Although Vps34^{dn} rescued Rb-deficient myotubes twitched, due to low expression of Vps34^{dn} in primary mouse myoblasts, the extent of myotube rescue was not as robust as with 3-MA treatment. **(D)** Immunostaining for BrdU incorporation (green) and MHC (red) in 3-MA treated ctrl and Rb-deficient myotubes at 2 or 10 days post-differentiation. Cultures were induced to differentiate and treated with 20μM BrdU for 16hr in the presence GM or DM. Note that Rb-deficient myotubes incorporate BrdU at day 2 but not 10 post-differentiation. **(E)** Brightfield images (left and center) and MHC staining (right) of ctrl and Rb-deficient myoblasts induced to differentiate for 7 days in the absence (DMSO/vehicle) or presence of bezafibrate. Arrowheads label bezafibrate-rescued Rb-deficient myotubes. **(F)** Immunostaining for cytochrome c of ctrl or Rb-deficient myotubes treated with bezafibrate and induced to differentiate for 2 days. DAPI was used to counterstain nuclei (blue).

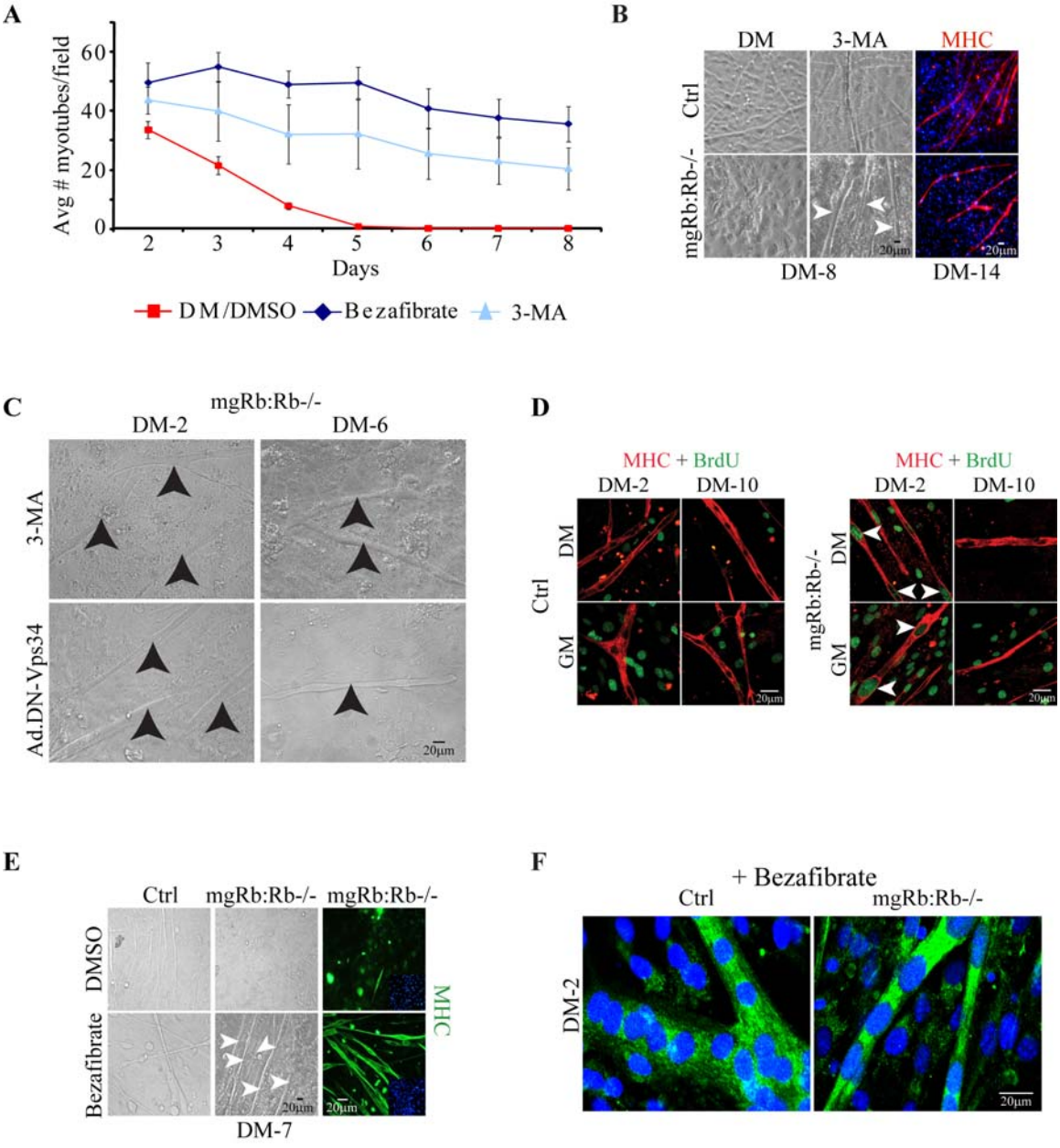
A
Avg # myotubes/field
60
40
20
0
2
3
4
5
6
7
8
Days
DM/DMSO
Bezafibrate
3-MA
B
DM
3-MA
MHC
Ctrl
mgRb:Rb-/-
20μm
DM-8
DM-14
C
mgRb:Rb-/-
DM-2
DM-6
3-MA
Ad.DN-Vps34
20μm
D
MHC + BrdU
DM-2
DM-10
Ctrl
DM
GM
mgRb:Rb-/-
20μm
E
Ctrl
mgRb:Rb-/-
mgRb:Rb-/-
DMSO
Bezafibrate
MHC
20μm
DM-7
F
+ Bezafibrate
Ctrl
mgRb:Rb-/-
DM-2
20μm

Figure 3. 9. Cell-cycle inhibitors aphidicolin and $p27^{Kip1}$ accelerate degeneration of Rb-deficient myotubes.

(A) Ctrl and Rb-deficient myoblasts were induced to differentiate for 2 days, treated with aphidicolin and incubated in the presence of BrdU for 16hr. BrdU was detected using a FITC-conjugated anti-BrdU antibody (green) and MHC antibody was used to visualize myotubes (red). Nuclei were counterstained with DAPI (blue). Note the reduced BrdU positive nuclei in ctrl cells and diminished myotube formation in Rb-deficient myoblasts following aphidicolin treatment. **(B)** Immunostaining for $p27^{Kip1}$ in ctrl myoblasts transduced with Ad.$p27^{Kip1}$. **(C)** Quantification of myotube formation in ctrl and Rb-deficient myoblasts transduced with Ad.GFP or Ad.$p27^{Kip1}$ and then induced to differentiate for the indicated days. Counts are an average of 6 representative fields from 2 independent experiments. **(D)** Brightfield images of ctrl and Rb-deficient myoblasts transduced with Ad.GFP or Ad.$p27^{Kip1}$, and induced to differentiate for the indicated days. Note the absence of Rb-deficient myotubes at day 2 post-differentiation in Ad.$p27^{Kip1}$ transduced cells.

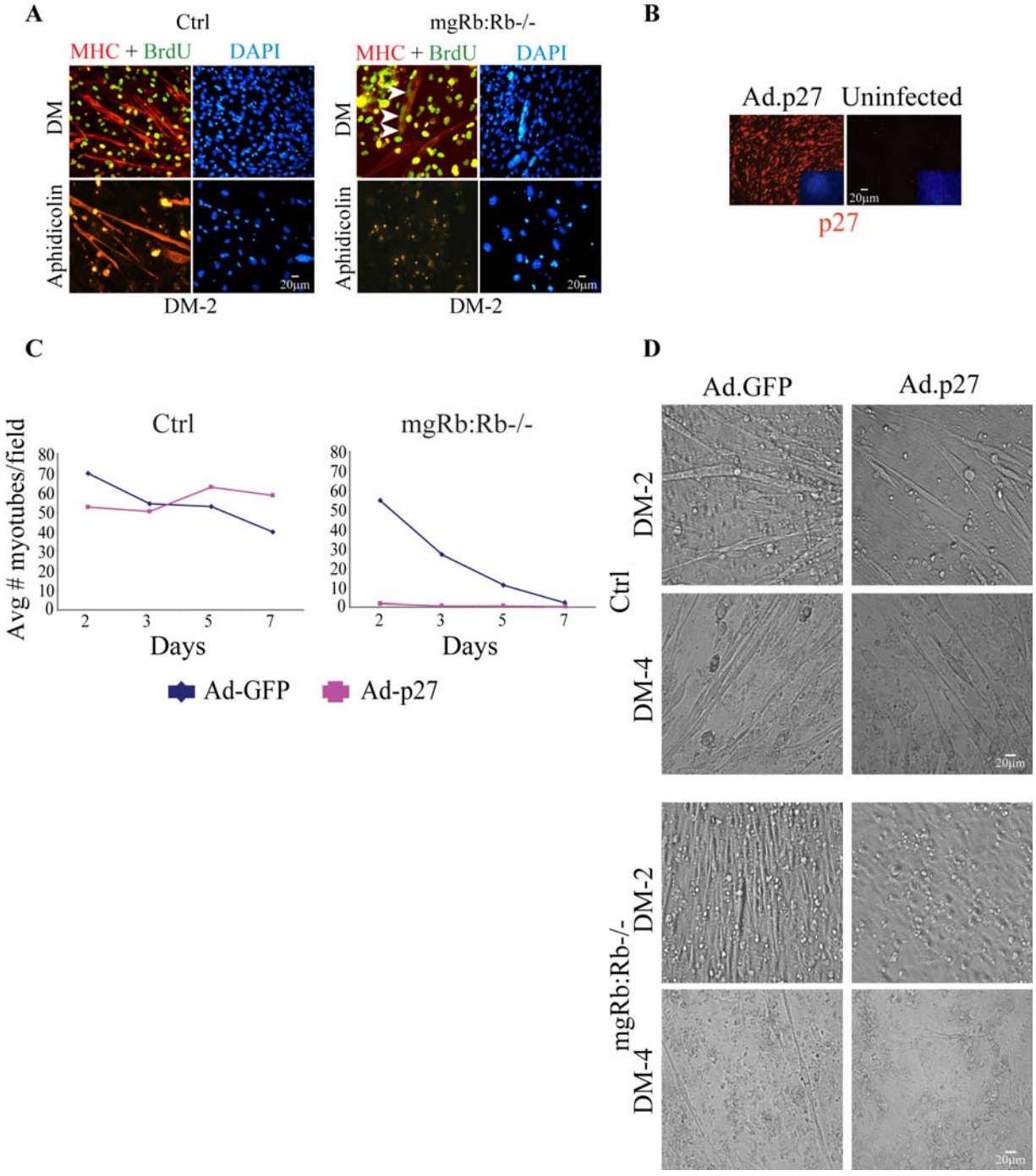
A
Ctrl
mgRb:Rb-/-
MHC + BrdU
DAPI
DM
Aphidicolin
20μm
DM-2
B
Ad.p27
Uninfected
20μm
p27
C
Ctrl
mgRb:Rb-/-
Avg # myotubes/field
Days
Ad-GFP
Ad-p27
D
Ad.GFP
Ad.p27
Ctrl
DM-2
DM-4
mgRb:Rb-/-
20μm

Figure 3. 10. Expression and enhanced differentiation of control myoblasts after transduction of dominant-negative FOXO3 and constitutively active mTOR.

(A) Immunostaining for HA-tagged wild-type (cytoplasmic) and dominant negative (nuclear) FOXO3adn using an anti-HA antibody (red) in indicated cultures transduced with Ad.wt-FoxO3a or Ad.DN-FoxO3a at day 2 post-differentiation. **(B)** Western blot analysis of ctrl myoblasts transduced with Ad.GFP, Ad.ca-mTOR or Ad.wt-mTOR at DM-2. An antibody recognizing anti-phospho-S6 ribosomal protein (ser240/244), a direct target of mTOR, was used. Tubulin served as the loading control. Note the elevated pS6 in cells transduced by constitutively activated (ca) mTOR. **(C)** Immunostaining with anti-phospho-S6 ribosomal protein (ser240/244) antibodies of ctrl and Rb-deficient myoblasts infected with Ad.GFP, Ad.ca-mTOR or Ad.wt-mTOR at DM-2. Note the increased intensity of pS6 within myotubes in mTOR transduced cells. **(D)** Brightfield images of differentiating myotubes after infection with indicated recombinant adenoviruses. Note the increase in the number of myotubes in cultures transduced with mTOR and dominant negative FOXO3a.

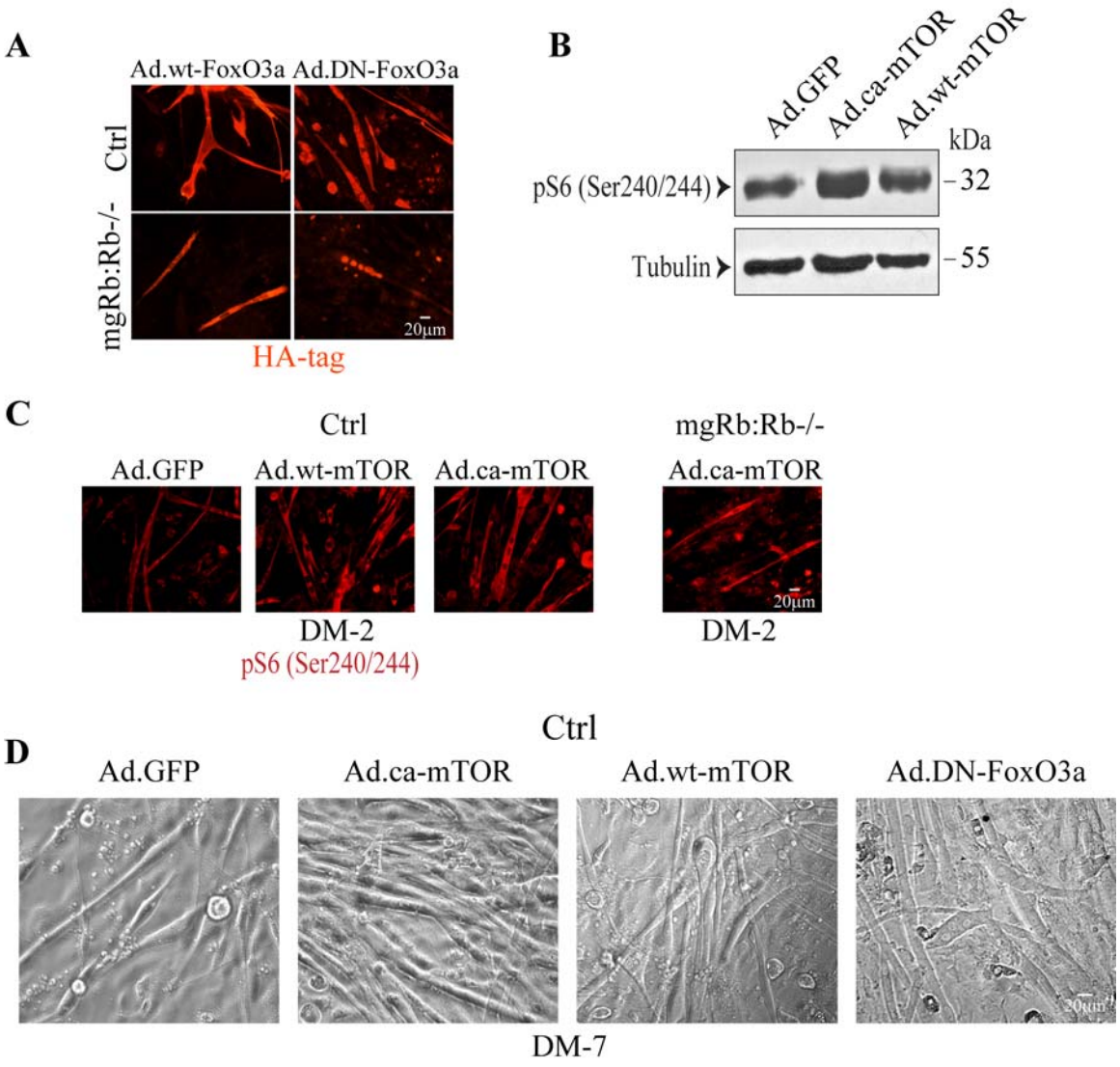
A
Ad.wt-FoxO3a
Ad.DN-FoxO3a
Ctrl
mgRb:Rb-/-
20μm
HA-tag
B
Ad.GFP
Ad.ca-mTOR
Ad.wt-mTOR
kDa
pS6 (Ser240/244)
32
Tubulin
55
C
Ctrl
mgRb:Rb-/-
Ad.GFP
Ad.wt-mTOR
Ad.ca-mTOR
Ad.ca-mTOR
20μm
DM-2
DM-2
pS6 (Ser240/244)
D
Ctrl
Ad.GFP
Ad.ca-mTOR
Ad.wt-mTOR
Ad.DN-FoxO3a
30μm
DM-7

Figure 3. 11. Minocycline but not XIAP can suppress the degeneration of Rb-deficient myotubes.

(A) Brightfield images of Rb-deficient myotubes after treatment with minocycline for 5 days. Note the presence of myotubes in treated but not untreated Rb-deficient cultures (arrowheads). **(B)** Western blot analysis for XIAP in myoblasts infected with Ad.GFP or Ad.XIAP. Tubulin served as a loading control. **(C)** Brightfield images of ctrl and Rb-deficient myoblasts infected with Ad.XIAP and induced to differentiate for 2 or 7 days. Note absence of Rb-deficient myotubes by 7 days post-differentiation irrespective of XIAP expression.

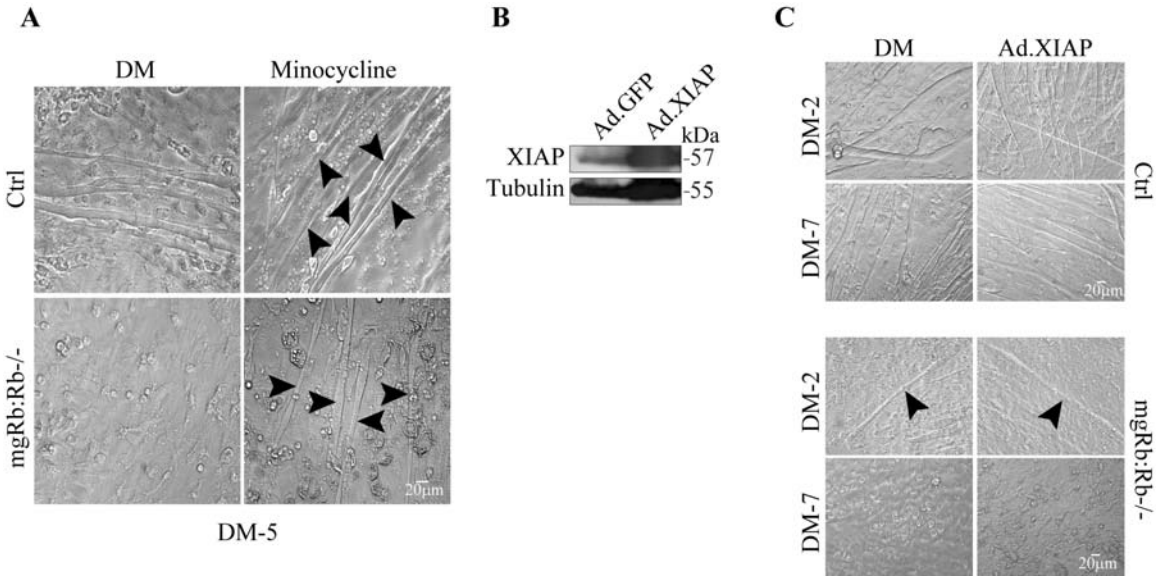
A
DM
Minocycline
Ctrl
mgRb:Rb-/-
20μm
DM-5
B
Ad.GFP
Ad.XIAP
kDa
XIAP
-57
Tubulin
-55
C
DM
Ad.XIAP
DM-2
DM-7
Ctrl
20μm
DM-2
DM-7
mgRb:Rb-/-
20μm

Figure 3. 12. HIF-1 hypoxia-mediated glycolytic shift rescues the Rb myogenic defect.

(A) Immunostaining for MHC (green) in indicated myoblasts induced to differentiate under normoxia or hypoxia treated or not with lonidamine. Note shortened myotubes in the presence of lonidamine. **(B)** Representative immunoblot (left) and average expression of myogenin and MCK normalized for MHC expression (n=3). **(C)** $Rb^{f/f}$ myoblasts transduced with Ad.GFP or Ad.cre and immunoblotted for pRb. Tubulin served as a loading control. **(D)** $Rb^{f/f}$ myoblasts transduced with Ad.GFP or Ad.cre and immunostained for pRb (red). Inlets, DAPI staining for nuclei (blue). **(E)** Immunostaining for MHC in $Rb^{f/f}$ myoblasts transduced with Ad.cre, and induced to differentiate in normoxia (top and middle) or hypoxia (bottom). **(F)** Top, brightfield images of $Rb^{f/f}$ myoblasts transduced with Ad.Empty Vector (EV) or Ad.cre and induced to differentiate under hypoxia. Bottom, larger view of indicated field - arrowheads point to rescued $Rb^{-/-}$ myotubes. A corresponding video for this field showing myotube contractions is presented in Video S6. **(G)** Quantification of myotube formation in $Rb^{f/f}$ myoblasts transduced with Ad.EV or Ad.cre and induced to differentiate under hypoxia. Counts are an average of 6 representative fields (n=3); error bars represent standard deviation. Asterisk (*), p=0.004. **(H)** Quantification of myotube formation in indicated myoblasts induced to differentiate under indicated conditions. Myotube counts are the average of 6 fields at 200X (n=4); error bars represent standard deviation. **(I)** MHC staining (red) of indicated myoblasts transduced with Ad.NfkB-Hif-1α and induced to differentiate in normoxia. **(J)** Quantification of myotube formation in indicated myoblasts transduced with Ad.EV or Ad.NfkB-Hif-1α and induced to differentiate in normoxia. Myotube counts are the average ± standard deviation of 6 fields at 200X (n=3).

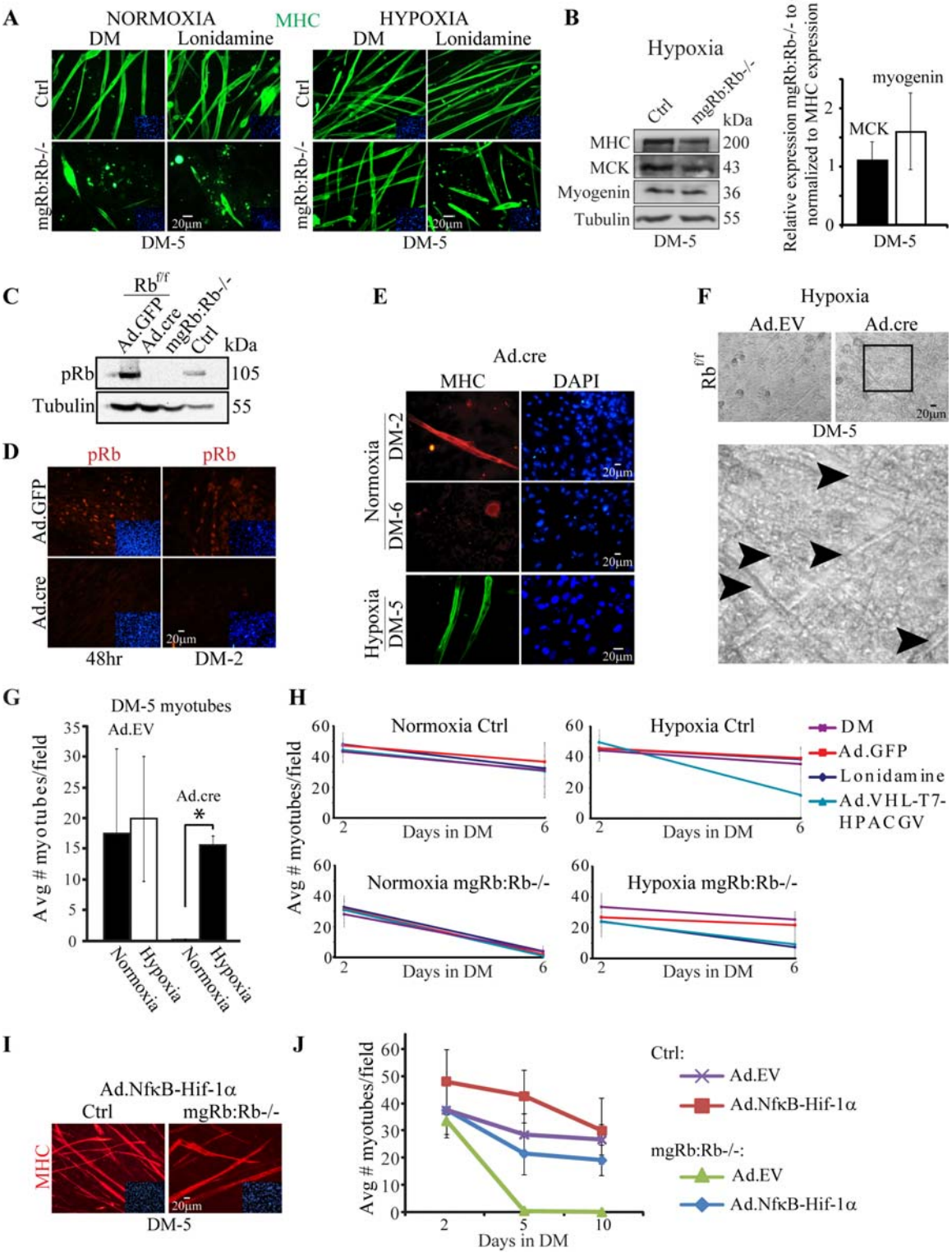
A
NORMOXIA
MHC
HYPOXIA
DM
Lonidamine
DM
Lonidamine
Ctrl
mgRb:Rb-/-
20μm
DM-5
B
Hypoxia
Ctrl
mgRb:Rb-/-
kDa
MHC
200
MCK
43
Myogenin
36
Tubulin
55
DM-5
Relative expression mgRb:Rb-/- to ctrl normalized to MHC expression
myogenin
MCK
DM-5
C
Rb f/f
Ad.GFP
Ad.cre
mgRb:Rb-/-
Ctrl
kDa
pRb
105
Tubulin
55
D
pRb
pRb
Ad.GFP
Ad.cre
20μm
48hr
DM-2
E
Ad.cre
MHC
DAPI
Normoxia
DM-2
DM-6
Hypoxia
DM-5
20μm
F
Hypoxia
Ad.EV
Ad.cre
Rb f/f
20μm
DM-5
G
DM-5 myotubes
Ad.EV
Ad.cre
*
Avg # myotubes/field
Normoxia
Hypoxia
Normoxia
Hypoxia
H
Normoxia Ctrl
Hypoxia Ctrl
Normoxia mgRb:Rb-/-
Hypoxia mgRb:Rb-/-
Avg # myotubes/field
Days in DM
DM
Ad.GFP
Lonidamine
Ad.VHL-T7-HPACGV
I
Ad.NfκB-Hif-1α
Ctrl
mgRb:Rb-/-
MHC
20μm
DM-5
J
Avg # myotubes/field
Days in DM
Ctrl:
Ad.EV
Ad.NfκB-Hif-1α
mgRb:Rb-/-:
Ad.EV
Ad.NfκB-Hif-1α

CHAPTER 4: UNIQUE AND REDUNDANT FUNCTIONS OF THE RETINOBLASTOMA PROTEIN FAMILY DURING SKELETAL MYOGENESIS

The results from this chapter have been submitted for publication:

Ciavarra et. al. Critical role of the Rb family in myoblast fusion and survival.

Note: Dr. Andrew T. Ho contributed Figures 4.1A and 4.1B as described in [542].

4.1 Abstract

Results from chapter 3 showed $Rb^{-/-}$ myoblasts fuse to form short myotubes which collapse as a result of an autophagy-dependent mechanism, and that autophagy inhibitors or hypoxia rescue the defect leading to long, twitching myotubes. Here, the contribution of pRb relatives, p107 and p130, to this process was determined. In particular, chronic or acute inactivation of Rb plus p130 or Rb plus p107 increased myoblast cell death and reduced myotube formation, yet expression of Bcl-2, treatment with autophagy antagonist, lithium or exposure to hypoxia extended myotube survival, leading to long, contracting myotubes that appeared indistinguishable from control myotubes. Mutations in Rb, p107 and p130 accelerated myoblast cell death and led to elongated unfused myocytes and bi-nuclear myotubes that twitched under hypoxia. Thus, when maintained by alternative survival pathways, $Rb^{-/-}$ myoblasts can efficiently differentiate even in the absence of p107 or p130 but not both. Whereas nuclei in $Rb^{-/-}$ myotubes were unable to stably exit the cell cycle, myotubes lacking both p107 and p130, but containing functional Rb, became permanently post-mitotic. Together these results demonstrate that p107 and p130 contribute to myoblast survival during myogenesis, but that such myoblasts can differentiate even in the absence of Rb function if survival is maintained by alternative pathways. This suggests that pRb, but not its relatives, play a critical role in cancer because of its unique requirement for cell cycle exit during terminal differentiation.

4.2 Introduction

The retinoblastoma tumor suppressor (Rb) plays important roles in development and homeostasis, and is commonly inactivated in human malignancies [519, 520]. Rb is a member of a family of proteins including p107 and p130 that exhibit similar or opposing

functions in different tissues. Rb controls cell proliferation and survival by binding transcription factors such as activator E2F factors [8, 543], whereby E2F-bound pRb complexes recruit histone modifying enzymes to repress transcription of genes required for S-phase progression, DNA replication and apoptosis [23-25, 30-37]. pRb is also thought to stimulate activity of lineage-specific transcription factors such as the bHLH factors MyoD and myogenin to activate the muscle differentiation program [99, 101-103, 149, 544]. There is evidence that pRb may also regulate differentiation by controlling expression of differentiation factors such as PPARγ and PGC-1α as well as by sequestering inhibitors of differentiation including Id2, HDAC1, EID-1 and RBP2 [140, 325, 329, 330, 545].

Analyses of $Rb^{-/-}$ mice and derived myoblasts are consistent with the notion that pRb is required for skeletal myogenesis. Rb-null embryos die at embryonic day (E) 13.5-14.5, exhibiting ectopic proliferation, massive apoptosis and incomplete differentiation in a number of tissues where Rb is normally expressed [116, 127, 546-550]. Thus, studies of terminal skeletal myogenesis, which occurs after embryonic day (E) 14.5, were precluded. To circumvent this early embryonic death, an Rb mini-gene (mgRb), expressed exclusively in the placenta and the nervous system, but not in skeletal muscles, was used to extend the life-span of $Rb^{-/-}$ embryos to birth [93, 131], (Z. Jiang and EZ, unpublished). In mgRb:$Rb^{-/-}$ embryos, myotubes are initially formed at E14.5-15.5, but degenerate thereafter in a process accompanied by massive apoptosis, primarily in myoblasts, endoreduplication and normal expression of early myogenic differentiation markers (MHC, cardiac actin), but not late markers (MCK, MRF4) [93]. Similar myogenic defects were subsequently reported after Rb-null embryos were partially

rescued by other means [129, 140, 551]. Moreover, a muscle-specific ablation of a floxed Rb allele (Rb^f) using Myf5-Cre demonstrated impaired muscle differentiation both *in vitro* and *in vivo* [150]. Finally, analysis of $Rb^{-/-}$ myoblasts *in vitro* revealed a similar pattern seen *in vivo* in Rb-null fetuses where the myoblasts initially fuse to form short myotubes, but quickly degenerate and never twitch [552].

Although these *in vivo* and *in vitro* experiments implicate pRb in terminal muscle differentiation, attributing an active differentiation function to pRb has been hampered by the fact that terminal differentiation is closely coupled to cell cycle exit and survival. Recently, these processes were uncoupled by providing differentiating $Rb^{-/-}$ myoblasts with survival factors such as Bcl-2 [552]. Remarkably, ectopic expression of Bcl-2 rescued the Rb defect leading to long myotubes that twitched for weeks in culture [552]. Further analyses revealed that Rb-deficient myotubes exhibit perinuclear mitochondrial aggregation and autophagy, not apoptosis, and that inhibition of autophagy or exposure to hypoxia suppressed the degeneration [552]. Interestingly, although $Rb^{-/-}$ myotubes initially fail to exit the cell cycle, the rescued myotubes eventually become stably post-mitotic despite the absence of Rb [552]. Together these results suggest that Rb is required for proper cell cycle exit and survival but not for stimulating the differentiation program.

As mentioned previously, Rb family members play distinct and redundant roles during development and it remains unresolved whether p107 and p130 compensate or exacerbate the differentiation defect of Rb-deficient myoblasts. Specifically, it was questioned whether the cell fusion and myotube formation that occurs prior to degeneration in the absence of pRb is mediated by p107 and/or p130, or whether these

events are independent of Rb family function. There are several notable differences among these family members. First, they exhibit differential affinity to E2F family members and other factors [8]. For example, pRb primarily binds activator E2Fs (E2F1, E2F2 and E2F3) as well as a repressor E2F (E2F4), whereas p107 and p130 preferentially bind repressor E2Fs (E2F4-E2F5). In addition, p107 and p130, but not pRb, share cyclin binding and CDK inhibitory domains to suppress cell growth [112-118, 553]. Inhibition of cell proliferation by the CDK inhibitor $p16^{INK4a}$ is dependent on the presence of pRb and a second function provided by either p107 or p130, indicating that in this context, loss of either: Rb or p107 plus p130 has similar consequences [554]. Rb also has a non-redundant role in suppressing DNA replication during senescence [555], and it was suggested that this unique role of pRb underlies its exclusive effect on cancer. The Rb family is also differentially regulated during embryogenesis and the cell cycle: Rb alone is highly expressed during embryogenesis in the nervous system, liver and muscles [116], whereas during the cell cycle, Rb expression is relatively constant, p107 expression is low in quiescence and increases sharply as cells re-enter the cell cycle and p130 is robustly expressed in quiescent and differentiated cells and down-regulated during proliferation [109]. Indeed, Rb family members play distinct roles during cell growth and development. For example, on a C57BL/6J background, Rb is essential whereas both p107 and p130 are dispensable [142]. However, on a BALB/cJ background, p130-null embryos die at E11-13 whereas p107-null mice develop myeloproliferative disorder [144-146]. During adipogenesis, fibroblasts lacking p107 and p130 are competent to differentiate into adipocytes while Rb-deficient cells are not [159]. However, while over-expression of pRb promotes adipocyte differentiation, overexpression of p107 suppresses

adipogenic differentiation [159]. In contrast, during myogenesis, over-expression of p107 suppressed ectopic cell proliferation in $Rb^{-/-}$ myotubes [149], whereas over-expression of p130, but not pRb, inhibited myogenic differentiation in the Rb proficient C2C12 myoblast cell line [160]. Taken together, these observations suggest that inactivation of p107 would exacerbate, whereas mutation in p130 would ameliorate the myogenic defect of Rb-deficient myoblasts.

To address the combined function of the Rb protein family during terminal muscle differentiation, double $Rb^{-/-}$:$p107^{-/-}$ and $Rb^{-/-}$:$p130^{-/-}$ as well as triple $Rb^{-/-}$:$p107^{-/-}$:$p130^{-/-}$ mutant myoblasts were analyzed following chronic or acute inactivation of Rb. The data suggest that combined mutations in Rb and p107 and/or p130 increase myoblast cell death, and consequently reduce multinucleated myotube formation. However, once formed, mutant myotubes persist if treated with survival factors or hypoxia, which bypass the requirement for pRb. In contrast, triple knockout (TKO) myoblasts formed short, bi-nuclear myotubes, which may represent fusion of TKO myocytes or acytokinetic mitosis, which often occurs in cardiac myocytes and other tissues [556]. Additionally, in contrast to the effect of $p16^{INK4a}$ on fibroblasts [554], pRb, but not p107/p130, is critical for cell cycle exit during myogenic differentiation, suggesting that this defect may underlie the unique role of Rb – but not its relatives - in cancer.

4.3 Combined mutations in Rb and p130 do not counteract Rb myogenic defects in mgRb:$Rb^{-/-}$:$p130^{-/-}$ fetuses

Ectopic expression of p130, but not Rb, in the mouse C2C12 myoblast cell line inhibits myogenesis [160], suggesting that p130 loss may ameliorate the muscle defects in Rb-deficient embryos. In contrast, p107 over expression was shown to suppress ectopic

proliferation in myotubes derived from $Rb^{-/-}$ teratoma [149]. However, whether its loss would affect myoblast fusion and survival in the absence of Rb is not known. To determine the combined effects of Rb protein family on skeletal myogenesis, mgRb:$Rb^{+/-}$:$p107^{+/-}$ and mgRb:$Rb^{+/-}$:$p130^{+/-}$ double heterozygote mice were generated and intercrossed. Despite multiple attempts, live E14.5-E16.5 mgRb:$Rb^{-/-}$:$p107^{-/-}$ embryos were never recovered after intercrossing mgRb:$Rb^{+/-}$:$p107^{+/-}$ mice (not shown). In contrast, E14.5-E16.5 mgRb:$Rb^{-/-}$:$p130^{-/-}$ fetuses were identified following mgRb:$Rb^{+/-}$:$p130^{+/-}$ and/or mgRb:$Rb^{+/-}$:$p130^{-/-}$ interbreeding at the expected Mendelian frequency (6.25%, 12.5% [542]). At E17.5, the frequency of mgRb:$Rb^{-/-}$:$p130^{-/-}$ double knockout (DKO) embryos dropped to 1/59 [542]. Compared to E16.5 mgRb:$Rb^{-/-}$ single KO embryos, mgRb:$Rb^{-/-}$:$p130^{-/-}$ DKO fetuses displayed a more pronounced hunchback, suggesting reduced muscle toning (Figure 4. 1A; top panels). Indeed, histological sections through the epaxial and hypaxial skeletal muscles of mgRb:$Rb^{-/-}$:$p130^{-/-}$ fetuses revealed similar defects as in $Rb^{-/-}$ littermates, including shorter myofibers, and enlarged nuclei within myotubes compared to control (Figure 4. 1A, white arrowheads). Expression of MHC and troponin T, markers of early and late muscle differentiation, respectively, were similarly reduced relative to control (Figure 4. 1B). Analysis of apoptosis by terminal deoxynucleotidyl transferase biotin-dUTP nick end labeling (TUNEL) revealed no obvious differences: 22.2 ±9.3% and 20.1 ±4.7% for single KO and DKO, respectively (not shown) [542].

4.4 Combined mutations in Rb and p130 accelerate myotube degeneration *in vitro*

To test for a cell-autonomous effect of combined mutations in Rb and p130, we derived primary myoblasts from E16.5 mgRb:$Rb^{-/-}$:$p130^{-/-}$ limb muscles. Western blot analysis

verified that pRb and p130 were undetectable in mgRb:$Rb^{-/-}$:$p130^{-/-}$ cultures at DM-2 (Figure 4. 1C). Importantly, expression of p107, which was undetectable in DM-2 control myotube cultures, was readily detected in $Rb^{-/-}$ and mgRb:$Rb^{-/-}$:$p130^{-/-}$ DKO cultures (Figure 4. 1C). This increase in p107 is consistent with the presence of E2F binding sites in the p107 promoter and its regulation by pRb [148, 557], and may partly compensate for the combined loss of pRb and p130 in mgRb:$Rb^{-/-}$:$p130^{-/-}$ myoblasts.

Under differentiation conditions, control myoblasts fused to form long multinucleated myotubes that twitched for weeks *in vitro*. In contrast, both mgRb:$Rb^{-/-}$ and mgRb:$Rb^{-/-}$:$p130^{-/-}$ myoblasts initially fused to form short myotubes containing 3-6 nuclei, but underwent rapid degeneration by DM-2 to -3 so that by DM-5 to -6 all myotubes had degenerated (Figure 4. 1D). Reproducibly, the mgRb:$Rb^{-/-}$:$p130^{-/-}$ myoblasts exhibited reduced myotube formation, but similar degeneration kinetics relative to mgRb:$Rb^{-/-}$ cultures (Figure 4. 1D).

In contrast to control myotubes, which remained stably post-mitotic (Figure 4.2A, top panel), nuclei in $Rb^{-/-}$ myotubes incorporated BrdU when stimulated with mitogens, indicating they are unable to permanently exit the cell cycle (Figure 4.2A, middle) [149, 531, 552]. To test the cell cycle status of mgRb:$Rb^{-/-}$:$p130^{-/-}$ DKO myotubes, cultures were differentiated for 2 days and then re-fed growth medium in the presence of BrdU. Like $Rb^{-/-}$ myotubes, the mgRb:$Rb^{-/-}$:$p130^{-/-}$ myotubes failed to permanently exit the cell cycle and labeled positive for BrdU (Figure 4.2A, bottom). Next, it was assessed whether mgRb:$Rb^{-/-}$:$p130^{-/-}$ myotube degeneration was associated with increased apoptosis. TUNEL-positive nuclei were detected in unfused myoblasts and not within myotubes, and were more abundant in $Rb^{-/-}$ and mgRb:$Rb^{-/-}$:$p130^{-/-}$ cultures compared to control

(Figure 4.2B). Importantly, the level of apoptosis was slightly but reproducibly elevated in mgRb:Rb$^{-/-}$:p130$^{-/-}$ relative to mgRb:Rb$^{-/-}$ cultures (Figure 4.2B).

To examine the status of the mitochondrial network, MitoTracker®, a live-cell probe that accumulates in mitochondria with intact membrane potential was used. In control DM-2 myotubes, MitoTracker® staining revealed a uniform, net-like organization of mitochondria throughout the cytoplasm (Figure 4.2C, top). In contrast, both mgRb:Rb$^{-/-}$ and mgRb:Rb$^{-/-}$:p130$^{-/-}$ myotubes exhibited relatively sparse cytosolic staining and strong perinuclear MitoTracker®-positive aggregates in ~70% of myotubes (Figure 4.2C). Together, these results indicate that p130 loss does not ameliorate the Rb myogenic, but rather, exacerbates it by reducing myoblast survival before cell fusion.

4.5 Efficient rescue of mgRb:Rb$^{-/-}$:p130$^{-/-}$ DKO myotube degeneration by Bcl-2, 3-MA and hypoxia

I next asked whether inhibition of autophagy would rescue muscle degeneration of mgRb:Rb$^{-/-}$:p130$^{-/-}$ myotubes, as it does for mgRb:Rb$^{-/-}$ myotubes [552]. Remarkably, adenovirus-mediated transduction of Bcl-2, an inhibitor of apoptosis and autophagy [558], effectively rescued myogenic degeneration of mgRb:Rb$^{-/-}$:p130$^{-/-}$ myotubes, leading to long twitching myotubes (Figure 4.3A). This striking result demonstrates that when provided with a survival signal to counteract the effect of Rb loss, mgRb:Rb$^{-/-}$:p130$^{-/-}$ myotube formation and maintenance is sustained without active participation of pRb or p130. In chapter 3, it was demonstrated that inhibition of autophagy by 3-methyladenine (3-MA) - an antagonist of a class III phosphatidylinositol 3-kinase, Vps34, whose activity is necessary for autophagic vesicle nucleation [524] - rescued mgRb:Rb$^{-/-}$ myotubes from collapse [552]. Similarly, mgRb:Rb$^{-/-}$:p130$^{-/-}$ myotubes were rescued by

3-MA (Figure 4.3B) and the myotubes twitched for weeks in culture and were indistinguishable from control myotubes (Video S7). The pan-PPAR agonist bezafibrate [476, 478] also rescued the collapse of mgRb:$Rb^{-/-}$:$p130^{-/-}$ double mutant myotubes with similar efficiency as 3-MA (Figure 4.3B). As control, ectopic expression of a constitutively active, phospho-mutant pRb (Ad.$Rb^{\Delta K11}$) [528] prevented degeneration of mgRb:$Rb^{-/-}$:$p130^{-/-}$ myotubes (Figure 4.3A, bottom panel).

Finally, I tested whether hypoxia could rescue the myogenic defect induced by loss of Rb plus p130. Strikingly, despite reduced myotube formation in mgRb:$Rb^{-/-}$:$p130^{-/-}$ DKO cultures relative to mgRb:$Rb^{-/-}$, hypoxia efficiently maintained the survival of the DKO myotubes (Figure 4.3C). Together, these results indicate that combined loss of Rb and p130 reduces myoblast survival relative to Rb loss alone, yet when cell death is inhibited by various mechanisms, mgRb:$Rb^{-/-}$:$p130^{-/-}$ DKO myotubes, once formed, can survive like $Rb^{-/-}$ cultures, indicating that neither factor is required for stimulating or maintaining the differentiation program.

4.6 Lithium also rescues the Rb myogenic defect following acute or chronic inactivation of Rb

A previous report suggested that pRb is required during myogenic differentiation to protect cyclin D3 from glycogen synthase kinase-3β (GSK-3β)-mediated phosphorylation and proteosomal degradation [301]. Using a teratoma-derived $Rb^{-/-}$ myoblast cell line, it was shown that lithium chloride (LiCl), a GSK-3β inhibitor, enhanced myogenic differentiation of these cells by promoting cyclin D3 stabilization [301]. Indeed, LiCl also moderately rescued mgRb:$Rb^{-/-}$ myotube degeneration so that by DM-6 many MHC, MCK and troponin T positive myotubes persisted (Figure 3.8A & C). However, by DM-

10 most myotubes had degenerated (Figure 3.8A), and as shown in Figure 4.3D, cyclin D3 was robustly expressed in untreated mgRb:$Rb^{-/-}$ myotubes at DM-2, as well as in Bcl-2 rescued mgRb:$Rb^{-/-}$:$p130^{-/-}$ myotubes at DM-6 (Figure 4.3D), indicating that cyclin D3 stabilization is not pRb-dependent. Moreover, the LiCl-partial rescue mechanism also seems to be β-catenin independent. Normally, inhibition of GSK-3β leads to activation of β-catenin where it accumulates in the nucleus and complexes with the TCF/LEF (T cell factor/lymphoid enhancer factor) family of DNA-binding transcription factors to enhance gene expression [559]; a process effectively mimicked by LiCl [560]. However, transduction of an activated β-catenin allele [561] did not prevent degeneration of mgRb:$Rb^{-/-}$ myotubes (Figure 3.8A), suggesting a β-catenin-independent mechanism is involved in LiCl rescued Rb-deficient myotubes .

To assess cyclin D3 expression following acute inactivation of Rb, primary myoblasts were isolated from E16.5 $Rb^{f/f}$ fetuses, where exon 19 of Rb on both chromosomes is flanked by loxP sites [562]. $Rb^{f/f}$ myoblasts were then transduced with an adenovirus expressing cre recombinase (Ad.cre) at a relatively high multiplicity of infection (MOI) of 1250. Under these conditions, cre induced recombination of the $Rb^{f/f}$ allele was complete as determined by western blot analysis and immunostaining for pRb (Figure 4.4A-B). At 48hr post-transduction, $Rb^{\Delta f}$ myoblasts were induced to differentiate with DM and monitored for myotube formation. Like after chronic inactivation of Rb in mgRb:$Rb^{-/-}$ myoblasts, acute inactivation of Rb led to transient formation of short myotubes by DM-2 which progressively degenerated, so that by day 6 virtually no myotubes survived (Figure 4.4C & E (top)). At DM-2, cyclin D3 expression was indistinguishable in $Rb^{\Delta f}$ versus control myotubes (Figure 4.4D). LiCl partially

suppressed the collapse of $Rb^{\Delta f}$ myotubes leading to long myotubes that survived for more than 6 days post-differentiation (Figure 4.4C & E). Cyclin D3 was detected in these $Rb^{\Delta f}$ myotubes with intensity similar to control myotubes (Figure 4.4F). These results indicate that cyclin D3 expression may not be affected by Rb status and LiCl resuces the Rb myogenic defect in a cyclin D3-independent manner.

4.7 Inactivation of Rb but not p107 plus p130 leads to ectopic DNA synthesis and myotube degeneration

Next, the consequences of combined mutations in p130 and p107 on myogenic differentiation were investigated. Attempts to knock-down p107 by lenti-shRNA [148] failed as the primary myoblasts senesced or apoptosed following transduction (not shown). As another approach, primary myoblasts were isolated from E16.5 $Rb^{f/f}$ and $Rb^{f/f}$:$p107^{-/-}$:$p130^{-/-}$ composite mutant embryos. Deletions of p107 and p130 were determined by PCR (not shown) and confirmed by immunoblotting (Figure 4.5A). To test whether combined mutations in p107 and p130 resulted in deregulated cell proliferation in response to differentiation, $Rb^{f/f}$:$p107^{-/-}$:$p130^{-/-}$ myoblasts were induced to differentiate for 2 days and then transferred to high serum medium in the presence of BrdU. Whereas $Rb^{\Delta f}$ mutant myotubes incorporated BrdU (Figure 4.5B), $Rb^{f/f}$:$p107^{-/-}$:$p130^{-/-}$ myotubes stably exited the cell cycle (Figure 4.5C) and differentiated into long myotubes that twitched like control cultures (not shown). Thus, a unique function of Rb during terminal differentiation is to enforce cell cycle exit.

4.8 Acute inactivation of Rb protein family leads to reduced myotube formation whereas TKO myoblasts form short bi-nuclear myotubes

The effect of acute inactivation of Rb plus p130, Rb plus p107 or the entire Rb family protein on myogenic differentiation was investigated. $Rb^{f/f}$, $Rb^{f/f}$:$p130^{-/-}$, $Rb^{f/f}$:$p107^{-/-}$ and $Rb^{f/f}$:$p130^{-/-}$:$p107^{-/-}$ myoblasts were transduced with Ad.cre or control empty vector (Ad.EV) and induced to differentiate. First, the p107 status in proliferating myoblasts where Rb was acutely deleted was probed. In contrast to a study that showed senescence associated cell cycle arrest can be reversed by acute loss of Rb (due to a failure to upregulate p107), proliferating $Rb^{\Delta f}$ and $Rb^{\Delta f}$:$p130^{-/-}$ myoblasts robustly expressed p107 48hr post-transduction of Ad.cre (Figure 4.6A) and both $Rb^{\Delta f}$ and $Rb^{\Delta f}$:$p130^{-/-}$ myoblasts differentiated to form myotubes by DM-2 (Figure 4.6B-C). In addition, $Rb^{\Delta f}$:$p107^{-/-}$ myoblasts also formed short myotubes by DM-2 but slightly less than $Rb^{\Delta f}$:$p130^{-/-}$ cultures (Figure 4.6B-C). Notably, $Rb^{\Delta f}$:$p107^{-/-}$ and to lesser extent $Rb^{\Delta f}$ and $Rb^{\Delta f}$:$p130^{-/-}$ myoblasts formed a mixture of myotubes and elongated MHC-positive myocytes that did not fuse into multinucleated myotubes. Quantification of the percentage of multinucleated myotubes relative to total MHC-positive cells (i.e. myocytes and myotubes) revealed that $Rb^{\Delta f}$, $Rb^{\Delta f}$:$p130^{-/-}$ and $Rb^{\Delta f}$:$p107^{-/-}$ cultures contained, 52%, 44% and 32% myotubes relative to total MHC-positive cells, respectively (Figure 4.6C). For $Rb^{\Delta f}$:$p107^{-/-}$:$p130^{-/-}$ TKO cultures, mostly single cell myocytes formed in addition to some short bi-nuclear myotubes (~8%) (Figure 4.6B-C).

The reduced myotube formation in $Rb^{\Delta f}$:$p130^{-/-}$, $Rb^{\Delta f}$:$p107^{-/-}$ and $Rb^{\Delta f}$:$p107^{-/-}$:$p130^{-/-}$ cultures relative to $Rb^{\Delta f}$ and control myoblasts could be a result of intrinsic defects in differentiation or due to excessive myoblast cell death that reduces the availability of competent neighboring myocytes for cell fusion. To address these possibilities, I first used Mitotracker® to monitor the level of autophagy in differentiating

myotubes. Following acute inactivation of Rb, transiently formed $Rb^{\Delta f}$ myotubes, like mgRb:$Rb^{-/-}$ myotubes, exhibited abnormal perinuclear clustering of mitochondria (Figure 4.7A, bottom left panel). The level of mitochondrial aggregation in $Rb^{\Delta f}$:$p107^{-/-}$ and $Rb^{\Delta f}$:$p130^{-/-}$ DKO myotubes was similar to that seen in $Rb^{\Delta f}$ cultures. Interestingly, the bi-nuclear TKO myotubes seemed to exhibit mitochondrial aggregation throughout the cytosol and not specifically in the perinuclear region.

Next, the number of TUNEL-positive cells was used to quantitate the level of apoptosis in the different cultures at DM-2. The TKO cultures exhibited the highest level of apoptosis (~119%) followed by $Rb^{\Delta f}$:$p107^{-/-}$ (49%), $Rb^{\Delta f}$:$p130^{-/-}$ (24%) and $Rb^{\Delta f}$ (19%) myoblasts (Figure 4.7B-C). Thus, the reduction in myotube number, and increased elongated myocytes, was correlated to the level of apoptosis in the various mutant cultures. Myoblasts seeded at low-density do not fuse under differentiation conditions and instead form elongated myocytes that undergo differentiation in the absence of fusion [563]. Therefore, the reduced myotubes and increase in myocytes in the DKO and TKO cultures could reflect the increased apoptosis and reduced number of competent myocytes available for fusion.

4.9 Hypoxia rescues myotubes formed in the absence of Rb, p130 and/or p107

In chapter 3 it was shown that hypoxia rescued the myogenic defect following acute inactivation of Rb [552]. To test whether hypoxia could prevent myotube degeneration following acute inactivation of Rb plus its relatives, $Rb^{f/f}$, $Rb^{f/f}$:$p130^{-/-}$, $Rb^{f/f}$:$p107^{-/-}$ and $Rb^{f/f}$:$p130^{-/-}$:$p107^{-/-}$ myoblasts were transduced with Ad.cre or Ad.EV and then either maintained in normoxia or shifted to hypoxia (1% O_2). Under normoxia, no myotube survived at DM-5 (Figure 4.8A, top row). Remarkably, despite the enhanced cell death,

and consequently, reduced number of myotubes, many $Rb^{\Delta f}$, $Rb^{\Delta f}$:$p130^{-/-}$ and $Rb^{\Delta f}$:$p107^{-/-}$ myotubes survived and twitched under hypoxia (Figure 4.8A-C, Figure 4.9A) (videos S8-10). In constrast, TKO myotubes degenerated, forming very thin myotubes, some of which twitched nonetheless (video S11). The ratio of myotubes to myocytes at DM-5 was similar to that observed at DM-2 (compare Figure 4.6C to Figure 4.8C). To directly test this, I induced the various cultures to differentiate under hypoxia and then counted the number of myotubes at DM-2 and DM-6. As shown in figure 4.8D, the ratio of myotubes at days 6 and 2 was similar in all cultures, suggesting that once myotubes are formed, they are capable of surviving in hypoxia independent of the Rb protein family. Together, these results suggest that the reduced differentiation capacity of $Rb^{\Delta f}$:$p130^{-/-}$ and $Rb^{\Delta f}$:$p107^{-/-}$ relative to $Rb^{\Delta f}$ myoblasts reflects an increase in apoptosis, which in turn limits the availability of surrounding myocytes capable of fusion, and not an inherent impairment in differentiation *per se*. In contrast, the $Rb^{f/f}$:$p130^{-/-}$:$p107^{-/-}$ myoblasts exhibited a severe differentiation defect even under hypoxia that may reflect the massive cell death outside the myotubes as well as the complete dysregulation of E2Fs in myotubes that may hinder differentiation and/or metabolism.

4.10 The nature of the bi-nuclear TKO myotubes

If TKO myotubes originate from cell fusion, this would suggest that the complete Rb family is dispensable for this process, and thus, these myotubes were analyzed further. I first asked whether the bi-nucleus TKO myotubes represent some rare $Rb^{f/f}$:$p130^{-/-}$:$p107^{-/-}$ myoblasts in which the $Rb^{f/f}$ allele had not been deleted. This was tested by immunostaining DM-2 TKO myotube cultures for pRb. None of over 80 short bi-nuclear myotubes from two independent cultures expressed pRb (Figure 4.9B). Interestingly, the

short bi-nuclear myotubes may represent fusion of TKO myocytes or acytokinetic mitosis, which occurs normally in cardiac myocytes and other tissues [556]. In many of the bi-nuclear TKO myotubes, which represent about 12.5% of total MHC-positive cells, the two nuclei were in very close proximity or in contact with each other. Further, in many of the single-nucleus myocytes, there was a single enlarged nucleus that appeared to contain a septation, suggestive of endomitosis (Figure 4.9C). Presently, the source of the two nuclei, whether from fusion or duplication, within the short TKO myotubes remains to be determined.

Figure 4. 1. Exacerbated myogenic defects in mgRb:$Rb^{-/-}$:$p130^{-/-}$ compared to mgRb:$Rb^{-/-}$ fetuses

(A) Macro-images of ctrl, mgRb:$Rb^{-/-}$ and mgRb:$Rb^{-/-}$:$p130^{-/-}$ embryos at E16.5 (A-C). Hematoxylin &eosin (H&E) histology staining reveals the cellular morphology at mid-sagittal section (D-F), epaxial muscles (G-I) and hypaxial muscles (J-L). Arrowheads point to enlarged nuclei within myofibers. **(B)** Confocal images show Troponin T (green) expression in skeletal muscle sections of control (ctrl) (A-B) mgRb:$Rb^{-/-}$ (C-D) and mgRb:$Rb^{-/-}$:$p130^{-/-}$ (E-F) embryos using an anti-fast troponin T antibody. MHC (green) expression in skeletal muscle sections of ctrl (G) mgRb:$Rb^{-/-}$ (H) and mgRb:$Rb^{-/-}$:$p130^{-/-}$ (I) embryos using an anti-MHC antibody. DAPI counterstained nuclei (blue). **(C)** Average number of myotubes counted on indicated days post-differentiation. Each time point is an average ± s.d. of 6 fields at 200X (n=4). **(D)** Western blot analysis for pRb and p107 in DM-2 (ctrl), mgRb:$Rb^{-/-}$ and mgRb:$Rb^{-/-}$:$p130^{-/-}$ myoblast cultures. Tubulin: loading control. Western blot analysis of p130 in DM-2 ctrl and mgRb:$Rb^{-/-}$:$p130^{-/-}$ cultures. Arrow indicates location of p130. Lower bands are non-specific and also served as the loading control.

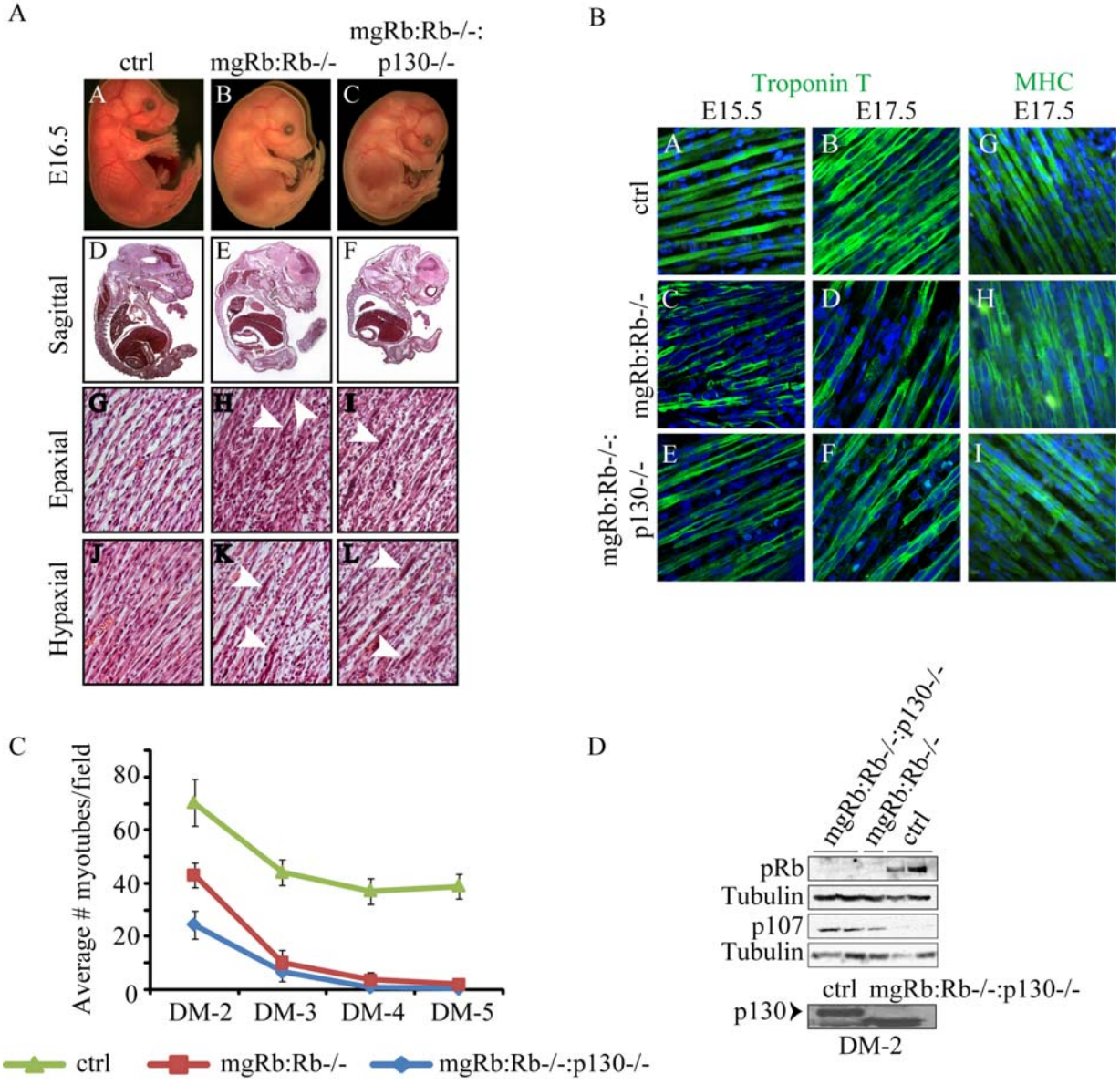
A
ctrl
mgRb:Rb-/-
mgRb:Rb-/-:
p130-/-
E16.5
Sagittal
Epaxial
Hypaxial
B
Troponin T
E15.5
E17.5
MHC
E17.5
ctrl
mgRb:Rb-/-
mgRb:Rb-/-:
p130-/-
C
Average # myotubes/field
80
60
40
20
0
DM-2
DM-3
DM-4
DM-5
ctrl
mgRb:Rb-/-
mgRb:Rb-/-:p130-/-
D
mgRb:Rb-/-:p130-/-
mgRb:Rb-/-
ctrl
pRb
Tubulin
p107
Tubulin
ctrl
mgRb:Rb-/-:p130-/-
p130
DM-2

Figure 4. 2. Rb:p130 double-mutant myotubes exhibit ectopic DNA synthesis, are TUNEL-negative & have perinuclear clustering of mitochondria

(A) Immunostaining for BrdU in ctrl, mgRb:$Rb^{-/-}$ and mgRb:$Rb^{-/-}$:$p130^{-/-}$ myotubes at DM-2. Myoblasts were differentiated for 1 day, exposed to 20μM BrdU for 16 hr in the presence of growth medium (GM) and stained for MHC (red) and BrdU (green). Arrowheads label BrdU positive nuclei within myotubes. **(B)** MHC (red) and TUNEL (green) staining at DM-2. Arrowheads indicate TUNEL positive nuclei which are invariably located outside myotubes. **(C)** Mitotracker® (red) staining at DM-2. Arrowheads point to large Mitotracker®-positive perinuclear aggregates.

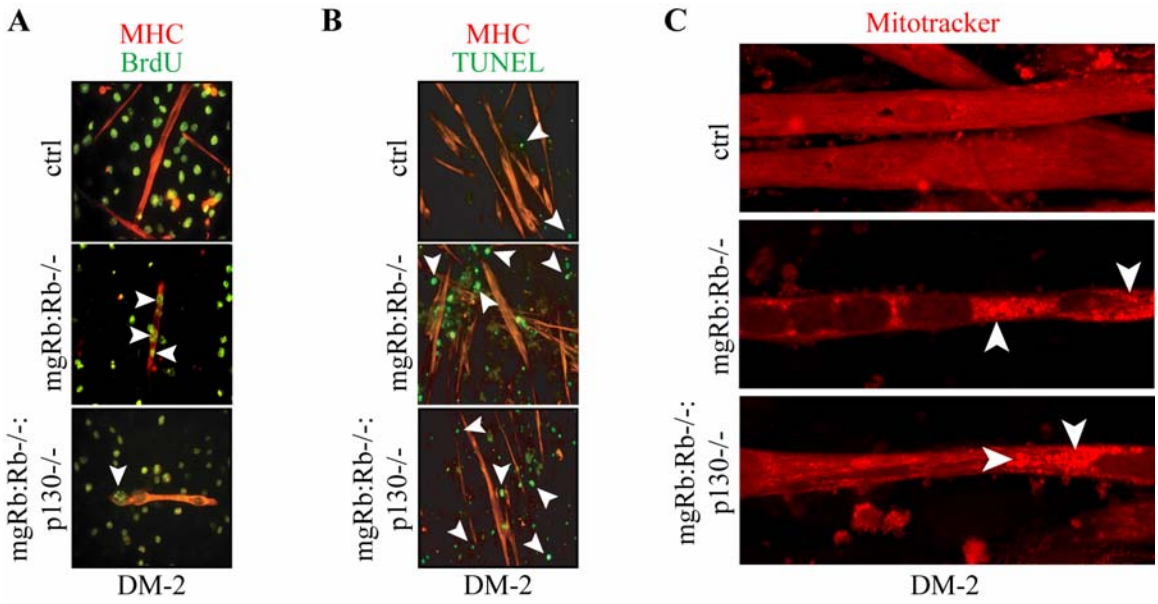
A
MHC
BrdU
ctrl
mgRb:Rb-/-
mgRb:Rb-/-:
p130-/-
DM-2
B
MHC
TUNEL
ctrl
mgRb:Rb-/-
mgRb:Rb-/-:
p130-/-
DM-2
C
Mitotracker
ctrl
mgRb:Rb-/-
mgRb:Rb-/-:
p130-/-
DM-2

Figure 4. 3. Rescue of Rb:p130 double-mutant myotubes by Bcl-2, hypoxia and 3-MA

(A) Brightfield images of mgRb:$Rb^{-/-}$:$p130^{-/-}$ myoblasts transduced with Ad.GFP, Ad.Bcl-2 or Ad.RbΔK11 and then induced to differentiate for 14 days. Arrowheads point to myotubes. Note: absence of myotubes in Ad.GFP transduced culture. **(B)** Average number of mgRb:$Rb^{-/-}$:$p130^{-/-}$ myotubes following treatment with 3-MA, bezafibrate or DM as indicated. Counts are average ± s.d. of 6 fields at 200X (n=3). **(C)** Immunostaining for MHC (green) in ctrl and mgRb:Rb-/-:p130-/- cultures differentiated under normoxia or hypoxia. Note the absence of myotubes in mgRb:$Rb^{-/-}$:$p130^{-/-}$ culture at DM-5 normoxia compared to robust myotubes under hypoxia at DM-5. DAPI counterstained nuclei (blue). **(D)** Top panel. Ctrl and $Rb^{-/-}$ myoblasts were induced to differentiate and immunostained for cyclin D3 at DM-2 (red). Nuclei were counterstained with DAPI (blue). Pink color in merged images is overlap between red and blue, indicating nuclear localization of cyclin D3. Bottom panel. Expression of cyclin D3 (red) in Bcl-2 rescued mgRb:$Rb^{-/-}$:$p130^{-/-}$ myotubes at DM-6.

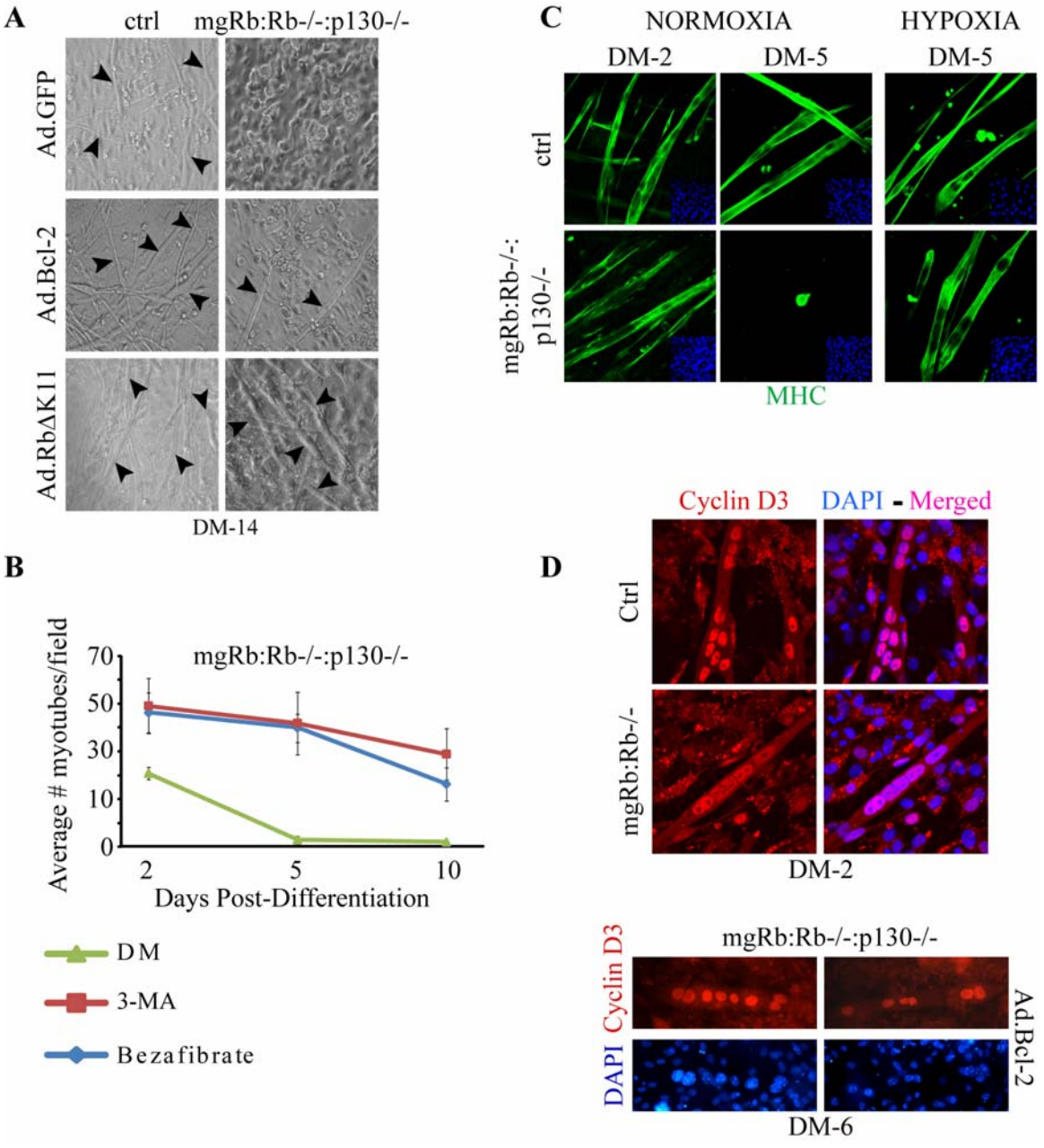
A
ctrl
mgRb:Rb-/-:p130-/-
Ad.GFP
Ad.Bcl-2
Ad.RbΔK11
DM-14
B
mgRb:Rb-/-:p130-/-
Average # myotubes/field
70
50
30
10
0
2
5
10
Days Post-Differentiation
DM
3-MA
Bezafibrate
C
NORMOXIA
HYPOXIA
DM-2
DM-5
DM-5
ctrl
mgRb:Rb-/-:
p130-/-
MHC
D
Cyclin D3
DAPI - Merged
Ctrl
mgRb:Rb-/-
DM-2
mgRb:Rb-/-:p130-/-
Cyclin D3
DAPI
Ad.Bcl-2
DM-6

Figure 4. 4. LiCl delays degeneration of myotubes with acutely inactivated Rb

(A) $Rb^{f/f}$ myoblasts were transduced with Ad.GFP or Ad.cre. At 48hr post-transduction cultures were immunostained for pRb (red). DAPI counterstained nuclei (blue). **(B)** $Rb^{f/f}$ myoblasts were transduced with Ad.GFP or Ad.cre and immunoblotted for pRb 48hr post-transduction. Tubulin served as loading control. **(C)** Average number of $Rb^{\Delta f}$ myotubes following LiCl treatment or untreated (DM) as indicated. Counts are average ± s.d. of 6 fields at 200X (n=3). **(D)** Expression of cyclin D3 (red) in Ad.EV and Ad.cre $Rb^{f/f}$ myotubes at DM-2. DAPI counterstained nuclei (blue). **(E)** Immunostaining for MHC (red) of $Rb^{f/f}$ myoblast cultures transduced with Ad.cre and induced to differentiate 48hrs later in the absence (top) or presence (bottom) of LiCl for 2 or 6 days. DAPI counterstained nuclei (blue). **(F)** Immunostaining for cyclin D3 (red) of $Rb^{f/f}$ myoblast cultures transduced with Ad.GFP or Ad.cre, and induced to differentiate 48hrs later in the absence (top) or presence (bottom) of LiCl for 5 days. DAPI counterstained nuclei (blue).

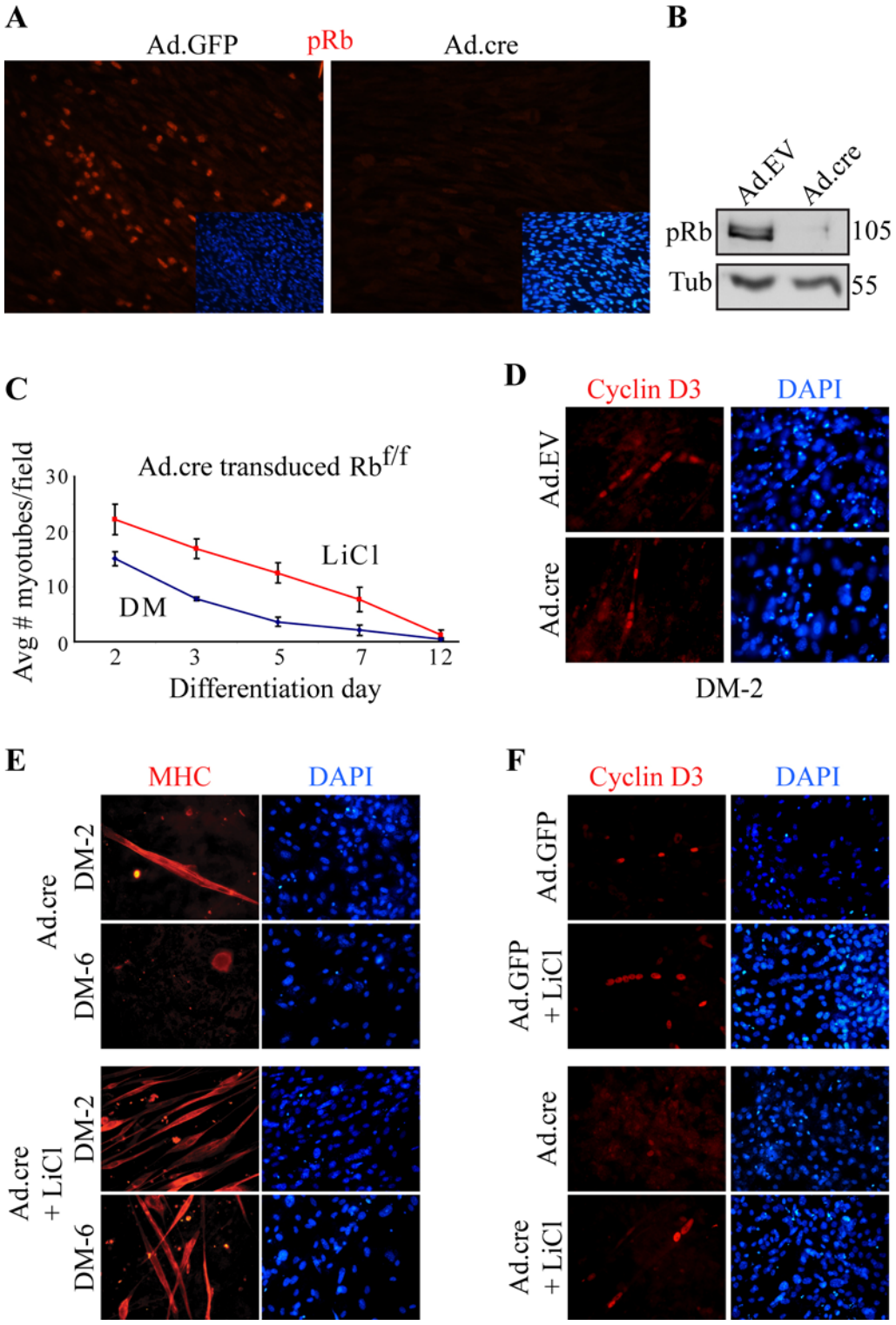
A
Ad.GFP
pRb
Ad.cre
B
Ad.EV
Ad.cre
pRb
105
Tub
55
C
Ad.cre transduced Rb^f/f
Avg # myotubes/field
30
20
10
0
LiCl
DM
2
3
5
7
12
Differentiation day
D
Cyclin D3
DAPI
Ad.EV
Ad.cre
DM-2
E
MHC
DAPI
Ad.cre
DM-2
DM-6
Ad.cre + LiCl
DM-2
DM-6
F
Cyclin D3
DAPI
Ad.GFP
Ad.GFP + LiCl
Ad.cre
Ad.cre + LiCl

Figure 4. 5. Inactivation of Rb but not p107:p130 leads to ectopic DNA synthesis and degeneration

(A) Western blot analysis of pRb, p107 and p130 in skeletal muscle of E16.5 $Rb^{f/f}$:p107+/-:p130+/- (ctrl) and $Rb^{f/f}$:p107-/-:p130-/- fetus. **(B)** Immunostaining for BrdU and MHC in Ad.EV and Ad.cre transduced $Rb^{f/f}$ myoblasts at DM-2. Myoblasts were differentiated for 1 day, exposed to 20μM BrdU for 16 hr in the presence of GM and stained for MHC (red) and BrdU (green). Arrowheads label BrdU positive nuclei. **(C)** Immunostaining for BrdU and MHC in $Rb^{f/f}$, $Rb^{f/f}$:$p107^{-/-}$, $Rb^{f/f}$:$p130^{-/-}$ and $Rb^{f/f}$:$p107^{-/-}$:$p130^{-/-}$ myoblasts at DM-2. Myoblasts were differentiated for 1 day, exposed to 20μM BrdU for 16 hr in the presence of GM and stained for MHC (red) and BrdU (green). Note absence of BrdU-positive nuclei in myotubes.

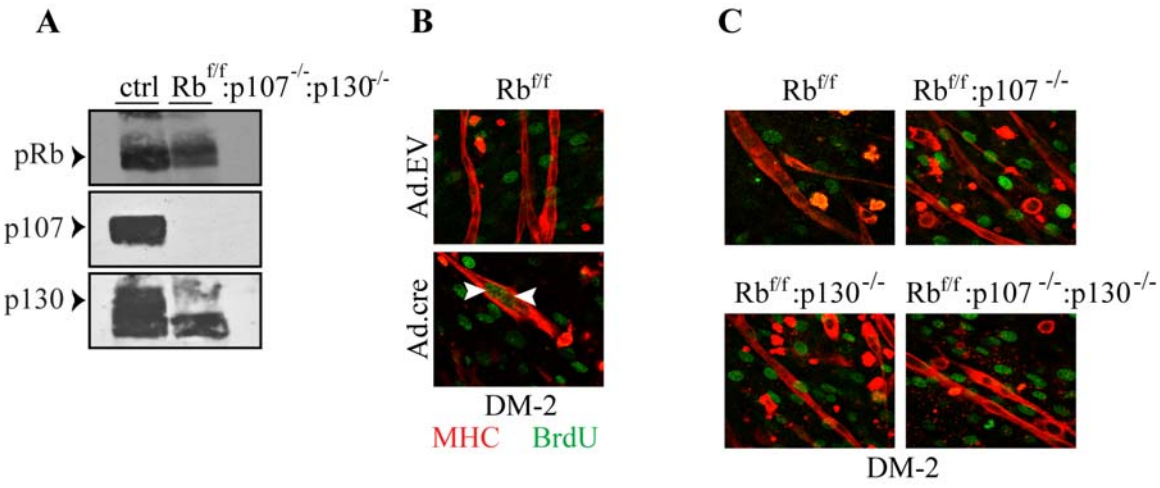
A
ctrl
Rb f/f :p107 -/- :p130 -/-
pRb
p107
p130
B
Rb f/f
Ad.EV
Ad.cre
DM-2
MHC
BrdU
C
Rb f/f
Rb f/f :p107 -/-
Rb f/f :p130 -/-
Rb f/f :p107 -/- :p130 -/-
DM-2

Figure 4. 6. Acute inactivation of Rb protein family leads to reduced myotube formation

(A) Western blot analysis of p107 and pRb 48hr post-transduction of Ad.EV and Ad.cre in $Rb^{f/f}$ and $Rb^{f/f}$:$p130^{-/-}$ myoblasts. Tubulin: loading control. **(B)** Immunostaining for MHC (green) in Ad.EV and Ad.cre transduced $Rb^{f/f}$ (a-b), $Rb^{f/f}$:$p107^{-/-}$ (c-d), $Rb^{f/f}$:$p130^{-/-}$ (e-f) and $Rb^{f/f}$:$p107^{-/-}$:$p130^{-/-}$ (g-h) myoblast cultures at DM-2. DAPI counterstained nuclei (blue). **(C)** Quantification of percent multinucleated myotubes relative to the number of total number of MHC-positive cells in Ad.EV and Ad.cre transduced $Rb^{f/f}$, $Rb^{f/f}$:$p107^{-/-}$, $Rb^{f/f}$:$p130^{-/-}$ and $Rb^{f/f}$:$p107^{-/-}$:$p130^{-/-}$ cultures at DM-2 in normoxia. Numbers on bars represent % for the respective samples.

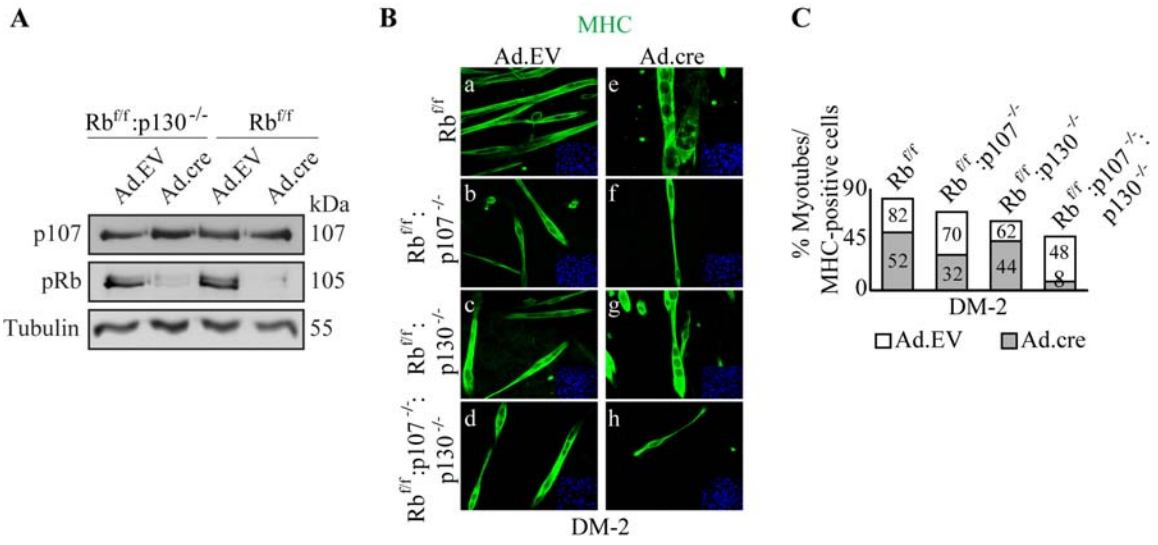
A
Rb f/f :p130 -/-
Rb f/f
Ad.EV
Ad.cre
Ad.EV
Ad.cre
kDa
p107
107
pRb
105
Tubulin
55
B
MHC
Ad.EV
Ad.cre
Rb f/f
Rb f/f : p107 -/-
Rb f/f : p130 -/-
Rb f/f :p107 -/- : p130 -/-
a
b
c
d
e
f
g
h
DM-2
C
% Myotubes/ MHC-positive cells
90
45
0
Rb f/f
Rb f/f :p107 -/-
Rb f/f :p130 -/-
Rb f/f :p107 -/- : p130 -/-
82
52
70
32
62
44
48
8
DM-2
Ad.EV
Ad.cre

Figure 4. 7. Acute inactivation of Rb protein family leads to perinuclear clustering of mitochondria and increased apoptosis

(A) Mitotracker staining of Ad.EV and Ad.cre transduced $Rb^{f/f}$, $Rb^{f/f}$:$p107^{-/-}$, $Rb^{f/f}$:$p130^{-/-}$ and $Rb^{f/f}$:$p107^{-/-}$:$p130^{-/-}$ cultures at DM-2. Arrowheads point to large perinuclear aggregates in Ad.cre transduced myotubes. **(B)** TUNEL staining (green) of Ad.EV and Ad.cre transduced $Rb^{f/f}$ (a-b), $Rb^{f/f}$:$p107^{-/-}$ (c-d), $Rb^{f/f}$:$p130^{-/-}$ (e-f) and $Rb^{f/f}$:$p107^{-/-}$:$p130^{-/-}$ (g-h) cultures at DM-2. DAPI counterstained nuclei (blue). Note TUNEL positive nuclei are never located within myotubes. **(C)** Percent increase in TUNEL-positive cells in Ad.cre relative to Ad.EV transduced cultures. Error bars represent s.d.

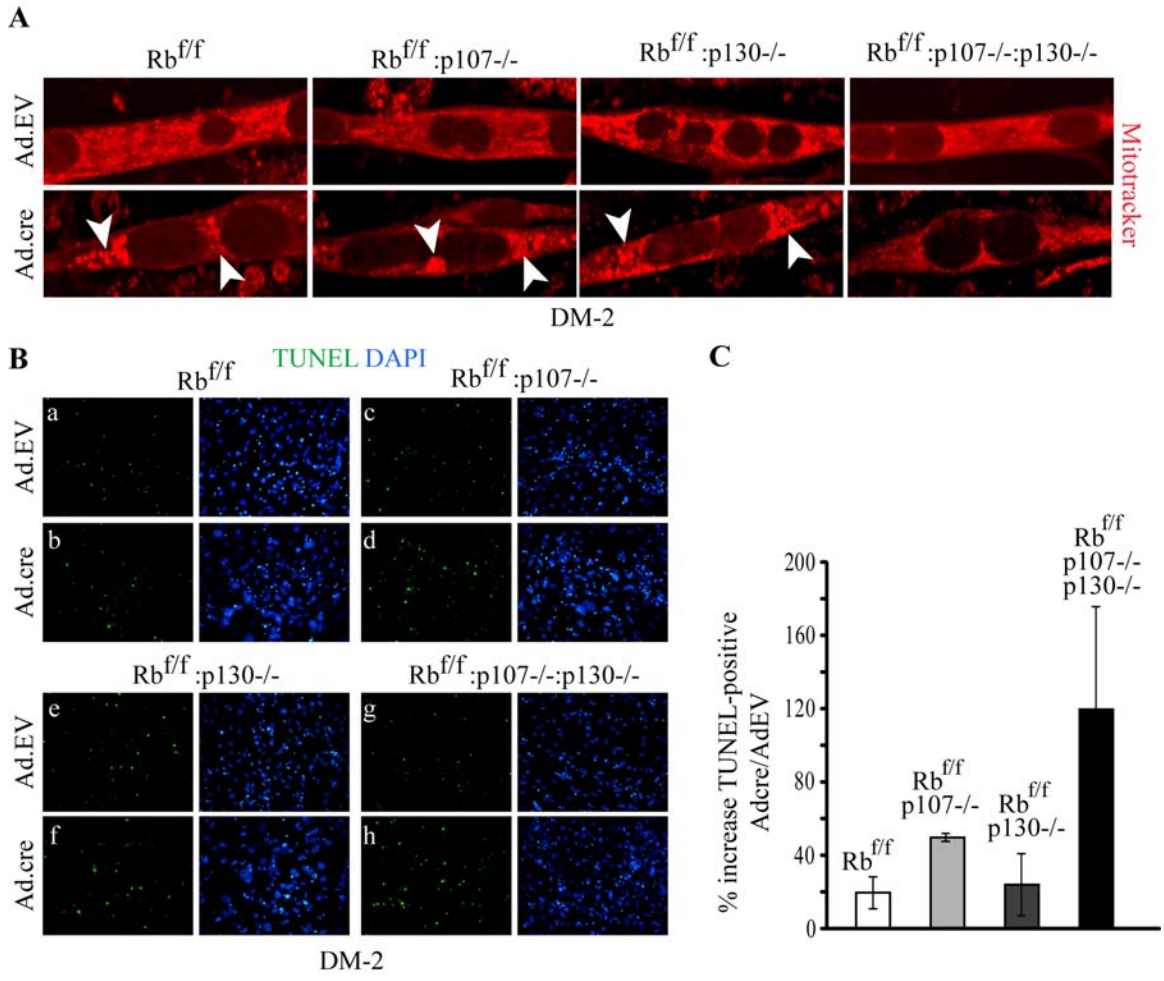
A
Rb f/f
Rb f/f :p107-/-
Rb f/f :p130-/-
Rb f/f :p107-/-:p130-/-
Ad.EV
Ad.cre
Mitotracker
DM-2
B
TUNEL DAPI
Rb f/f
Rb f/f :p107-/-
Rb f/f :p130-/-
Rb f/f :p107-/-:p130-/-
a
b
c
d
e
f
g
h
Ad.EV
Ad.cre
DM-2
C
% increase TUNEL-positive Adcre/AdEV
200
160
120
80
40
0
Rb f/f
Rb f/f p107-/-
Rb f/f p130-/-
Rb f/f p107-/- p130-/-

Figure 4. 8. Hypoxia rescues myotubes in absence of Rb family members

(A) Top row panels. Immunostaining for MHC (green) of Ad.cre transduced $Rb^{f/f}$, $Rb^{f/f}$:$p107^{-/-}$, $Rb^{f/f}$:$p130^{-/-}$ and $Rb^{f/f}$:$p107^{-/-}$:$p130^{-/-}$ cultures at DM-5 in normoxia. Middle and bottom panels. Immunostaining for MHC (green) of Ad.EV and Ad.cre transduced $Rb^{f/f}$, $Rb^{f/f}$:$p107^{-/-}$, $Rb^{f/f}$:$p130^{-/-}$ and $Rb^{f/f}$:$p107^{-/-}$:$p130^{-/-}$ cultures at DM-5 in hypoxia. DAPI counterstained nuclei (blue). **(B)** Quantification of myotube formation in $Rb^{f/f}$, $Rb^{f/f}$:$p107^{-/-}$, $Rb^{f/f}$:$p130^{-/-}$ and $Rb^{f/f}$:$p107^{-/-}$:$p130^{-/-}$ cultures transduced with Ad.EV or Ad.cre and induced to differentiate 48hr later for 5 days. Counts were conducted at DM-5. Counts are an average of 6 representative fields (n=4); error bars represent s.d. Test of statistical significance performed between Ad.EV and Ad.cre data. * $p < 0.05$ and ** $p < 0.07$. **(C)** Quantification of percent multinucleated myotubes relative to the number of total number of MHC-positive cells in Ad.EV and Ad.cre transduced $Rb^{f/f}$, $Rb^{f/f}$:$p107^{-/-}$, $Rb^{f/f}$:$p130^{-/-}$ and $Rb^{f/f}$:$p107^{-/-}$:$p130^{-/-}$ cultures at DM-5 in hypoxia. Numbers on bars represent % for the respective samples. **(D)** Quantification of myotube formation in $Rb^{f/f}$, $Rb^{f/f}$:$p107^{-/-}$, $Rb^{f/f}$:$p130^{-/-}$ and $Rb^{f/f}$:$p107^{-/-}$:$p130^{-/-}$ cultures transduced with Ad.EV or Ad.cre and induced to differentiate 48hr in hypoxia. Counts were conducted at DM-2 and DM-6. Error bars represent s.d.

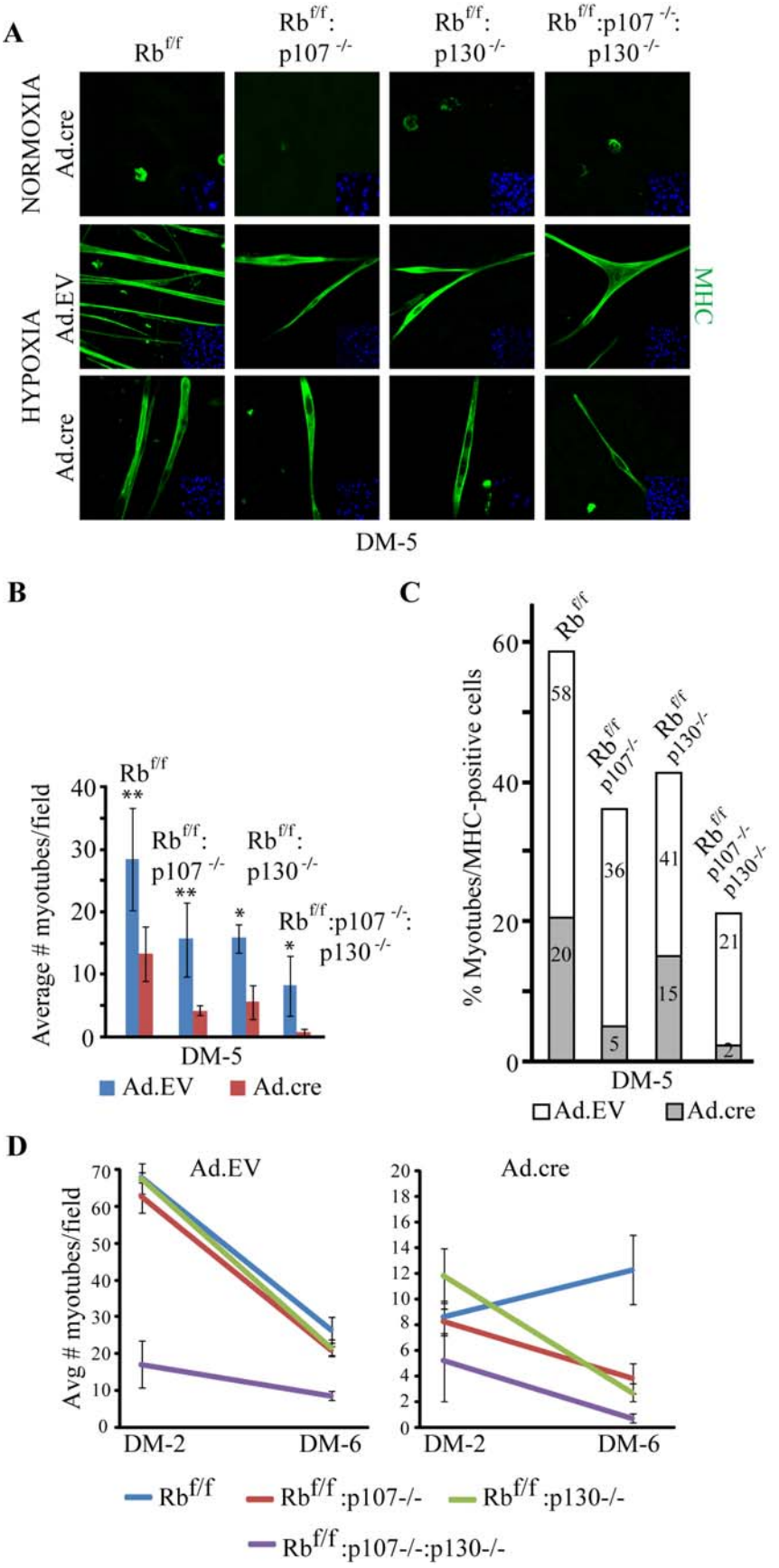
A
Rb f/f
Rb f/f: p107 -/-
Rb f/f: p130 -/-
Rb f/f:p107 -/-: p130 -/-
NORMOXIA
Ad.cre
HYPOXIA
Ad.EV
Ad.cre
MHC
DM-5
B
Average # myotubes/field
Rb f/f
Rb f/f: p107 -/-
Rb f/f: p130 -/-
Rb f/f:p107 -/-: p130 -/-
DM-5
Ad.EV
Ad.cre
C
% Myotubes/MHC-positive cells
Rb f/f
Rb f/f p107 -/-
Rb f/f p130 -/-
Rb f/f p107 -/- p130 -/-
58
20
36
5
41
15
21
2
DM-5
Ad.EV
Ad.cre
D
Avg # myotubes/field
Ad.EV
Ad.cre
DM-2
DM-6
Rb f/f
Rb f/f :p107-/-
Rb f/f :p130-/-
Rb f/f :p107-/-:p130-/-

Figure 4. 9. Rare TKO myotubes survive under hypoxia

(A) Brightfield images of Ad.EV and Ad.cre transduced $Rb^{f/f}$:$p107^{-/-}$:$p130^{-/-}$ cultures at DM-6 in hypoxia. Arrowheads point to myotubes. Note: presence of thin putative myotube in Ad.cre transduced culture. **(B)** Top row (Low). Immunostaining for pRb (green) of Ad.EV and Ad.cre transduced $Rb^{f/f}$:$p107^{-/-}$:$p130^{-/-}$ cultures at DM-2 (captured at 400x). Bottom Row (High). Higher magnification (630x) of Ad.cre transduced $Rb^{f/f}$:$p107^{-/-}$:$p130^{-/-}$ two-nucleus myotube immunostained for pRb (green) demonstrating absence of detectable pRb. DAPI counterstained nuclei (blue). Arrowheads point to nuclei within myotube. **(C)** Top row (Low). Immunostaining for MHC (red) and DAPI nuclear stain (blue) of Ad.cre transduced $Rb^{f/f}$:$p107^{-/-}$:$p130^{-/-}$ culture at DM-2 (captured at 400x). Arrowhead points to nucleus. Bottom row (High). Higher magnification (630x) of the Ad.cre transduced $Rb^{f/f}$:$p107^{-/-}$:$p130^{-/-}$ myotube shown in top row immunostained for MHC (red) and DAPI nuclear stain (blue) demonstrating what appears to be single nucleus with a septation.

A

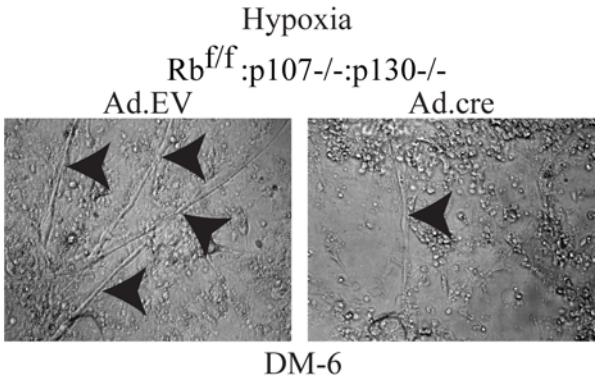
Hypoxia
Rb^f/f:p107-/-:p130-/-
Ad.EV
Ad.cre
DM-6

B

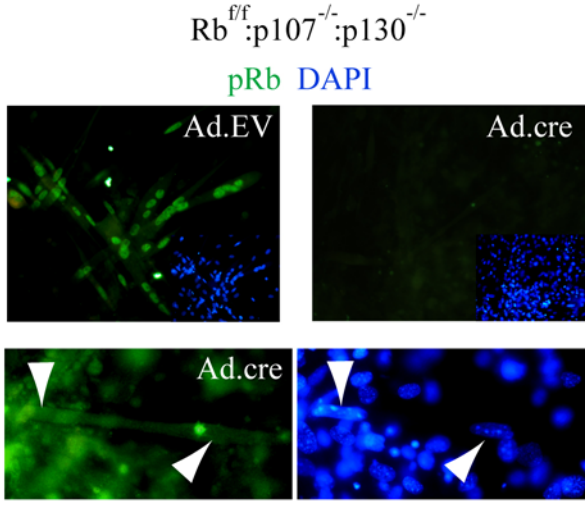
Rb^f/f:p107^-/-:p130^-/-
pRb DAPI
Low
High
Ad.EV
Ad.cre
Ad.cre

C

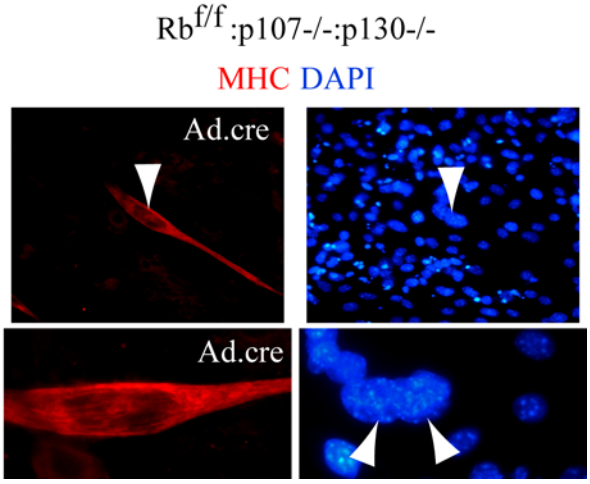
Rb^f/f:p107-/-:p130-/-
MHC DAPI
Low
High
Ad.cre
Ad.cre

CHAPTER 5: DISCUSSION

5.1 Discussion

In this thesis, I demonstrate that Rb is not required to actively participate during terminal muscle differentiation, as commonly thought, but is required to enforce cell cycle exit and to suppress cell death. In contrast to control myoblasts, which formed long myotubes that survived for weeks in culture, $Rb^{-/-}$ myoblasts fused to form short myotubes that failed to exit the cell cycle and progressively degenerated, so that by day 5 post-differentiation, virtually no myotubes remained. Myotube degeneration was associated with perinuclear mitochondrial clustering, autophagic degradation and reduced ATP levels. When treated with autophagy inhibitors (Bcl-2, 3-MA) or shifted to hypoxic conditions (1% O_2), $Rb^{-/-}$ myotubes twitched and survived for weeks and expressed normal levels of myogenic markers comparable to control myotubes. Thus, Rb is not required to stimulate muscle-specific transcription factors during myogenesis, but is required to inhibit apoptosis in myoblasts, for cell cycle exit and to suppress autophagy in myotubes. Subsequently, I investigated the contribution of the pRb relatives, p107 and p130, to the $Rb^{-/-}$ myogenic defect. I show that chronic or acute inactivation of Rb plus p130 or Rb plus p107 increases myoblast cell death and reduces myotube formation. Bcl-2, autophagy antagonist, lithium or hypoxia, extended myotube survival, leading to contracting myotubes that appeared indistinguishable from control. Mutations in all three family members (TKO) accelerated myoblast cell death and led to elongated myocytes and short, bi-nuclear myotubes, some of which twitched under hypoxia. Whereas nuclei in $Rb^{-/-}$ myotubes were unable to stably exit the cell cycle, myotubes lacking both p107 and p130, but containing functional Rb, became permanently post-mitotic. Together these results demonstrate that p107 and p130 contribute to myoblast survival during myogenesis but

that they can differentiate in the absence of Rb function if survival is maintained by alternative pathways.

5.2 Rescue of myogenic defects in Rb-deficient cells by inhibition of autophagy or by hypoxia-induced glycolytic shift

It is commonly thought that Rb is required for cell cycle exit, apoptosis and differentiation [91, 93, 127, 564-566]. Specifically in the case of skeletal muscle differentiation, Rb is believed to be needed for cell cycle exit and to actively participate in differentiation according to the three models outlined in section 1.3 [102, 103, 149, 151, 325]. However, the early stages of muscle differentiation proceed apparently normal in mouse $Rb^{-/-}$ myoblasts, including myotube formation, *in vitro* [552], but as opposed to control myotubes, fail to exit the cell cycle and undergo rapid degeneration beginning 3 days post-differentiation. Importantly, this *in vitro* abortive muscle differentiation phenotype recapitulates the *in vivo* muscle differentiation defects observed in partially rescued Rb-deficient embryos [93]. Strikingly, by uncoupling differentiation from survival and cell-cycle exit in differentiating $Rb^{-/-}$ myoblasts, data from this thesis support the view that pRb is required during muscle differentiation to maintain the post-mitotic state and suppress degeneration and not for differentiation *per se*.

This contrasts studies suggesting pRb actively participates in myogenesis by cooperating with muscle-specific transcription factors and sequestering inhibitors of differentiation (described in section 1.3). Despite the fusion of Rb-deficient myoblasts into myotubes, cell cycle exit and survival are impaired, opening the possibility that an interaction between pRb and p130 with MyoD, for example, may be necessary for proper cell cycle exit and survival of the differentiated state. Indeed, studies have shown that

MyoD induces p21 and cell cycle exit, but whether pRb/p130 is required for this function is unknown [278, 307]. Since the first report describing a pRb-MyoD interaction in 1993 [102], it still remains unresolved whether these factors form a *bona fide* interaction *in vivo* and if they do, what the role of this complex is. A recent genome-wide screen for interactions among transcription factors in both human and mouse using a mammalian two-hybrid system independently demonstrated that human pRb and p130, but not p107, interact with MYOD and C/EBP β (among many other factors) [106]. In comparison, mouse pRb and p130, but not p107, were found to interact with RUNX2 but not with MYOD [106]. However, mouse pRb did not bind E2Fs either and may form very weak interactions in this system and might, for example, reflect intrinsic differences between mouse and human proteins (mouse pRb (921a.a.) [121] compared to human pRb (928a.a.) [567] and mouse p130 (1135a.a.) [568] compared to human p130 (1139a.a.) [568]). In either system, an interaction between p107 and MYOD or other differentiation factors was not detected, which contrasts a previous report [149], but the data are consistent with the reduced expression of p107 during differentiation. This questions the concept that pRb is actively required for differentiation and even the common idea that p107 functionally compensates for Rb loss during muscle differentiation [149, 150].

The notion that pRb is not required to actively participate in differentiation, but for cell cycle exit and survival of the differentiated state may also hold in other cell-types [98, 99, 101]. For example, it was observed that $Rb^{-/-}$ cells contribute to most adult tissues in $Rb^{-/-}$:$Rb^{+/+}$ chimeric mice [569, 570], whereby most of these tissues were morphologically normal despite containing large proportions of $Rb^{-/-}$ cells. In addition, impaired differentiation of starburst amacrine cells (SACs) in $Rb^{-/-}$ retina is reversed in

$Rb^{-/-}$:$E2F3a^{-/-}$ mice, whereby rather than activating cell-type specific differentiation factors, Rb regulates SAC differentiation by suppressing E2F3a [9]. Also, Rb-deficient preadipocytes differentiate into adipocytes provided PPAR-γ, the master regulator of adipocyte differentiation, is activated [571, 572]. In another report it was shown that Rb-deficient erythroblasts failed to differentiate due to failure of proper coupling of cell cycle exit with mitochondrial biogenesis [535]. However, it was not assessed empirically whether overcoming this block, for example by inducing mitochondrial biogenesis with bezafibrate, could bypass the function of Rb during erythroblast differentiation.

Interestingly, as reported in chapter 3, $Rb^{-/-}$ myotubes die in the presence of the cell cycle inhibitor aphidicolin (DNA polymerase α inhibitor). The mechanism of this collapse remains to be defined, but notably, others have reported that arresting cell cycle progression with aphidicolin in irradiated $Rb^{-/-}$ cells did not prevent cell death [573]. Thus, with respect to aphidicolin, inhibition of DNA Polymerase α is not capable of mimicking the death suppressing functions of pRb [573]. Suppression of the cell-cycle was also attempted by ectopic expression of $p27^{Kip1}$, which led to a blockade of differentiation of $Rb^{-/-}$ myoblasts but not control. The mechanism of this inhibition is not known, but the results demonstrate that $Rb^{-/-}$ myoblasts are extremely sensitive to cell cycle inhibitors.

Importantly, the results indicate that $Rb^{-/-}$ cells, which represent a large proportion of human cancers [519, 574], can differentiate and may be amenable to differentiation-induced tumor therapy, similar to the mode of therapy that has been exploited to induce differentiation of leukemic promyelocytes using all-*trans*-retinoic acid [575, 576].

A surprising discovery from chapter 3 was the non-apoptotic mode of Rb-deficient myotube cell death, notwithstanding the dramatic rescue of the myotubes by Bcl-2. This raised the possibility that Bcl-2 - which blocks both apoptosis and autophagy [577] - protected the myotubes by restraining autophagy, and thus suppressing this alternative mode of cell death which can often be detected in dying apoptosis-deficient cells [419, 421, 578]. This idea was supported by using two other inhibitors of autophagy - 3-MA and $Vps34^{dn}$ - which also prevented $Rb^{-/-}$ myotube collapse. Although endogenous levels of Bcl-2 may not be compromised in $Rb^{-/-}$ myotubes, an elevated level of Bnip3 - which displaces Bcl-2 from Beclin-1 to induce autophagy [579] - was detected in $Rb^{-/-}$ myotubes relative to control (Figure 3.2E). Thus, in the absence of Rb, it is speculated that elevated Bnip3 levels may bind and inhibit Bcl-2 activity, preventing Bcl-2-mediated suppression of autophagy. By supplying exogenous Bcl-2, the equilibrium was shifted in favor of Bcl-2, permitting free Bcl-2 to protect mitochondria and restrain autophagy, suggesting that the Bcl-2:Bnip3 ratio is critical in regulating autophagic cell death.

In most eukaryotic cells, mitochondrial permeability changes following exposure to apoptotic stimuli, which lead to the release of apoptogenic factors. In $Rb^{-/-}$ cells for example, de-regulated E2F activity can cause excessive mitochondrial damage via BH3-only factors such as Bnip3, which is thought to cause mitochondrial dysfunction via direct opening of the mPTP as well as via Bax/Bak activation [431]. Together, these processes promote loss of mitochondrial potential, apoptosis and autophagy/mitophagy [432, 580-582]. In addition, it was suggested that Bnip3 actively promotes autophagy by disrupting Bcl-2/Beclin-1 complexes [583]. However, in apoptosis-deficient cells,

autophagic activity, and not apoptosis, is enhanced by apoptotic stimuli and mPTP opening [420, 421, 584, 585]. Interestingly, data from chapter 3 imply that $Rb^{-/-}$ myotubes are apoptosis-defective and progressively degenerate due to excessive autophagy. Furthermore, ectopic expression of XIAP did not rescue $Rb^{-/-}$ myotube degeneration, whereas minocycline - a MOMP inhibitor [536] - did provide partial protection, signifying autophagic cell death required MOMP but not caspase activation. In contrast, XIAP did not provide protection suggesting that apoptosis is already blocked, possibly because endogenous XIAP levels are sufficiently high in myoblasts and therefore adding more XIAP is inconsequential, an idea supported by others [360, 586]. Thus, in $Rb^{-/-}$ myotubes, it is proposed that the intrinsic apoptotic machinery is inactive and that mitochondrial dysfunction leads to disruption of the mitochondrial network, mitochondrial perinuclear aggregation and autophagic degradation. Survival factors capable of restoring mitochondrial function or redirection of cell metabolism toward glycolysis can maintain $Rb^{-/-}$ cell survival and differentiation.

Another possible mechanism leading to Rb-deficient myotube degeneration is a defect in mitochondrial fusion and fission, processes regulated by the mitofusins (Mfn1 and Mfn2) and Drp1, respectively [587, 588]. Notably, the perinuclear clustering and rounded mitochondria phenotypes of Rb-deficient myotubes are comparable to mitofusin-null cells, whereby Mfn2-deficient skeletal muscle and other cell-types have fragmented spherical mitochondria [588-590] as well as inappropriate clustering of the mitochondria [591]. The status of mitofusin in $Rb^{-/-}$ myotubes remains to be explored (see Future Directions). Furthermore, the level of mtDNA from Rb-deficient skeletal muscle was reduced compared to control, and bezafibrate, which induces mitochondrial biogenesis,

rescued the collapse of the Rb-deficient myotubes. Thus, on one hand there is inappropriate mitochondrial distribution and on the other hand there is a reduction in mitochondrial mass. Collectively, these defects promote a bioenergetic failure due to insufficient ATP levels, which is detrimental in a highly oxidative tissue such as skeletal muscle.

Normally, loss of muscle mass, which occurs with disuse, fasting and many diseases, results mostly from accelerated breakdown of muscle proteins [592]. This process, thought to be coordinated by the FoxO3 transcription factor, occurs with the transcriptional upregulation of autophagy-related and atrophy-related genes [593]. Conversely, activated mTOR suppresses autophagy and induces protein synthesis and muscle hypertrophy [378]. Despite the role these factors play in survival-associated autophagy in response to starvation, they have not been implicated in death-associated autophagy [334]. This may explain why ectopic expression of DN-FoxO3 or activated-mTOR alleles did not suppress degeneration of Rb-deficient myotubes since the death-associated autophagy was likely induced by alternative pathways other than starvation.

A switch from OXPHOS to glycolysis and loss of the Rb tumor suppressor represent two major hallmarks of cancer. Results from chapter 3 indicate that Rb loss leads to inappropriate cell division, which is oncogenic, and to impaired mitochondrial function, which promotes cell death. Thus, for neoplastic transformation, Rb loss must cooperate with mutations that suppress mitochondrial damage or autophagy, or shift ATP production from OXPHOS to glycolysis.

Tumor cells generally exhibit increased glycolysis even in the presence of sufficient oxygen (Warburg effect) which is advantageous as oxygen becomes limiting in

the tumor mass. Under hypoxic conditions, HIF-1α is stabilized and coordinates angiogenesis, glycolysis, survival and tumor dissemination [506, 594-598]. It was also proposed that Rb directly stimulates the transcriptional activity of HIF-1α to affect glycolysis [599]; however, $Rb^{-/-}$ myotubes clearly undergo a HIF-1α dependent glycolytic-shift, indicating that HIF-1α is functional in the absence of pRb. Although this function may be compensated by p107/p130, other work has shown that Rb/p107/p130/p53 deficient tumor cells can survive under hypoxia [600], indicating that HIF-1α activity is Rb family independent. It was also shown that $Rb^{-/-}$ cells harbor high levels of the E2F1 regulated glycolysis enzyme 6-phosphofructo-2-kinase/fructose-2,6-bisphosphatase [601]. Together, the evidence supports the idea that $Rb^{-/-}$ cells can endure in hypoxia, and with cooperating oncogenic events, may accumulate mutations required for enhanced growth and dissemination from the primary tumor site. A likely cooperating event is inactivation of p53, since hypoxia-mediated activation of p53 can trigger cell death [602] and inactivation of p53 can directly cause a switch from OXPHOS to aerobic glycolysis [496, 512, 513, 603]. Another likely cooperating oncogenic event is the deregulation of myc in $Rb^{-/-}$ cells. Myc in cooperation with HIF-1α, were shown to induce glycolysis by upregulating hexokinase 2 and pyruvate dehydrogenase kinase 1 and to inhibit mitochondrial biogenesis and cellular respiration [604-606]. Thus, a novel role for pRb in maintaining mitochondrial integrity that is important for normal differentiation has been identified and has implications for cancer metabolism.

Three models are proposed to describe the degeneration of $Rb^{-/-}$ myotubes: **1st model:** Impaired mitochondria cause bioenergetic stress, which triggers starvation

signals despite an abundance of oxidizable nutrients in the environment (serum lipids, amino acids and glucose). As a consequence, adaptive, non-selective, autophagy is induced to preserve cellular bioenergetics by reusing degraded autolysosomal contents to maintain basal macromolecule synthesis and to fuel any possible mitochondrial ATP production. However, the excessive autophagy causes irreversible damage leading to myotube demise via autophagic cell death (type II cell death) [334]. This model is limited by the observation that Rb-deficient myotubes are not dependent on autophagy for survival, since inhibition of autophagy rescues, rather than accelerates the collapse of the Rb-deficient myotubes. **2nd model:** Substantial mitochondrial damage activates mitophagy, whereby mitochondria are selectively eliminated, which results in massive ATP-depletion followed by myotube death. **3rd model:** Macroautophagy is initiated in response to intracellular damage allowing for the elimination of apoptosis-deficient cells. This would be similar to what has been reported for: a) Bax/Bak deficient MEFs, whereby cell death after death stimulation is dependent on ATG5 and Beclin-1 and inhibited by 3-MA [419]; and b) Cells with inhibited caspase-8 induce ATG7 and Beclin-1 to promote autophagic cell death [578]. Consistent with this model, pharmacologic and genetic inhibition of autophagy prevent Rb-deficient myotube death which is not TUNEL-positive and is not rescued by ectopic expression of XIAP.

By uncoupling differentiation from cell-cycle exit and survival during skeletal myogenesis, it was shown that Rb is not actively required for differentiation *per se*, but is required for cell cycle exit and to suppress degeneration associated with excess autophagy. The exact mediators of this degeneration remain to be defined and some putative possibilities are outlined in the Future Directions section.

5.3 Combined role of the Rb family during skeletal myogenesis

The prevailing view is that the tumor suppressor pRb plays at least two independent functions: control of cell division and apoptosis through inhibition of E2F regulated genes, and differentiation through activation of lineage-specific differentiation factors. However, results from chapter 3 demonstrate that survival factors, autophagy inhibitors and hypoxia can prevent the degeneration of $Rb^{-/-}$ myotubes [552]. Although these observations challenge the idea that pRb is actively required to stimulate the differentiation program, the data do not rule out the possibility that the Rb relatives, p107 and p130, partially compensate for Rb loss during differentiation. Specifically, p107 and p130 may account for the ability of $Rb^{-/-}$ myoblasts to fuse and form short myotubes before they degenerate. In addition, it was not clear whether p130 compensated for pRb or counteracted its function. These issues were addressed by analyzing primary myoblasts with combined mutations in the Rb gene family. I found that mutations in pRb plus p107 or pRb plus p130 increased apoptosis in myoblasts and accordingly reduced the number of myotubes, but myotubes that did form survived and twitched under hypoxia or following treatment with autophagy-antagonists. Also, p107 was more critical than p130 in preventing myoblast apoptosis during differentiation, and both exhibit partially overlapping functions with pRb. As noted previously, several studies have suggested that the Rb family may affect differentiation and lineage commitment by transcriptionally regulating the expression of differentiation factors such as PPARγ and PGC1α, by sequestering inhibitors of differentiation like ID2, HDAC1, EID-1 and RBP2 [140, 325, 329, 330, 545], or by binding and stimulating differentiation factors such as CBFA1 (RUNX2) during osteoblast differentiation, C/EBPβ during adipocyte differentiation and

MyoD and myogenin during myogenesis [98-102, 544]. As noted, in the recent genome-wide protein-protein interaction analysis [106], p107 does not seem to interact with MyoD or any other differentiation factor in human or mouse and this is consistent with the reduced expression of p107 during differentiation. Therefore, the ability of Rb/p130 DKO myoblasts to fully differentiate when treated with autophagy inhibitors or hypoxia is stunning and supports the notion that pRb is not actively required for differentiation. The interaction of pRb and/or p130 with MyoD may potentially be required for cell survival or cell cycle exit, but it does not seem essential for differentiation *per se*.

Cyclin D3 levels were assessed since it was suggested that pRb is required for accumulation of cyclin D3 during myogenic differentiation by protecting the cyclin from GSK3-β mediated phosphorylation and proteosomal degradation [301]. Also, it was reported that LiCl, a GSK3-β inhibitor, enhanced the differentiation of an Rb-deficient myoblast cell line by promoting cyclin D3 stabilization [301]. This is consistent with results from chapters 3 and 4 whereby LiCl enhanced the survival of Rb-deficient myotubes following either chronic or acute inactivation of Rb (Figures 3.7A and C, 4.4C and E). However, cyclin D3 stabilization may not be pRb-dependent *per se*, since even in the absence of LiCl, cyclin D3 is highly expressed in mgRb:$Rb^{-/-}$, mgRb:$Rb^{-/-}$:$p130^{-/-}$ and $Rb^{\Delta f}$ myotubes. Instead, lithium may extend survival of $Rb^{-/-}$ myotubes by attenuating autophagy via GSK3-β inhibition [607].

The observation that p130 mutation exacerbated the Rb-deficient myogenic defect is in contrast to a report by *Carnac et al.* [160]. Their data propose that p130 is highly expressed in "reserve" cells, which is a population of cells maintained in a quiescent state during the course of *in vitro* differentiation from myoblasts to myotubes [160], and over-

expression of p130 antagonizes muscle differentiation in the C2C12 muscle cell line [160]. This suggests p130-deficient myoblasts would have an improved differentiation phenotype. However, I found that loss of p130 worsens rather than improves the myogenic defect seen in $Rb^{-/-}$ embryos and derived myoblasts. This notion is also supported by data showing a reduction in the number of differentiated desmin-positive myocytes in the myotome of p130-null embryos on a Balb/cJ background [146]. One possibility to explain this discrepancy is that p130 counteracts the activity of pRb and inhibits differentiation of reserve/satellite cells, but plays a partially redundant role with pRb in fetal myoblasts. Eliminating both Rb and p130 in satellite cells (for example, using a Pax7-cre-ER deleter line) may resolve this issue.

In TKO myoblast cultures, excessive cell death led to elongated unfused MHC-positive myocytes and short bi-nuclear myotubes. Under hypoxia, these myotubes became abnormally thin, yet, some surviving myotubes twitched. This is remarkable given TKO fibroblasts are prone to cell death and to genomic instability associated with telomere shortening [154, 608, 609]. The formation of the bi-nuclear TKO myotubes may be due to some low level of fusion and/or acytokinetic mitosis, which often occurs in cardiac myocytes and other tissues [556]. Notably, the appearance of some rare TKO myotubes with three nuclei, as well as twitching under hypoxia, suggests that at least some fusion does occur. Furthermore, some nuclei were enlarged and exhibited a septation suggestive of endomitosis [556] and interestingly, it was suggested previously that p107 and p130 enforce a G2/M phase checkpoint that prevents Rb-deficient cells from progressing into mitosis [610]. Both of these processes (acytokinetic mitosis and endomitosis) may contribute to genetic instability and cancer in the absence of Rb.

Presently, the most plausible interpretation of the data is that the primary defect of DKO and TKO myoblasts is cell death, which reduces opportunities for myocyte fusion, but that surviving myoblasts are inherently capable of differentiation. The TKO myoblasts have a more severe differentiation defect and may be prone to nuclear duplication and polyploidy. Thus, while a quantitative reduction in myotube formation was observed between single and DKO cultures, there is a qualitative difference between double and triple mutants and the diminished differentiation and survival of TKO myoblasts may be due to the complete deregulation of E2Fs. There also exists the possibility that some Rb function may be required to direct lineage decisions at the stem-cell stage, but not in already committed cells such as myoblasts. This was recently suggested in a study showing Rb status dictates the fate choice of mesenchymal stem cells between osteogenic and adipogenic differentiation by positively regulating the osteogenic factor RUNX2 and negatively regulating the adipogenic factor PPAR-γ [611]. Thus, Rb may be required to stimulate differentiation factors and sequester inhibitors of differentiation such as such as Id2, HDAC1 and EID-1 [248, 329] in bipotent stem/progenitor cells in the somite or Pax3/Pax7-double positive muscle stem cells in the dermomyotome [612], but this function may not be essential once cells, such as embryonic myoblasts, become committed to a specific lineage.

The effect of Rb family loss seems to be cell-type dependent as suggested in various studies. In TKO hematopoietic stem cells (HSCs), hyperproliferation of early hematopoietic progenitors occurs concomitantly with an increase in apoptosis of the lymphoid progenitor population [613]. In this context, the Rb family maintains the balance between these cell types, and interestingly, a single p107 allele is sufficient to

rescue the defect. In the retina, Rb loss alone is not sufficient to induce tumors; combined mutations with p107 or p130 in retinal precursors is required to prevent cell cycle exit and induce retinoblastoma [133, 141, 147]. In post-mitotic differentiated neurons of the inner nuclear layer of the retina, $Rb^{-/-}$:$p107^{+/-}$:$p130^{-/-}$ horizontal interneurons re-entered the cell cycle and expanded to form metastatic retinoblastoma. In contrast, horizontal interneurons were not affected in $Rb^{+/-}$:$p107^{-/-}$:$p130^{-/-}$ or $Rb^{-/-}$:$p107^{-/-}$:$p130^{+/-}$ retinae, suggesting that a single copy of Rb or p130, but not p107, is sufficient to prevent horizontal interneuron proliferation [614]. In mammary epithelium, Rb loss alone in ductal but not alveolar progenitors induces mammary tumors, and combined mutations with p53 but not p107 acclerated tumor formation [138]. In skeletal muscle, inactivation of Rb in myoblasts or satellite cells disrupts the myogenic program, but has little effect on post-mitotic myotubes as demonstrated in chapter 4 and by others [150, 158]. The combined inactivation of Rb family members leads to even more severe myogenic defects, which can be rescued by inhibiting autophagy or by hypoxia. Additionally, the post-mitotic state in differentiated skeletal muscle is thought to be preserved in an Rb family independent manner [158] and was recently suggested to require inactivation of Rb and ARF [297]. Overall, depending on cell-type, lineage and position of the cell in the stem-cell hierarchy, eliminating all Rb family members has a varied effect, which may be suppressed by the presence of one Rb family member, and may lead to lineage deletion, hyperproliferation and tumorigenesis.

Rb but not p107 or p130 is often lost in cancer, and as p107 and p130 are more highly related to each other than to pRb, both may need to be inactivated to observe an effect. In experimental systems, when both p107 and p130 are mutated, they produce

similar or different effects as Rb loss alone. For example, in response to $p16^{INK4a}$ over-expression, mutations in p107 plus p130 allow cells to escape cell cycle inhibition as efficient as Rb loss alone [554]. On the other hand, oncogene-induced senescence was shown to be Rb but not p107/p130-dependent [555]. This latter study suggested that Rb is uniquely required for cancer because only its loss permits tumor cells to escape senescence under oncogenic stress. In this thesis, I have shown that Rb, but not its closely related relatives p107 and p130, is uniquely required for cell cycle exit during terminal differentiation. Thus, the exclusive role of Rb in cancer may be due to its sole requirement for cell cycle exit during terminal differentiation and perhaps disruption of either pRb function, senescence or cell cycle exit, may cause neoplastic transformation depending on the cell and biological context.

5.4 Future Directions

Contribution of E2Fs to $Rb^{-/-}$ muscle phenotype

As a broad approach to help pinpoint the downstream mediators of the Rb-deficient muscle phenotype, microarray analysis of mgRb:$Rb^{-/-}$ skeletal muscle compared to control would be a useful starting point. This will help identify factors that are de-regulated in mgRb:$Rb^{-/-}$ muscle and have a documented role in muscle degeneration, autophagy/mitophagy. Furthermore, since the activator E2Fs are the best-characterized targets of Rb, it would be useful to characterize their contributions to the Rb myogenic defect. Notably, mgRb:$Rb^{-/-}$:$E2F1^{-/-}$ [95], $Rb^{-/-}$:$E2F1^{-/-}$ [12, 14], $Rb^{-/-}$:$E2F2^{-/-}$ [14], $Rb^{-/-}$:$E2F3^{-/-}$ [13], and $Rb^{-/-}$:$E2F3a^{-/-}$ & $Rb^{-/-}$:$E2F3b^{-/-}$ [615] mice have been previously generated. While partial rescue of the proliferative and/or apoptotic phenotypes were observed, the myogenic defect was not rescued. Importantly, there is considerable

functional redundancy within the E2F family, and thus, compound mutant mice deficient for Rb and multiple activator E2Fs will need to be generated to assess the extent by which the Rb muscle defect is mediated by the E2Fs. In preliminary work, which was done in collaboration with Dr. Rod Bremner, $Rb^{f/f}$:$E2F1^{-/-}$:$E2F3^{f/f}$ myoblasts were transduced with Ad.cre or Ad.GFP and induced to differentiate. However, elimination of both E2F1 and E2F3 was not sufficient to rescue the Rb-deficient myotubes.

What is the nature of the apoptotic block?

As discussed in section 5.1, Rb-deficient myotubes are apoptosis-deficient. To explore the nature of this block, the levels of endogenous XIAP and Smac/DIABLO could be manipulated (knock-down or over-expression, respectively) to test whether they are critical in establishing the apoptotic block. This may be important in the context of some Rb mutant cancer cells that may be apoptosis-deficient due to de-regulated XIAP levels. If an XIAP-mediated apoptotic-block is found in Rb mutant cancer cells, XIAP inhibitors may unleash the apoptotic machinery to kill the cells.

Testing the effect of inhibiting autophagy *in vivo*

Genetic ablation of autophagy *in vivo* will be useful to corroborate the *in vitro* results that demonstrate Rb-deficient muscle degeneration occurs as a result of excessive autophagy. This can be done by generating mgRb:$Rb^{-/-}$:$Atg5^{-/-}$ or Myf5.cre:$Rb^{f/f}$:$Atg5^{-/-}$ [616] and analyzing the extent of muscle degeneration in the late stages of embryogenesis (E16.5-E20.5) relative to mgRb:$Rb^{-/-}$ muscle.

Given that bezafibrate rescued the degeneration of $Rb^{-/-}$ myotubes *in vitro*, the effect of inducing mitochondrial biogenesis *in vivo* should also be explored. This can be done by administering bezafibrate to pregnant mgRb:$Rb^{+/-}$ mice using bezafibrate-

containing chow [476] or via intraperitoneal injection [617]. Provided a therapeutic dose is delivered to the embryo, the consequence of inducing mitochondrial biogenesis in Rb-deficient embryos may extend beyond skeletal muscle. For instance, in the absence of Rb there is ineffective erythroid differentiation partially due to failed mitochondrial biogenesis [535]. Thus, this approach will not only test the extent by which mitochondrial biogenesis can rescue the muscle defect in the absence of Rb, but may alleviate other differentiation defects as well.

Role of Bnip3 and the type of autophagy accompanying $Rb^{-/-}$ muscle degeneration

To address the possibility that Bnip3 is the mediator of $Rb^{-/-}$ myotube degeneration, for reasons described in section 1.4.4 and the observation that Bnip3 levels are elevated in DM-2 $Rb^{-/-}$ myotubes (Figure 3.2E), Bnip3 as well as the related protein Bnip3L, could be knocked-down individually and in combination because of the unique and/or redundant roles of these proteins. If Bnip3 knock-down alone rescues Rb-deficient myotubes from collapse, this can be corroborated *in vivo* by creating mgRb:$Rb^{-/-}$:$Bnip3^{-/-}$ double-knock out embryos [618].

Another outstanding question is the nature of the autophagy detected in Rb-deficient myotubes. That is, is non-discriminate macroautophagy occurring - which engulfs bulk cytoplasm - or is mitophagy specifically eliminating mitochondria? To distinguish these possibilities, the knock-down of mitophagy-specific proteins such as Parkin [427, 428], Atg32 [426] and bnip3L (Nix) [417] can be used to test the effect on Rb-deficient myotube survival and probing the status of the mitochondrial network. Presumably, if mitophagy is the mechanism by which the mitochondrial-network

collapses, perinuclear clustering of mitochondria would be prevented after knock-down of these factors.

The mitofusins and Drp1

Mitochondrial morphology and distribution is determined by the equilibrium of fusion and fission, processes moderated by the mitofusins (Mfn1 and Mfn2) and Drp1. Interestingly, overexpression of Mfn1 in numerous cell-types results in perinuclear clustering of mitochondria [619] and such defects create a dysfunctional mitochondrial network which lead to bioenergetic failure. To investigate the involvement of a mitochondrial fusion/fission defect in Rb-deficient myotubes, the level of mitofusins (mitochondrial fusion) and Drp1 (mitochondrial fission) could be probed in skeletal muscle of mgRb:$Rb^{-/-}$ embryos using western blot analysis and qPCR. If any of the proteins are found to be dysregulated, the factors could be knocked-down or overexpressed to restore the equilibrium and possibly the mitochondrial network.

Identification of dying cells in cultures with acutely inactivated Rb

A progressive increase in cell death was observed in $Rb^{\Delta f}$, $Rb^{\Delta f}$:$p130^{-/-}$, $Rb^{\Delta f}$:$p107^{-/-}$ and $Rb^{\Delta f}$:$p107^{-/-}$:$p130^{-/-}$ differentiating primary cultures and this correlated with corresponding reduction in myotube number. To determine whether this increase was due to a *bona fide* increase in myoblast cell death specifically (since primary cultures are a mix of myoblasts plus non-myogenic cells such as fibroblasts), a double-labeling experiment - TUNEL plus Myf5/MyoD - could be conducted and analyzed by flow cytometry.

Assessing the fusion potential of TKO myoblasts *in vivo*

The contribution of TKO myoblasts to skeletal muscle *in vivo* could be assessed by analyzing embryonic skeletal muscle from Myf5.cre:$Rb^{f/f}$:$p107^{-/-}$:$p130^{-/-}$ embryos for evidence of multinucleated myotubes. Such myotubes would strongly suggest that TKO myoblasts are competent to fuse and differentiation can occur independently of Rb family function. This could also be done on an $Atg5^{f/f}$ background or following bezafibrate treatment.

Deciphering whether Rb-mutant cancer cells are glycolytic

Another outstanding question is whether Rb-mutant cancer cells are glycolytic in a Rb-dependent manner as this could provide another mode of killing these cells. To do this, a tetracycline-inducible Rb can be introduced into Rb-mutant tumor cells and the effect of Rb on glycolysis can be evaluated using two approaches *in vitro*: 1) Glycolytic tumor cells are usually extremely sensitive to the glucose antagonist 2-deoxy-D-glucose. 2) Glycolytic cells display elevated lactate dehydrogenase A (LDH-A) activity, and knock-down of this enzyme under hypoxic conditions kills highly glycolytic cells. *In vivo*, the glycolytic status of Rb-mutant tumors could be evaluated using positron emission tomography (PET) after intravenous injection of the glucose analogue ^{18}F-fluorodeoxyglucose (^{18}FDG), a technique used to detect increased cellular glucose uptake. Targeting tumor-associated glycolysis as a therapy is currently under investigation and the many metabolic enzymes and intermediates provide an attractive array of new possible therapeutics.

APPENDIX

Appendix 1: Legends for Videos

Video S1 Twitching of control myotubes transduced with Ad.Bcl-2. Control myoblasts were transduced with Ad.Bcl-2, induced to differentiate and video captured at day 10 post-differentiation. Similar results were obtained without Ad.Bcl-2.

Video S2 Twitching of Rb-deficient myotubes transduced with Ad.Bcl-2. $Rb^{-/-}$ myoblasts were transduced with Ad.Bcl-2, induced to differentiate and video captured at day 10 post-differentiation.

Video S3 Twitching of control myotubes treated with 3-MA. Control myoblasts were induced to differentiate in the presence of 3-MA and video captured at day 7 post-differentiation. Similar results were obtained without 3-MA treatment

Video S4 Twitching of Rb-deficient myotubes treated with 3-MA. $Rb^{-/-}$ myoblasts were induced to differentiate and treated with 3-MA and video captured at day 7 post-differentiation.

Video S5 Twitching of Ad.EV transduced $Rb^{f/f}$ myotubes in hypoxia. $Rb^{f/f}$ myoblasts were transduced with Ad.EV, induced to differentiate after 48hrs, transferred to hypoxia and video captured 4 days later.

Video S6 Twitching of $Rb^{\Delta f}$ myotubes under hypoxia. $Rb^{f/f}$ myoblasts were transduced with Ad.cre, induced to differentiate after 48hrs, transferred to hypoxia and video captured 4 days later.

Video S7 Twitching of mgRb:$Rb^{-/-}$:$p130^{-/-}$ myotubes treated with 3-MA. mgRb:$Rb^{-/-}$:$p130^{-/-}$ myoblasts were induced to differentiate and treated with 3-MA and video captured at DM-5.

Video S8 Twitching Ad.cre transduced $Rb^{\Delta f}$ myotubes under hypoxia. $Rb^{f/f}$ myoblasts were transduced with Ad.cre, induced to differentiate after 48hr, transferred to hypoxia and video captured at DM-5.

Video S9 Twitching Ad.cre transduced $Rb^{\Delta f}$:$p107^{-/-}$ myotubes under hypoxia. $Rb^{f/f}$:$p107^{-/-}$ myoblasts were transduced with Ad.cre, induced to differentiate after 48hr, transferred to hypoxia and video captured at DM-5.

Video S10 Twitching Ad.cre transduced $Rb^{\Delta f}$:p130-/- myotubes under hypoxia. $Rb^{f/f}$:$p130^{-/-}$ myoblasts were transduced with Ad.cre, induced to differentiate after 48hr, transferred to hypoxia and video captured at DM-5.

Video S11 Twitching Ad.cre transduced $Rb^{\Delta f}$:$p107^{-/-}$:$p130^{-/-}$ myotube under hypoxia. $Rb^{f/f}$:$p107^{-/-}$:$p130^{-/-}$ myoblasts were transduced with Ad.cre, induced to differentiate after 48hr, transferred to hypoxia and video captured at DM-5.

REFERENCES

1. Lohmann, D.R. and B.L. Gallie, *Retinoblastoma: revisiting the model prototype of inherited cancer.* Am J Med Genet C Semin Med Genet, 2004. **129**(1): p. 23-8.
2. Knudson, A.G., Jr., *Mutation and cancer: statistical study of retinoblastoma.* Proc Natl Acad Sci U S A, 1971. **68**(4): p. 820-3.
3. Friend, S.H., et al., *A human DNA segment with properties of the gene that predisposes to retinoblastoma and osteosarcoma.* Nature, 1986. **323**(6089): p. 643-6.
4. Tsai, S.Y., et al., *Mouse development with a single E2F activator.* Nature, 2008. **454**(7208): p. 1137-41.
5. Danielian, P.S., et al., *E2f3a and E2f3b make overlapping but different contributions to total E2f3 activity.* Oncogene, 2008. **27**(51): p. 6561-70.
6. Attwooll, C., E.L. Denchi, and K. Helin, *The E2F family: specific functions and overlapping interests.* Embo J, 2004. **23**(24): p. 4709-16.
7. Nevins, J.R., *The Rb/E2F pathway and cancer.* Hum Mol Genet, 2001. **10**(7): p. 699-703.
8. Chen, H.Z., S.Y. Tsai, and G. Leone, *Emerging roles of E2Fs in cancer: an exit from cell cycle control.* Nat Rev Cancer, 2009. **9**(11): p. 785-97.
9. Chen, D., et al., *Rb-mediated neuronal differentiation through cell-cycle-independent regulation of E2f3a.* PLoS Biol, 2007. **5**(7): p. e179.
10. Wu, L., et al., *The E2F1-3 transcription factors are essential for cellular proliferation.* Nature, 2001. **414**(6862): p. 457-62.
11. Liu, Y. and E. Zacksenhaus, *E2F1 mediates ectopic proliferation and stage-specific p53-dependent apoptosis but not aberrant differentiation in the ocular lens of Rb deficient fetuses.* Oncogene, 2000. **19**(52): p. 6065-73.
12. Tsai, K.Y., et al., *Mutation of E2f-1 suppresses apoptosis and inappropriate S phase entry and extends survival of Rb-deficient mouse embryos.* Mol Cell, 1998. **2**(3): p. 293-304.
13. Ziebold, U., et al., *E2F3 contributes both to the inappropriate proliferation and to the apoptosis arising in Rb mutant embryos.* Genes Dev, 2001. **15**(4): p. 386-91.
14. Saavedra, H.I., et al., *Specificity of E2F1, E2F2, and E2F3 in mediating phenotypes induced by loss of Rb.* Cell Growth Differ, 2002. **13**(5): p. 215-25.
15. Gaubatz, S., et al., *E2F4 and E2F5 play an essential role in pocket protein-mediated G1 control.* Mol Cell, 2000. **6**(3): p. 729-35.
16. Li, J., et al., *Synergistic function of E2F7 and E2F8 is essential for cell survival and embryonic development.* Dev Cell, 2008. **14**(1): p. 62-75.
17. Bandara, L.R., et al., *Functional synergy between DP-1 and E2F-1 in the cell cycle-regulating transcription factor DRTF1/E2F.* Embo J, 1993. **12**(11): p. 4317-24.
18. Girling, R., et al., *A new component of the transcription factor DRTF1/E2F.* Nature, 1993. **365**(6445): p. 468.
19. Helin, K., et al., *Heterodimerization of the transcription factors E2F-1 and DP-1 leads to cooperative trans-activation.* Genes Dev, 1993. **7**(10): p. 1850-61.
20. Wu, C.L., et al., *In vivo association of E2F and DP family proteins.* Mol Cell Biol, 1995. **15**(5): p. 2536-46.

21. Zhang, Y. and S.P. Chellappan, *Cloning and characterization of human DP2, a novel dimerization partner of E2F.* Oncogene, 1995. **10**(11): p. 2085-93.
22. Helin, K., E. Harlow, and A. Fattaey, *Inhibition of E2F-1 transactivation by direct binding of the retinoblastoma protein.* Mol Cell Biol, 1993. **13**(10): p. 6501-8.
23. Brehm, A., et al., *Retinoblastoma protein recruits histone deacetylase to repress transcription.* Nature, 1998. **391**(6667): p. 597-601.
24. Magnaghi-Jaulin, L., et al., *Retinoblastoma protein represses transcription by recruiting a histone deacetylase.* Nature, 1998. **391**(6667): p. 601-5.
25. Dahiya, A., et al., *Role of the LXCXE binding site in Rb function.* Mol Cell Biol, 2000. **20**(18): p. 6799-805.
26. Dunaief, J.L., et al., *The retinoblastoma protein and BRG1 form a complex and cooperate to induce cell cycle arrest.* Cell, 1994. **79**(1): p. 119-30.
27. Stevaux, O. and N.J. Dyson, *A revised picture of the E2F transcriptional network and RB function.* Curr Opin Cell Biol, 2002. **14**(6): p. 684-91.
28. Dyson, N., *The regulation of E2F by pRB-family proteins.* Genes Dev, 1998. **12**(15): p. 2245-62.
29. Johnson, D.G., et al., *Expression of transcription factor E2F1 induces quiescent cells to enter S phase.* Nature, 1993. **365**(6444): p. 349-52.
30. Thalmeier, K., et al., *Nuclear factor E2F mediates basic transcription and trans-activation by E1a of the human MYC promoter.* Genes Dev, 1989. **3**(4): p. 527-36.
31. Blake, M.C. and J.C. Azizkhan, *Transcription factor E2F is required for efficient expression of the hamster dihydrofolate reductase gene in vitro and in vivo.* Mol Cell Biol, 1989. **9**(11): p. 4994-5002.
32. Ohtani, K., J. DeGregori, and J.R. Nevins, *Regulation of the cyclin E gene by transcription factor E2F1.* Proc Natl Acad Sci U S A, 1995. **92**(26): p. 12146-50.
33. DeGregori, J., T. Kowalik, and J.R. Nevins, *Cellular targets for activation by the E2F1 transcription factor include DNA synthesis- and G1/S-regulatory genes.* Mol Cell Biol, 1995. **15**(8): p. 4215-24.
34. Muller, H., et al., *E2Fs regulate the expression of genes involved in differentiation, development, proliferation, and apoptosis.* Genes Dev, 2001. **15**(3): p. 267-85.
35. Leone, G., et al., *E2F3 activity is regulated during the cell cycle and is required for the induction of S phase.* Genes Dev, 1998. **12**(14): p. 2120-30.
36. Ishida, S., et al., *Role for E2F in control of both DNA replication and mitotic functions as revealed from DNA microarray analysis.* Mol Cell Biol, 2001. **21**(14): p. 4684-99.
37. Zhu, W., P.H. Giangrande, and J.R. Nevins, *E2Fs link the control of G1/S and G2/M transcription.* Embo J, 2004. **23**(23): p. 4615-26.
38. Dagnino, L., et al., *Expression patterns of the E2F family of transcription factors during mouse nervous system development.* Mech Dev, 1997. **66**(1-2): p. 13-25.
39. Asp, P., et al., *E2f3b plays an essential role in myogenic differentiation through isoform-specific gene regulation.* Genes Dev, 2009. **23**(1): p. 37-53.
40. Alberts, B., et al., *Molecular Biology of the Cell*. Vol. 4th Ed. 2002: Garland Science.
41. Norbury, C. and P. Nurse, *Animal cell cycles and their control.* Annu Rev Biochem, 1992. **61**: p. 441-70.

42. Cross, F., J. Roberts, and H. Weintraub, *Simple and complex cell cycles.* Annu Rev Cell Biol, 1989. **5**: p. 341-96.
43. Chen, P.L., et al., *Phosphorylation of the retinoblastoma gene product is modulated during the cell cycle and cellular differentiation.* Cell, 1989. **58**(6): p. 1193-8.
44. Buchkovich, K., L.A. Duffy, and E. Harlow, *The retinoblastoma protein is phosphorylated during specific phases of the cell cycle.* Cell, 1989. **58**(6): p. 1097-105.
45. Durfee, T., et al., *The retinoblastoma protein associates with the protein phosphatase type 1 catalytic subunit.* Genes Dev, 1993. **7**(4): p. 555-69.
46. Baldin, V., et al., *Cyclin D1 is a nuclear protein required for cell cycle progression in G1.* Genes Dev, 1993. **7**(5): p. 812-21.
47. Kitagawa, M., et al., *The consensus motif for phosphorylation by cyclin D1-Cdk4 is different from that for phosphorylation by cyclin A/E-Cdk2.* Embo J, 1996. **15**(24): p. 7060-9.
48. Connell-Crowley, L., J.W. Harper, and D.W. Goodrich, *Cyclin D1/Cdk4 regulates retinoblastoma protein-mediated cell cycle arrest by site-specific phosphorylation.* Mol Biol Cell, 1997. **8**(2): p. 287-301.
49. Harbour, J.W., et al., *Cdk phosphorylation triggers sequential intramolecular interactions that progressively block Rb functions as cells move through G1.* Cell, 1999. **98**(6): p. 859-69.
50. Duronio, R.J., et al., *E2F-induced S phase requires cyclin E.* Genes Dev, 1996. **10**(19): p. 2505-13.
51. Lundberg, A.S. and R.A. Weinberg, *Functional inactivation of the retinoblastoma protein requires sequential modification by at least two distinct cyclin-cdk complexes.* Mol Cell Biol, 1998. **18**(2): p. 753-61.
52. Hochegger, H., S. Takeda, and T. Hunt, *Cyclin-dependent kinases and cell-cycle transitions: does one fit all?* Nat Rev Mol Cell Biol, 2008. **9**(11): p. 910-6.
53. Hinds, P.W., et al., *Regulation of retinoblastoma protein functions by ectopic expression of human cyclins.* Cell, 1992. **70**(6): p. 993-1006.
54. Henglein, B., et al., *Structure and cell cycle-regulated transcription of the human cyclin A gene.* Proc Natl Acad Sci U S A, 1994. **91**(12): p. 5490-4.
55. Resnitzky, D., L. Hengst, and S.I. Reed, *Cyclin A-associated kinase activity is rate limiting for entrance into S phase and is negatively regulated in G1 by p27Kip1.* Mol Cell Biol, 1995. **15**(8): p. 4347-52.
56. Girard, F., et al., *Cyclin A is required for the onset of DNA replication in mammalian fibroblasts.* Cell, 1991. **67**(6): p. 1169-79.
57. Rosenberg, A.R., et al., *Overexpression of human cyclin A advances entry into S phase.* Oncogene, 1995. **10**(8): p. 1501-9.
58. Norbury, C., J. Blow, and P. Nurse, *Regulatory phosphorylation of the p34cdc2 protein kinase in vertebrates.* Embo J, 1991. **10**(11): p. 3321-9.
59. Li, J., A.N. Meyer, and D.J. Donoghue, *Nuclear localization of cyclin B1 mediates its biological activity and is regulated by phosphorylation.* Proc Natl Acad Sci U S A, 1997. **94**(2): p. 502-7.
60. Jin, P., S. Hardy, and D.O. Morgan, *Nuclear localization of cyclin B1 controls mitotic entry after DNA damage.* J Cell Biol, 1998. **141**(4): p. 875-85.

61. Hagting, A., et al., *Human securin proteolysis is controlled by the spindle checkpoint and reveals when the APC/C switches from activation by Cdc20 to Cdh1.* J Cell Biol, 2002. **157**(7): p. 1125-37.
62. Sherr, C.J. and J.M. Roberts, *CDK inhibitors: positive and negative regulators of G1-phase progression.* Genes Dev, 1999. **13**(12): p. 1501-12.
63. Serrano, M., G.J. Hannon, and D. Beach, *A new regulatory motif in cell-cycle control causing specific inhibition of cyclin D/CDK4.* Nature, 1993. **366**(6456): p. 704-7.
64. Hannon, G.J. and D. Beach, *p15INK4B is a potential effector of TGF-beta-induced cell cycle arrest.* Nature, 1994. **371**(6494): p. 257-61.
65. Guan, K.L., et al., *Growth suppression by p18, a p16INK4/MTS1- and p14INK4B/MTS2-related CDK6 inhibitor, correlates with wild-type pRb function.* Genes Dev, 1994. **8**(24): p. 2939-52.
66. Hirai, H., et al., *Novel INK4 proteins, p19 and p18, are specific inhibitors of the cyclin D-dependent kinases CDK4 and CDK6.* Mol Cell Biol, 1995. **15**(5): p. 2672-81.
67. Chan, F.K., et al., *Identification of human and mouse p19, a novel CDK4 and CDK6 inhibitor with homology to p16ink4.* Mol Cell Biol, 1995. **15**(5): p. 2682-8.
68. Besson, A., S.F. Dowdy, and J.M. Roberts, *CDK inhibitors: cell cycle regulators and beyond.* Dev Cell, 2008. **14**(2): p. 159-69.
69. Nakanishi, M., et al., *Identification of the active region of the DNA synthesis inhibitory gene p21Sdi1/CIP1/WAF1.* Embo J, 1995. **14**(3): p. 555-63.
70. Chen, J., et al., *Cyclin-binding motifs are essential for the function of p21CIP1.* Mol Cell Biol, 1996. **16**(9): p. 4673-82.
71. Russo, A.A., et al., *Crystal structure of the p27Kip1 cyclin-dependent-kinase inhibitor bound to the cyclin A-Cdk2 complex.* Nature, 1996. **382**(6589): p. 325-31.
72. Harper, J.W., et al., *The p21 Cdk-interacting protein Cip1 is a potent inhibitor of G1 cyclin-dependent kinases.* Cell, 1993. **75**(4): p. 805-16.
73. Xiong, Y., et al., *p21 is a universal inhibitor of cyclin kinases.* Nature, 1993. **366**(6456): p. 701-4.
74. Dulic, V., et al., *p53-dependent inhibition of cyclin-dependent kinase activities in human fibroblasts during radiation-induced G1 arrest.* Cell, 1994. **76**(6): p. 1013-23.
75. Polyak, K., et al., *Cloning of p27Kip1, a cyclin-dependent kinase inhibitor and a potential mediator of extracellular antimitogenic signals.* Cell, 1994. **78**(1): p. 59-66.
76. Toyoshima, H. and T. Hunter, *p27, a novel inhibitor of G1 cyclin-Cdk protein kinase activity, is related to p21.* Cell, 1994. **78**(1): p. 67-74.
77. Lee, M.H., I. Reynisdottir, and J. Massague, *Cloning of p57KIP2, a cyclin-dependent kinase inhibitor with unique domain structure and tissue distribution.* Genes Dev, 1995. **9**(6): p. 639-49.
78. Matsuoka, S., et al., *p57KIP2, a structurally distinct member of the p21CIP1 Cdk inhibitor family, is a candidate tumor suppressor gene.* Genes Dev, 1995. **9**(6): p. 650-62.

79. Cheng, M., et al., *The p21(Cip1) and p27(Kip1) CDK 'inhibitors' are essential activators of cyclin D-dependent kinases in murine fibroblasts.* Embo J, 1999. **18**(6): p. 1571-83.
80. Bienvenu, F., et al., *Transcriptional role of cyclin D1 in development revealed by a genetic-proteomic screen.* Nature. **463**(7279): p. 374-8.
81. Sherr, C.J. and J.D. Weber, *The ARF/p53 pathway.* Curr Opin Genet Dev, 2000. **10**(1): p. 94-9.
82. Kamijo, T., et al., *Tumor suppression at the mouse INK4a locus mediated by the alternative reading frame product p19ARF.* Cell, 1997. **91**(5): p. 649-59.
83. Bates, S., et al., *p14ARF links the tumour suppressors RB and p53.* Nature, 1998. **395**(6698): p. 124-5.
84. DeGregori, J., et al., *Distinct roles for E2F proteins in cell growth control and apoptosis.* Proc Natl Acad Sci U S A, 1997. **94**(14): p. 7245-50.
85. el-Deiry, W.S., et al., *WAF1/CIP1 is induced in p53-mediated G1 arrest and apoptosis.* Cancer Res, 1994. **54**(5): p. 1169-74.
86. Miyashita, T. and J.C. Reed, *Tumor suppressor p53 is a direct transcriptional activator of the human bax gene.* Cell, 1995. **80**(2): p. 293-9.
87. Yu, J., et al., *Identification and classification of p53-regulated genes.* Proc Natl Acad Sci U S A, 1999. **96**(25): p. 14517-22.
88. Nakano, K. and K.H. Vousden, *PUMA, a novel proapoptotic gene, is induced by p53.* Mol Cell, 2001. **7**(3): p. 683-94.
89. Moroni, M.C., et al., *Apaf-1 is a transcriptional target for E2F and p53.* Nat Cell Biol, 2001. **3**(6): p. 552-8.
90. Oda, E., et al., *Noxa, a BH3-only member of the Bcl-2 family and candidate mediator of p53-induced apoptosis.* Science, 2000. **288**(5468): p. 1053-8.
91. Nahle, Z., et al., *Direct coupling of the cell cycle and cell death machinery by E2F.* Nat Cell Biol, 2002. **4**(11): p. 859-64.
92. Hershko, T. and D. Ginsberg, *Up-regulation of Bcl-2 homology 3 (BH3)-only proteins by E2F1 mediates apoptosis.* J Biol Chem, 2004. **279**(10): p. 8627-34.
93. Zacksenhaus, E., et al., *pRb controls proliferation, differentiation, and death of skeletal muscle cells and other lineages during embryogenesis.* Genes Dev, 1996. **10**(23): p. 3051-64.
94. MacPherson, D., et al., *Conditional mutation of Rb causes cell cycle defects without apoptosis in the central nervous system.* Mol Cell Biol, 2003. **23**(3): p. 1044-53.
95. Jiang, Z., et al., *E2F1 and p53 are dispensable, whereas p21(Waf1/Cip1) cooperates with Rb to restrict endoreduplication and apoptosis during skeletal myogenesis.* Dev Biol, 2000. **227**(1): p. 8-41.
96. Chen, D., et al., *Division and apoptosis of E2f-deficient retinal progenitors.* Nature, 2009. **462**(7275): p. 925-9.
97. Chong, J.L., et al., *E2f1-3 switch from activators in progenitor cells to repressors in differentiating cells.* Nature, 2009. **462**(7275): p. 930-4.
98. Chen, P.L., et al., *Retinoblastoma protein positively regulates terminal adipocyte differentiation through direct interaction with C/EBPs.* Genes Dev, 1996. **10**(21): p. 2794-804.

99. Chen, P.L., et al., *Retinoblastoma protein directly interacts with and activates the transcription factor NF-IL6.* Proc Natl Acad Sci U S A, 1996. **93**(1): p. 465-9.
100. Luan, Y., et al., *The retinoblastoma protein is an essential mediator of osteogenesis that links the p204 protein to the Cbfa1 transcription factor thereby increasing its activity.* J Biol Chem, 2007. **282**(23): p. 16860-70.
101. Thomas, D.M., et al., *The retinoblastoma protein acts as a transcriptional coactivator required for osteogenic differentiation.* Mol Cell, 2001. **8**(2): p. 303-16.
102. Gu, W., et al., *Interaction of myogenic factors and the retinoblastoma protein mediates muscle cell commitment and differentiation.* Cell, 1993. **72**(3): p. 309-24.
103. Novitch, B.G., et al., *pRb is required for MEF2-dependent gene expression as well as cell-cycle arrest during skeletal muscle differentiation.* Curr Biol, 1999. **9**(9): p. 449-59.
104. Smialowski, P., et al., *NMR and mass spectrometry studies of putative interactions of cell cycle proteins pRb and CDK6 with cell differentiation proteins MyoD and ID-2.* Biochim Biophys Acta, 2005. **1750**(1): p. 48-60.
105. Zhang, J.M., et al., *Direct inhibition of G(1) cdk kinase activity by MyoD promotes myoblast cell cycle withdrawal and terminal differentiation.* Embo J, 1999. **18**(24): p. 6983-93.
106. Ravasi, T., et al., *An atlas of combinatorial transcriptional regulation in mouse and man.* Cell. **140**(5): p. 744-52.
107. Ewen, M.E., et al., *Molecular cloning, chromosomal mapping, and expression of the cDNA for p107, a retinoblastoma gene product-related protein.* Cell, 1991. **66**(6): p. 1155-64.
108. Mayol, X., et al., *Cloning of a new member of the retinoblastoma gene family (pRb2) which binds to the E1A transforming domain.* Oncogene, 1993. **8**(9): p. 2561-6.
109. Classon, M. and N. Dyson, *p107 and p130: versatile proteins with interesting pockets.* Exp Cell Res, 2001. **264**(1): p. 135-47.
110. Claudio, P.P., T. Tonini, and A. Giordano, *The retinoblastoma family: twins or distant cousins?* Genome Biol, 2002. **3**(9): p. reviews3012.
111. Wirt, S.E. and J. Sage, *p107 in the public eye: an Rb understudy and more.* Cell Div. **5**: p. 9.
112. Nevins, J.R., *Toward an understanding of the functional complexity of the E2F and retinoblastoma families.* Cell Growth Differ, 1998. **9**(8): p. 585-93.
113. Smith, E.J., G. Leone, and J.R. Nevins, *Distinct mechanisms control the accumulation of the Rb-related p107 and p130 proteins during cell growth.* Cell Growth Differ, 1998. **9**(4): p. 297-303.
114. Hurford, R.K., Jr., et al., *pRB and p107/p130 are required for the regulated expression of different sets of E2F responsive genes.* Genes Dev, 1997. **11**(11): p. 1447-63.
115. Morris, E.J. and N.J. Dyson, *Retinoblastoma protein partners.* Adv Cancer Res, 2001. **82**: p. 1-54.
116. Jiang, Z., et al., *The retinoblastoma gene family is differentially expressed during embryogenesis.* Oncogene, 1997. **14**(15): p. 1789-97.

117. Leng, X., et al., *Reversal of growth suppression by p107 via direct phosphorylation by cyclin D1/cyclin-dependent kinase 4.* Mol Cell Biol, 2002. **22**(7): p. 2242-54.
118. Hansen, K., et al., *Phosphorylation-dependent and -independent functions of p130 cooperate to evoke a sustained G1 block.* Embo J, 2001. **20**(3): p. 422-32.
119. Kiess, M., R.M. Gill, and P.A. Hamel, *Expression and activity of the retinoblastoma protein (pRB)-family proteins, p107 and p130, during L6 myoblast differentiation.* Cell Growth Differ, 1995. **6**(10): p. 1287-98.
120. Dick, F.A., *Structure-function analysis of the retinoblastoma tumor suppressor protein - is the whole a sum of its parts?* Cell Div, 2007. **2**: p. 26.
121. Bernards, R., et al., *Structure and expression of the murine retinoblastoma gene and characterization of its encoded protein.* Proc Natl Acad Sci U S A, 1989. **86**(17): p. 6474-8.
122. Harbour, J.W. and D.C. Dean, *Chromatin remodeling and Rb activity.* Curr Opin Cell Biol, 2000. **12**(6): p. 685-9.
123. Lee, J.O., A.A. Russo, and N.P. Pavletich, *Structure of the retinoblastoma tumour-suppressor pocket domain bound to a peptide from HPV E7.* Nature, 1998. **391**(6670): p. 859-65.
124. Hiebert, S.W., et al., *The interaction of RB with E2F coincides with an inhibition of the transcriptional activity of E2F.* Genes Dev, 1992. **6**(2): p. 177-85.
125. Ewen, M.E., et al., *Interaction of p107 with cyclin A independent of complex formation with viral oncoproteins.* Science, 1992. **255**(5040): p. 85-7.
126. Lees, E., et al., *Cyclin E/cdk2 and cyclin A/cdk2 kinases associate with p107 and E2F in a temporally distinct manner.* Genes Dev, 1992. **6**(10): p. 1874-85.
127. Jacks, T., et al., *Effects of an Rb mutation in the mouse.* Nature, 1992. **359**(6393): p. 295-300.
128. Lee, E.Y., et al., *Mice deficient for Rb are nonviable and show defects in neurogenesis and haematopoiesis.* Nature, 1992. **359**(6393): p. 288-94.
129. Wu, L., et al., *Extra-embryonic function of Rb is essential for embryonic development and viability.* Nature, 2003. **421**(6926): p. 942-7.
130. Clarke, A.R., et al., *Requirement for a functional Rb-1 gene in murine development.* Nature, 1992. **359**(6393): p. 328-30.
131. Jiang, Z., et al., *Retinoblastoma gene promoter directs transgene expression exclusively to the nervous system.* J Biol Chem, 2001. **276**(1): p. 593-600.
132. Vooijs, M., et al., *Tumor formation in mice with somatic inactivation of the retinoblastoma gene in interphotoreceptor retinol binding protein-expressing cells.* Oncogene, 2002. **21**(30): p. 4635-45.
133. Chen, D., et al., *Cell-specific effects of RB or RB/p107 loss on retinal development implicate an intrinsically death-resistant cell-of-origin in retinoblastoma.* Cancer Cell, 2004. **5**(6): p. 539-51.
134. MacLellan, W.R., et al., *Overlapping roles of pocket proteins in the myocardium are unmasked by germ line deletion of p130 plus heart-specific deletion of Rb.* Mol Cell Biol, 2005. **25**(6): p. 2486-97.
135. Ruiz, S., et al., *Unique and overlapping functions of pRb and p107 in the control of proliferation and differentiation in epidermis.* Development, 2004. **131**(11): p. 2737-48.

136. Bothe, G.W., et al., *Selective expression of Cre recombinase in skeletal muscle fibers.* Genesis, 2000. **26**(2): p. 165-6.
137. Ferguson, K.L., et al., *A cell-autonomous requirement for the cell cycle regulatory protein, Rb, in neuronal migration.* Embo J, 2005. **24**(24): p. 4381-91.
138. Jiang, Z., et al., *Rb deletion in mouse mammary progenitors induces luminal-B or basal-like/EMT tumor subtypes depending on p53 status.* J Clin Invest. **120**(9): p. 3296-309.
139. Guo, Z., et al., *Inactivation of the retinoblastoma tumor suppressor induces apoptosis protease-activating factor-1 dependent and independent apoptotic pathways during embryogenesis.* Cancer Res, 2001. **61**(23): p. 8395-400.
140. Lasorella, A., et al., *Id2 is a retinoblastoma protein target and mediates signalling by Myc oncoproteins.* Nature, 2000. **407**(6804): p. 592-8.
141. MacPherson, D., et al., *Cell type-specific effects of Rb deletion in the murine retina.* Genes Dev, 2004. **18**(14): p. 1681-94.
142. Lee, M.H., et al., *Targeted disruption of p107: functional overlap between p107 and Rb.* Genes Dev, 1996. **10**(13): p. 1621-32.
143. Marino, S., et al., *Rb and p107 are required for normal cerebellar development and granule cell survival but not for Purkinje cell persistence.* Development, 2003. **130**(15): p. 3359-68.
144. Cobrinik, D., et al., *Shared role of the pRB-related p130 and p107 proteins in limb development.* Genes Dev, 1996. **10**(13): p. 1633-44.
145. LeCouter, J.E., et al., *Strain-dependent myeloid hyperplasia, growth deficiency, and accelerated cell cycle in mice lacking the Rb-related p107 gene.* Mol Cell Biol, 1998. **18**(12): p. 7455-65.
146. LeCouter, J.E., et al., *Strain-dependent embryonic lethality in mice lacking the retinoblastoma-related p130 gene.* Development, 1998. **125**(23): p. 4669-79.
147. Robanus-Maandag, E., et al., *p107 is a suppressor of retinoblastoma development in pRb-deficient mice.* Genes Dev, 1998. **12**(11): p. 1599-609.
148. Sage, J., et al., *Acute mutation of retinoblastoma gene function is sufficient for cell cycle re-entry.* Nature, 2003. **424**(6945): p. 223-8.
149. Schneider, J.W., et al., *Reversal of terminal differentiation mediated by p107 in Rb-/- muscle cells.* Science, 1994. **264**(5164): p. 1467-71.
150. Huh, M.S., et al., *Rb is required for progression through myogenic differentiation but not maintenance of terminal differentiation.* J Cell Biol, 2004. **166**(6): p. 865-76.
151. Novitch, B.G., et al., *Skeletal muscle cells lacking the retinoblastoma protein display defects in muscle gene expression and accumulate in S and G2 phases of the cell cycle.* J Cell Biol, 1996. **135**(2): p. 441-56.
152. Dannenberg, J.H., et al., *Tissue-specific tumor suppressor activity of retinoblastoma gene homologs p107 and p130.* Genes Dev, 2004. **18**(23): p. 2952-62.
153. Lipinski, M.M. and T. Jacks, *The retinoblastoma gene family in differentiation and development.* Oncogene, 1999. **18**(55): p. 7873-82.
154. Sage, J., et al., *Targeted disruption of the three Rb-related genes leads to loss of G(1) control and immortalization.* Genes Dev, 2000. **14**(23): p. 3037-50.

155. Dannenberg, J.H., et al., *Ablation of the retinoblastoma gene family deregulates G(1) control causing immortalization and increased cell turnover under growth-restricting conditions.* Genes Dev, 2000. **14**(23): p. 3051-64.
156. Mayhew, C.N., et al., *Liver-specific pRB loss results in ectopic cell cycle entry and aberrant ploidy.* Cancer Res, 2005. **65**(11): p. 4568-77.
157. Slack, R.S., et al., *A critical temporal requirement for the retinoblastoma protein family during neuronal determination.* J Cell Biol, 1998. **140**(6): p. 1497-509.
158. Camarda, G., et al., *A pRb-independent mechanism preserves the postmitotic state in terminally differentiated skeletal muscle cells.* J Cell Biol, 2004. **167**(3): p. 417-23.
159. Classon, M., et al., *Opposing roles of pRB and p107 in adipocyte differentiation.* Proc Natl Acad Sci U S A, 2000. **97**(20): p. 10826-31.
160. Carnac, G., et al., *The retinoblastoma-like protein p130 is involved in the determination of reserve cells in differentiating myoblasts.* Curr Biol, 2000. **10**(9): p. 543-6.
161. MacIntosh, B.R., P.F. Gardiner, and A.J. McComas, *Skeletal Muscle. Form and Function. Second Edition.* 2006.
162. Buckingham, M., et al., *The formation of skeletal muscle: from somite to limb.* J Anat, 2003. **202**(1): p. 59-68.
163. Gridley, T., *The long and short of it: somite formation in mice.* Dev Dyn, 2006. **235**(9): p. 2330-6.
164. Gilbert, S.F., *The morphogenesis of evolutionary developmental biology.* Int J Dev Biol, 2003. **47**(7-8): p. 467-77.
165. Parker, M.H., P. Seale, and M.A. Rudnicki, *Looking back to the embryo: defining transcriptional networks in adult myogenesis.* Nat Rev Genet, 2003. **4**(7): p. 497-507.
166. Tajbakhsh, S., et al., *Differential activation of Myf5 and MyoD by different Wnts in explants of mouse paraxial mesoderm and the later activation of myogenesis in the absence of Myf5.* Development, 1998. **125**(21): p. 4155-62.
167. Hollway, G. and P. Currie, *Vertebrate myotome development.* Birth Defects Res C Embryo Today, 2005. **75**(3): p. 172-9.
168. Brent, A.E. and C.J. Tabin, *Developmental regulation of somite derivatives: muscle, cartilage and tendon.* Curr Opin Genet Dev, 2002. **12**(5): p. 548-57.
169. Ordahl, C.P. and N.M. Le Douarin, *Two myogenic lineages within the developing somite.* Development, 1992. **114**(2): p. 339-53.
170. Kassar-Duchossoy, L., et al., *Pax3/Pax7 mark a novel population of primitive myogenic cells during development.* Genes Dev, 2005. **19**(12): p. 1426-31.
171. Braun, T., et al., *Targeted inactivation of the muscle regulatory gene Myf-5 results in abnormal rib development and perinatal death.* Cell, 1992. **71**(3): p. 369-82.
172. Tajbakhsh, S., D. Rocancourt, and M. Buckingham, *Muscle progenitor cells failing to respond to positional cues adopt non-myogenic fates in myf-5 null mice.* Nature, 1996. **384**(6606): p. 266-70.
173. Lagha, M., et al., *Regulation of skeletal muscle stem cell behavior by Pax3 and Pax7.* Cold Spring Harb Symp Quant Biol, 2008. **73**: p. 307-15.

174. Francis-West, P.H., L. Antoni, and K. Anakwe, *Regulation of myogenic differentiation in the developing limb bud.* J Anat, 2003. **202**(1): p. 69-81.
175. Denetclaw, W.F., Jr., B. Christ, and C.P. Ordahl, *Location and growth of epaxial myotome precursor cells.* Development, 1997. **124**(8): p. 1601-10.
176. Buckingham, M., *Myogenic progenitor cells and skeletal myogenesis in vertebrates.* Curr Opin Genet Dev, 2006. **16**(5): p. 525-32.
177. Borello, U., et al., *The Wnt/beta-catenin pathway regulates Gli-mediated Myf5 expression during somitogenesis.* Development, 2006. **133**(18): p. 3723-32.
178. Tajbakhsh, S., et al., *Redefining the genetic hierarchies controlling skeletal myogenesis: Pax-3 and Myf-5 act upstream of MyoD.* Cell, 1997. **89**(1): p. 127-38.
179. Relaix, F., et al., *A Pax3/Pax7-dependent population of skeletal muscle progenitor cells.* Nature, 2005. **435**(7044): p. 948-53.
180. Buckingham, M., *Skeletal muscle progenitor cells and the role of Pax genes.* C R Biol, 2007. **330**(6-7): p. 530-3.
181. Buckingham, M. and F. Relaix, *The role of Pax genes in the development of tissues and organs: Pax3 and Pax7 regulate muscle progenitor cell functions.* Annu Rev Cell Dev Biol, 2007. **23**: p. 645-73.
182. Olivera-Martinez, I., et al., *Mediolateral somitic origin of ribs and dermis determined by quail-chick chimeras.* Development, 2000. **127**(21): p. 4611-7.
183. Gros, J., et al., *A common somitic origin for embryonic muscle progenitors and satellite cells.* Nature, 2005. **435**(7044): p. 954-8.
184. Bladt, F., et al., *Essential role for the c-met receptor in the migration of myogenic precursor cells into the limb bud.* Nature, 1995. **376**(6543): p. 768-71.
185. Epstein, J.A., et al., *Pax3 modulates expression of the c-Met receptor during limb muscle development.* Proc Natl Acad Sci U S A, 1996. **93**(9): p. 4213-8.
186. Sonnenberg, E., et al., *Scatter factor/hepatocyte growth factor and its receptor, the c-met tyrosine kinase, can mediate a signal exchange between mesenchyme and epithelia during mouse development.* J Cell Biol, 1993. **123**(1): p. 223-35.
187. Bajard, L., et al., *A novel genetic hierarchy functions during hypaxial myogenesis: Pax3 directly activates Myf5 in muscle progenitor cells in the limb.* Genes Dev, 2006. **20**(17): p. 2450-64.
188. Seale, P., et al., *Pax7 is required for the specification of myogenic satellite cells.* Cell, 2000. **102**(6): p. 777-86.
189. Mansouri, A., et al., *Dysgenesis of cephalic neural crest derivatives in Pax7-/- mutant mice.* Development, 1996. **122**(3): p. 831-8.
190. Oustanina, S., G. Hause, and T. Braun, *Pax7 directs postnatal renewal and propagation of myogenic satellite cells but not their specification.* Embo J, 2004. **23**(16): p. 3430-9.
191. Schultz, E., *Satellite cell proliferative compartments in growing skeletal muscles.* Dev Biol, 1996. **175**(1): p. 84-94.
192. Beauchamp, J.R., et al., *Expression of CD34 and Myf5 defines the majority of quiescent adult skeletal muscle satellite cells.* J Cell Biol, 2000. **151**(6): p. 1221-34.

193. Cornelison, D.D. and B.J. Wold, *Single-cell analysis of regulatory gene expression in quiescent and activated mouse skeletal muscle satellite cells.* Dev Biol, 1997. **191**(2): p. 270-83.
194. Garry, D.J., et al., *Persistent expression of MNF identifies myogenic stem cells in postnatal muscles.* Dev Biol, 1997. **188**(2): p. 280-94.
195. Darr, K.C. and E. Schultz, *Exercise-induced satellite cell activation in growing and mature skeletal muscle.* J Appl Physiol, 1987. **63**(5): p. 1816-21.
196. Rosenblatt, J.D., D. Yong, and D.J. Parry, *Satellite cell activity is required for hypertrophy of overloaded adult rat muscle.* Muscle Nerve, 1994. **17**(6): p. 608-13.
197. Bischoff, R. and C. Heintz, *Enhancement of skeletal muscle regeneration.* Dev Dyn, 1994. **201**(1): p. 41-54.
198. Appell, H.J., S. Forsberg, and W. Hollmann, *Satellite cell activation in human skeletal muscle after training: evidence for muscle fiber neoformation.* Int J Sports Med, 1988. **9**(4): p. 297-9.
199. Schultz, E., M.C. Gibson, and T. Champion, *Satellite cells are mitotically quiescent in mature mouse muscle: an EM and radioautographic study.* J Exp Zool, 1978. **206**(3): p. 451-6.
200. Collins, C.A., et al., *Stem cell function, self-renewal, and behavioral heterogeneity of cells from the adult muscle satellite cell niche.* Cell, 2005. **122**(2): p. 289-301.
201. Sacco, A., et al., *Self-renewal and expansion of single transplanted muscle stem cells.* Nature, 2008. **456**(7221): p. 502-6.
202. Cerletti, M., et al., *Regulation and function of skeletal muscle stem cells.* Cold Spring Harb Symp Quant Biol, 2008. **73**: p. 317-22.
203. Kuang, S., et al., *Asymmetric self-renewal and commitment of satellite stem cells in muscle.* Cell, 2007. **129**(5): p. 999-1010.
204. Smith, C.K., 2nd, M.J. Janney, and R.E. Allen, *Temporal expression of myogenic regulatory genes during activation, proliferation, and differentiation of rat skeletal muscle satellite cells.* J Cell Physiol, 1994. **159**(2): p. 379-85.
205. Yablonka-Reuveni, Z. and A.J. Rivera, *Temporal expression of regulatory and structural muscle proteins during myogenesis of satellite cells on isolated adult rat fibers.* Dev Biol, 1994. **164**(2): p. 588-603.
206. Fuchtbauer, E.M. and H. Westphal, *MyoD and myogenin are coexpressed in regenerating skeletal muscle of the mouse.* Dev Dyn, 1992. **193**(1): p. 34-9.
207. Cooper, R.N., et al., *In vivo satellite cell activation via Myf5 and MyoD in regenerating mouse skeletal muscle.* J Cell Sci, 1999. **112 (Pt 17)**: p. 2895-901.
208. Cornelison, D.D., et al., *MyoD(-/-) satellite cells in single-fiber culture are differentiation defective and MRF4 deficient.* Dev Biol, 2000. **224**(2): p. 122-37.
209. Davis, R.L., H. Weintraub, and A.B. Lassar, *Expression of a single transfected cDNA converts fibroblasts to myoblasts.* Cell, 1987. **51**(6): p. 987-1000.
210. Braun, T., et al., *A novel human muscle factor related to but distinct from MyoD1 induces myogenic conversion in 10T1/2 fibroblasts.* Embo J, 1989. **8**(3): p. 701-9.
211. Edmondson, D.G. and E.N. Olson, *A gene with homology to the myc similarity region of MyoD1 is expressed during myogenesis and is sufficient to activate the muscle differentiation program.* Genes Dev, 1989. **3**(5): p. 628-40.

212. Wright, W.E., D.A. Sassoon, and V.K. Lin, *Myogenin, a factor regulating myogenesis, has a domain homologous to MyoD.* Cell, 1989. **56**(4): p. 607-17.
213. Braun, T. and H.H. Arnold, *The four human muscle regulatory helix-loop-helix proteins Myf3-Myf6 exhibit similar hetero-dimerization and DNA binding properties.* Nucleic Acids Res, 1991. **19**(20): p. 5645-51.
214. Braun, T., et al., *Myf-6, a new member of the human gene family of myogenic determination factors: evidence for a gene cluster on chromosome 12.* Embo J, 1990. **9**(3): p. 821-31.
215. Braun, T., et al., *Differential expression of myogenic determination genes in muscle cells: possible autoactivation by the Myf gene products.* Embo J, 1989. **8**(12): p. 3617-25.
216. Miner, J.H. and B. Wold, *Herculin, a fourth member of the MyoD family of myogenic regulatory genes.* Proc Natl Acad Sci U S A, 1990. **87**(3): p. 1089-93.
217. Lassar, A.B., et al., *Functional activity of myogenic HLH proteins requires hetero-oligomerization with E12/E47-like proteins in vivo.* Cell, 1991. **66**(2): p. 305-15.
218. Rudnicki, M.A., et al., *Inactivation of MyoD in mice leads to up-regulation of the myogenic HLH gene Myf-5 and results in apparently normal muscle development.* Cell, 1992. **71**(3): p. 383-90.
219. Megeney, L.A., et al., *MyoD is required for myogenic stem cell function in adult skeletal muscle.* Genes Dev, 1996. **10**(10): p. 1173-83.
220. Kablar, B., et al., *MyoD and Myf-5 differentially regulate the development of limb versus trunk skeletal muscle.* Development, 1997. **124**(23): p. 4729-38.
221. Kaul, A., et al., *Myf-5 revisited: loss of early myotome formation does not lead to a rib phenotype in homozygous Myf-5 mutant mice.* Cell, 2000. **102**(1): p. 17-9.
222. Rudnicki, M.A., et al., *MyoD or Myf-5 is required for the formation of skeletal muscle.* Cell, 1993. **75**(7): p. 1351-9.
223. Kassar-Duchossoy, L., et al., *Mrf4 determines skeletal muscle identity in Myf5:Myod double-mutant mice.* Nature, 2004. **431**(7007): p. 466-71.
224. Venuti, J.M., et al., *Myogenin is required for late but not early aspects of myogenesis during mouse development.* J Cell Biol, 1995. **128**(4): p. 563-76.
225. Mak, K.L., et al., *The MRF4 activation domain is required to induce muscle-specific gene expression.* Mol Cell Biol, 1992. **12**(10): p. 4334-46.
226. Hinterberger, T.J., et al., *Expression of the muscle regulatory factor MRF4 during somite and skeletal myofiber development.* Dev Biol, 1991. **147**(1): p. 144-56.
227. Nabeshima, Y., et al., *Myogenin gene disruption results in perinatal lethality because of severe muscle defect.* Nature, 1993. **364**(6437): p. 532-5.
228. Olson, E.N., et al., *Know your neighbors: three phenotypes in null mutants of the myogenic bHLH gene MRF4.* Cell, 1996. **85**(1): p. 1-4.
229. Hasty, P., et al., *Muscle deficiency and neonatal death in mice with a targeted mutation in the myogenin gene.* Nature, 1993. **364**(6437): p. 501-6.
230. Zhang, W., R.R. Behringer, and E.N. Olson, *Inactivation of the myogenic bHLH gene MRF4 results in up-regulation of myogenin and rib anomalies.* Genes Dev, 1995. **9**(11): p. 1388-99.
231. Bassel-Duby, R. and E.N. Olson, *Signaling pathways in skeletal muscle remodeling.* Annu Rev Biochem, 2006. **75**: p. 19-37.

232. Subramanian, S.V. and B. Nadal-Ginard, *Early expression of the different isoforms of the myocyte enhancer factor-2 (MEF2) protein in myogenic as well as non-myogenic cell lineages during mouse embryogenesis.* Mech Dev, 1996. **57**(1): p. 103-12.
233. Edmondson, D.G., et al., *Mef2 gene expression marks the cardiac and skeletal muscle lineages during mouse embryogenesis.* Development, 1994. **120**(5): p. 1251-63.
234. Naidu, P.S., et al., *Myogenin and MEF2 function synergistically to activate the MRF4 promoter during myogenesis.* Mol Cell Biol, 1995. **15**(5): p. 2707-18.
235. Molkentin, J.D., et al., *Cooperative activation of muscle gene expression by MEF2 and myogenic bHLH proteins.* Cell, 1995. **83**(7): p. 1125-36.
236. Black, B.L. and E.N. Olson, *Transcriptional control of muscle development by myocyte enhancer factor-2 (MEF2) proteins.* Annu Rev Cell Dev Biol, 1998. **14**: p. 167-96.
237. Ludolph, D.C. and S.F. Konieczny, *Transcription factor families: muscling in on the myogenic program.* FASEB J, 1995. **9**(15): p. 1595-604.
238. Kaushal, S., et al., *Activation of the myogenic lineage by MEF2A, a factor that induces and cooperates with MyoD.* Science, 1994. **266**(5188): p. 1236-40.
239. Black, B.L., J.D. Molkentin, and E.N. Olson, *Multiple roles for the MyoD basic region in transmission of transcriptional activation signals and interaction with MEF2.* Mol Cell Biol, 1998. **18**(1): p. 69-77.
240. Cserjesi, P. and E.N. Olson, *Myogenin induces the myocyte-specific enhancer binding factor MEF-2 independently of other muscle-specific gene products.* Mol Cell Biol, 1991. **11**(10): p. 4854-62.
241. Naya, F.J., et al., *Transcriptional activity of MEF2 during mouse embryogenesis monitored with a MEF2-dependent transgene.* Development, 1999. **126**(10): p. 2045-52.
242. Perk, J., A. Iavarone, and R. Benezra, *Id family of helix-loop-helix proteins in cancer.* Nat Rev Cancer, 2005. **5**(8): p. 603-14.
243. Norton, J.D., *ID helix-loop-helix proteins in cell growth, differentiation and tumorigenesis.* J Cell Sci, 2000. **113 (Pt 22)**: p. 3897-905.
244. Benezra, R., et al., *The protein Id: a negative regulator of helix-loop-helix DNA binding proteins.* Cell, 1990. **61**(1): p. 49-59.
245. Benezra, R., et al., *Id: a negative regulator of helix-loop-helix DNA binding proteins. Control of terminal myogenic differentiation.* Ann N Y Acad Sci, 1990. **599**: p. 1-11.
246. Biederer, C.H., et al., *The basic helix-loop-helix transcription factors myogenin and Id2 mediate specific induction of caveolin-3 gene expression during embryonic development.* J Biol Chem, 2000. **275**(34): p. 26245-51.
247. Iavarone, A., et al., *The helix-loop-helix protein Id-2 enhances cell proliferation and binds to the retinoblastoma protein.* Genes Dev, 1994. **8**(11): p. 1270-84.
248. Lasorella, A., A. Iavarone, and M.A. Israel, *Id2 specifically alters regulation of the cell cycle by tumor suppressor proteins.* Mol Cell Biol, 1996. **16**(6): p. 2570-8.

249. Biressi, S., et al., *Intrinsic phenotypic diversity of embryonic and fetal myoblasts is revealed by genome-wide gene expression analysis on purified cells.* Dev Biol, 2007. **304**(2): p. 633-51.
250. Biressi, S., M. Molinaro, and G. Cossu, *Cellular heterogeneity during vertebrate skeletal muscle development.* Dev Biol, 2007. **308**(2): p. 281-93.
251. Duxson, M.J., Y. Usson, and A.J. Harris, *The origin of secondary myotubes in mammalian skeletal muscles: ultrastructural studies.* Development, 1989. **107**(4): p. 743-50.
252. Kelly, A.M. and S.I. Zacks, *The histogenesis of rat intercostal muscle.* J Cell Biol, 1969. **42**(1): p. 135-53.
253. Evans, D., et al., *During fetal muscle development, clones of cells contribute to both primary and secondary fibers.* Dev Biol, 1994. **162**(2): p. 348-53.
254. Hawke, T.J. and D.J. Garry, *Myogenic satellite cells: physiology to molecular biology.* J Appl Physiol, 2001. **91**(2): p. 534-51.
255. Seale, P. and M.A. Rudnicki, *A new look at the origin, function, and "stem-cell" status of muscle satellite cells.* Dev Biol, 2000. **218**(2): p. 115-24.
256. Craig, R.W. and R. Padron, *Molecular Structure of the Sarcomere*, in *Myology, 3rd edition*. 2004.
257. Huxley, A.F. and R. Niedergerke, *Structural changes in muscle during contraction; interference microscopy of living muscle fibres.* Nature, 1954. **173**(4412): p. 971-3.
258. Huxley, H. and J. Hanson, *Changes in the cross-striations of muscle during contraction and stretch and their structural interpretation.* Nature, 1954. **173**(4412): p. 973-6.
259. Gordon, A.M., E. Homsher, and M. Regnier, *Regulation of contraction in striated muscle.* Physiol Rev, 2000. **80**(2): p. 853-924.
260. Ohtsuki, I., *Calcium ion regulation of muscle contraction: the regulatory role of troponin T.* Mol Cell Biochem, 1999. **190**(1-2): p. 33-8.
261. Pette, D. and R.S. Staron, *Transitions of muscle fiber phenotypic profiles.* Histochem Cell Biol, 2001. **115**(5): p. 359-72.
262. Dagenais, G.R., R.G. Tancredi, and K.L. Zierler, *Free fatty acid oxidation by forearm muscle at rest, and evidence for an intramuscular lipid pool in the human forearm.* J Clin Invest, 1976. **58**(2): p. 421-31.
263. Rasmussen, B.B. and R.R. Wolfe, *Regulation of fatty acid oxidation in skeletal muscle.* Annu Rev Nutr, 1999. **19**: p. 463-84.
264. Berchtold, M.W., H. Brinkmeier, and M. Muntener, *Calcium ion in skeletal muscle: its crucial role for muscle function, plasticity, and disease.* Physiol Rev, 2000. **80**(3): p. 1215-65.
265. Olson, E.N. and R.S. Williams, *Remodeling muscles with calcineurin.* Bioessays, 2000. **22**(6): p. 510-9.
266. Murayama, T. and Y. Ogawa, *Roles of two ryanodine receptor isoforms coexisting in skeletal muscle.* Trends Cardiovasc Med, 2002. **12**(7): p. 305-11.
267. Anderson, K. and G. Meissner, *T-tubule depolarization-induced SR Ca2+ release is controlled by dihydropyridine receptor- and Ca(2+)-dependent mechanisms in cell homogenates from rabbit skeletal muscle.* J Gen Physiol, 1995. **105**(3): p. 363-83.

268. Rios, E. and G. Pizarro, *Voltage sensor of excitation-contraction coupling in skeletal muscle.* Physiol Rev, 1991. **71**(3): p. 849-908.
269. Jeon, K.W. and M. Friedlander, *International Review of Cytology: A survey of Cell Biology*. 1992.
270. Ebashi, S., *Excitation-contraction coupling and the mechanism of muscle contraction.* Annu Rev Physiol, 1991. **53**: p. 1-16.
271. Toyoshima, C., *Ion pumping by calcium ATPase of sarcoplasmic reticulum.* Adv Exp Med Biol, 2007. **592**: p. 295-303.
272. Schatzmann, H.J., *The calcium pump of the surface membrane and of the sarcoplasmic reticulum.* Annu Rev Physiol, 1989. **51**: p. 473-85.
273. Olson, E.N., *Interplay between proliferation and differentiation within the myogenic lineage.* Dev Biol, 1992. **154**(2): p. 261-72.
274. Clegg, C.H., et al., *Growth factor control of skeletal muscle differentiation: commitment to terminal differentiation occurs in G1 phase and is repressed by fibroblast growth factor.* J Cell Biol, 1987. **105**(2): p. 949-56.
275. Ohkubo, Y., et al., *SV40 large T antigen reinduces the cell cycle in terminally differentiated myotubes through inducing Cdk2, Cdc2, and their partner cyclins.* Exp Cell Res, 1994. **214**(1): p. 270-8.
276. Wang, J. and B. Nadal-Ginard, *Regulation of cyclins and p34CDC2 expression during terminal differentiation of C2C12 myocytes.* Biochem Biophys Res Commun, 1995. **206**(1): p. 82-8.
277. Myers, T.K., S.E. Andreuzza, and D.S. Franklin, *p18INK4c and p27KIP1 are required for cell cycle arrest of differentiated myotubes.* Exp Cell Res, 2004. **300**(2): p. 365-78.
278. Halevy, O., et al., *Correlation of terminal cell cycle arrest of skeletal muscle with induction of p21 by MyoD.* Science, 1995. **267**(5200): p. 1018-21.
279. Parker, S.B., et al., *p53-independent expression of p21Cip1 in muscle and other terminally differentiating cells.* Science, 1995. **267**(5200): p. 1024-7.
280. Zhang, P., et al., *p21(CIP1) and p57(KIP2) control muscle differentiation at the myogenin step.* Genes Dev, 1999. **13**(2): p. 213-24.
281. Nadal-Ginard, B., *Commitment, fusion and biochemical differentiation of a myogenic cell line in the absence of DNA synthesis.* Cell, 1978. **15**(3): p. 855-64.
282. Endo, T. and S. Goto, *Retinoblastoma gene product Rb accumulates during myogenic differentiation and is deinduced by the expression of SV40 large T antigen.* J Biochem (Tokyo), 1992. **112**(4): p. 427-30.
283. DeCaprio, J.A., et al., *SV40 large tumor antigen forms a specific complex with the product of the retinoblastoma susceptibility gene.* Cell, 1988. **54**(2): p. 275-83.
284. Ludlow, J.W., et al., *SV40 large T antigen binds preferentially to an underphosphorylated member of the retinoblastoma susceptibility gene product family.* Cell, 1989. **56**(1): p. 57-65.
285. Stubdal, H., J. Zalvide, and J.A. DeCaprio, *Simian virus 40 large T antigen alters the phosphorylation state of the RB-related proteins p130 and p107.* J Virol, 1996. **70**(5): p. 2781-8.
286. Bargonetti, J., et al., *Site-specific binding of wild-type p53 to cellular DNA is inhibited by SV40 T antigen and mutant p53.* Genes Dev, 1992. **6**(10): p. 1886-98.

287. Eckner, R., et al., *Association of p300 and CBP with simian virus 40 large T antigen.* Mol Cell Biol, 1996. **16**(7): p. 3454-64.
288. Ali, S.H. and J.A. DeCaprio, *Cellular transformation by SV40 large T antigen: interaction with host proteins.* Semin Cancer Biol, 2001. **11**(1): p. 15-23.
289. Iujvidin, S., et al., *SV40 immortalizes myogenic cells: DNA synthesis and mitosis in differentiating myotubes.* Differentiation, 1990. **43**(3): p. 192-203.
290. Endo, T. and B. Nadal-Ginard, *Reversal of myogenic terminal differentiation by SV40 large T antigen results in mitosis and apoptosis.* J Cell Sci, 1998. **111 (Pt 8)**: p. 1081-93.
291. Whyte, P., et al., *Association between an oncogene and an anti-oncogene: the adenovirus E1A proteins bind to the retinoblastoma gene product.* Nature, 1988. **334**(6178): p. 124-9.
292. Whyte, P., N.M. Williamson, and E. Harlow, *Cellular targets for transformation by the adenovirus E1A proteins.* Cell, 1989. **56**(1): p. 67-75.
293. de Stanchina, E., et al., *E1A signaling to p53 involves the p19(ARF) tumor suppressor.* Genes Dev, 1998. **12**(15): p. 2434-42.
294. Tiainen, M., et al., *Expression of E1A in terminally differentiated muscle cells reactivates the cell cycle and suppresses tissue-specific genes by separable mechanisms.* Mol Cell Biol, 1996. **16**(10): p. 5302-12.
295. Braun, T., E. Bober, and H.H. Arnold, *Inhibition of muscle differentiation by the adenovirus E1a protein: repression of the transcriptional activating function of the HLH protein Myf-5.* Genes Dev, 1992. **6**(5): p. 888-902.
296. Taylor, D.A., et al., *E1A-mediated inhibition of myogenesis correlates with a direct physical interaction of E1A12S and basic helix-loop-helix proteins.* Mol Cell Biol, 1993. **13**(8): p. 4714-27.
297. Pajcini, K.V., et al., *Transient Inactivation of Rb and ARF Yields Regenerative Cells from Postmitotic Mammalian Muscle.* Cell Stem Cell. **7**(2): p. 198-213.
298. Kiess, M., R.M. Gill, and P.A. Hamel, *Expression of the positive regulator of cell cycle progression, cyclin D3, is induced during differentiation of myoblasts into quiescent myotubes.* Oncogene, 1995. **10**(1): p. 159-66.
299. Bartkova, J., et al., *Cyclin D3: requirement for G1/S transition and high abundance in quiescent tissues suggest a dual role in proliferation and differentiation.* Oncogene, 1998. **17**(8): p. 1027-37.
300. Rao, S.S. and D.S. Kohtz, *Positive and negative regulation of D-type cyclin expression in skeletal myoblasts by basic fibroblast growth factor and transforming growth factor beta. A role for cyclin D1 in control of myoblast differentiation.* J Biol Chem, 1995. **270**(8): p. 4093-100.
301. De Santa, F., et al., *pRb-dependent cyclin D3 protein stabilization is required for myogenic differentiation.* Mol Cell Biol, 2007. **27**(20): p. 7248-65.
302. Rao, S.S., C. Chu, and D.S. Kohtz, *Ectopic expression of cyclin D1 prevents activation of gene transcription by myogenic basic helix-loop-helix regulators.* Mol Cell Biol, 1994. **14**(8): p. 5259-67.
303. Skapek, S.X., et al., *Inhibition of myogenic differentiation in proliferating myoblasts by cyclin D1-dependent kinase.* Science, 1995. **267**(5200): p. 1022-4.

304. Crescenzi, M., et al., *MyoD induces growth arrest independent of differentiation in normal and transformed cells.* Proc Natl Acad Sci U S A, 1990. **87**(21): p. 8442-6.
305. Sorrentino, V., et al., *Cell proliferation inhibited by MyoD1 independently of myogenic differentiation.* Nature, 1990. **345**(6278): p. 813-5.
306. Lassar, A.B., S.X. Skapek, and B. Novitch, *Regulatory mechanisms that coordinate skeletal muscle differentiation and cell cycle withdrawal.* Curr Opin Cell Biol, 1994. **6**(6): p. 788-94.
307. Guo, K., et al., *MyoD-induced expression of p21 inhibits cyclin-dependent kinase activity upon myocyte terminal differentiation.* Mol Cell Biol, 1995. **15**(7): p. 3823-9.
308. Pajalunga, D., et al., *Critical requirement for cell cycle inhibitors in sustaining nonproliferative states.* J Cell Biol, 2007. **176**(6): p. 807-18.
309. Deng, C., et al., *Mice lacking p21CIP1/WAF1 undergo normal development, but are defective in G1 checkpoint control.* Cell, 1995. **82**(4): p. 675-84.
310. Zhang, P., et al., *Altered cell differentiation and proliferation in mice lacking p57KIP2 indicates a role in Beckwith-Wiedemann syndrome.* Nature, 1997. **387**(6629): p. 151-8.
311. Nakayama, K., et al., *Mice lacking p27(Kip1) display increased body size, multiple organ hyperplasia, retinal dysplasia, and pituitary tumors.* Cell, 1996. **85**(5): p. 707-20.
312. Kiyokawa, H., et al., *Enhanced growth of mice lacking the cyclin-dependent kinase inhibitor function of p27(Kip1).* Cell, 1996. **85**(5): p. 721-32.
313. Fero, M.L., et al., *A syndrome of multiorgan hyperplasia with features of gigantism, tumorigenesis, and female sterility in p27(Kip1)-deficient mice.* Cell, 1996. **85**(5): p. 733-44.
314. Serrano, M., et al., *Role of the INK4a locus in tumor suppression and cell mortality.* Cell, 1996. **85**(1): p. 27-37.
315. Massague, J., et al., *Type beta transforming growth factor is an inhibitor of myogenic differentiation.* Proc Natl Acad Sci U S A, 1986. **83**(21): p. 8206-10.
316. Florini, J.R., et al., *Transforming growth factor-beta. A very potent inhibitor of myoblast differentiation, identical to the differentiation inhibitor secreted by Buffalo rat liver cells.* J Biol Chem, 1986. **261**(35): p. 16509-13.
317. Cusella-De Angelis, M.G., et al., *Differential response of embryonic and fetal myoblasts to TGF beta: a possible regulatory mechanism of skeletal muscle histogenesis.* Development, 1994. **120**(4): p. 925-33.
318. Olson, E.N., et al., *Regulation of myogenic differentiation by type beta transforming growth factor.* J Cell Biol, 1986. **103**(5): p. 1799-805.
319. Spizz, G., et al., *Serum and fibroblast growth factor inhibit myogenic differentiation through a mechanism dependent on protein synthesis and independent of cell proliferation.* J Biol Chem, 1986. **261**(20): p. 9483-8.
320. Vaidya, T.B., et al., *Fibroblast growth factor and transforming growth factor beta repress transcription of the myogenic regulatory gene MyoD1.* Mol Cell Biol, 1989. **9**(8): p. 3576-9.

321. Brennan, T.J., et al., *Transforming growth factor beta represses the actions of myogenin through a mechanism independent of DNA binding.* Proc Natl Acad Sci U S A, 1991. **88**(9): p. 3822-6.
322. Edmondson, D.G., T.J. Brennan, and E.N. Olson, *Mitogenic repression of myogenin autoregulation.* J Biol Chem, 1991. **266**(32): p. 21343-6.
323. Salminen, A., et al., *Transcription of the muscle regulatory gene Myf4 is regulated by serum components, peptide growth factors and signaling pathways involving G proteins.* J Cell Biol, 1991. **115**(4): p. 905-17.
324. Lassar, A.B., et al., *Transformation by activated ras or fos prevents myogenesis by inhibiting expression of MyoD1.* Cell, 1989. **58**(4): p. 659-67.
325. Puri, P.L., et al., *Class I histone deacetylases sequentially interact with MyoD and pRb during skeletal myogenesis.* Mol Cell, 2001. **8**(4): p. 885-97.
326. Eckner, R., et al., *Interaction and functional collaboration of p300/CBP and bHLH proteins in muscle and B-cell differentiation.* Genes Dev, 1996. **10**(19): p. 2478-90.
327. Yuan, W., et al., *Human p300 protein is a coactivator for the transcription factor MyoD.* J Biol Chem, 1996. **271**(15): p. 9009-13.
328. Puri, P.L., et al., *Differential roles of p300 and PCAF acetyltransferases in muscle differentiation.* Mol Cell, 1997. **1**(1): p. 35-45.
329. MacLellan, W.R., et al., *A novel Rb- and p300-binding protein inhibits transactivation by MyoD.* Mol Cell Biol, 2000. **20**(23): p. 8903-15.
330. Benevolenskaya, E.V., et al., *Binding of pRB to the PHD protein RBP2 promotes cellular differentiation.* Mol Cell, 2005. **18**(6): p. 623-35.
331. Schweichel, J.U. and H.J. Merker, *The morphology of various types of cell death in prenatal tissues.* Teratology, 1973. **7**(3): p. 253-66.
332. Kroemer, G., et al., *Classification of cell death: recommendations of the Nomenclature Committee on Cell Death 2009.* Cell Death Differ, 2009. **16**(1): p. 3-11.
333. Kroemer, G. and B. Levine, *Autophagic cell death: the story of a misnomer.* Nat Rev Mol Cell Biol, 2008. **9**(12): p. 1004-10.
334. Levine, B. and J. Yuan, *Autophagy in cell death: an innocent convict?* J Clin Invest, 2005. **115**(10): p. 2679-88.
335. Kerr, J.F., A.H. Wyllie, and A.R. Currie, *Apoptosis: a basic biological phenomenon with wide-ranging implications in tissue kinetics.* Br J Cancer, 1972. **26**(4): p. 239-57.
336. Riedl, S.J. and Y. Shi, *Molecular mechanisms of caspase regulation during apoptosis.* Nat Rev Mol Cell Biol, 2004. **5**(11): p. 897-907.
337. Earnshaw, W.C., L.M. Martins, and S.H. Kaufmann, *Mammalian caspases: structure, activation, substrates, and functions during apoptosis.* Annu Rev Biochem, 1999. **68**: p. 383-424.
338. Elmore, S., *Apoptosis: a review of programmed cell death.* Toxicol Pathol, 2007. **35**(4): p. 495-516.
339. Strasser, A., L. O'Connor, and V.M. Dixit, *Apoptosis signaling.* Annu Rev Biochem, 2000. **69**: p. 217-45.
340. Li, H., et al., *Cleavage of BID by caspase 8 mediates the mitochondrial damage in the Fas pathway of apoptosis.* Cell, 1998. **94**(4): p. 491-501.

341. Wang, C. and R.J. Youle, *The role of mitochondria in apoptosis*.* Annu Rev Genet, 2009. **43**: p. 95-118.
342. Shi, Y., *Mechanical aspects of apoptosome assembly.* Curr Opin Cell Biol, 2006. **18**(6): p. 677-84.
343. Tenev, T., et al., *IAPs are functionally non-equivalent and regulate effector caspases through distinct mechanisms.* Nat Cell Biol, 2005. **7**(1): p. 70-7.
344. Deveraux, Q.L., et al., *X-linked IAP is a direct inhibitor of cell-death proteases.* Nature, 1997. **388**(6639): p. 300-4.
345. Shi, Y., *Mechanisms of caspase activation and inhibition during apoptosis.* Mol Cell, 2002. **9**(3): p. 459-70.
346. Xu, D., et al., *Attenuation of ischemia-induced cellular and behavioral deficits by X chromosome-linked inhibitor of apoptosis protein overexpression in the rat hippocampus.* J Neurosci, 1999. **19**(12): p. 5026-33.
347. Duckett, C.S., et al., *Human IAP-like protein regulates programmed cell death downstream of Bcl-xL and cytochrome c.* Mol Cell Biol, 1998. **18**(1): p. 608-15.
348. Cregan, S.P., et al., *Apoptosis-inducing factor is involved in the regulation of caspase-independent neuronal cell death.* J Cell Biol, 2002. **158**(3): p. 507-17.
349. Cory, S. and J.M. Adams, *The Bcl2 family: regulators of the cellular life-or-death switch.* Nat Rev Cancer, 2002. **2**(9): p. 647-56.
350. Youle, R.J. and A. Strasser, *The BCL-2 protein family: opposing activities that mediate cell death.* Nat Rev Mol Cell Biol, 2008. **9**(1): p. 47-59.
351. Willis, S.N., et al., *Apoptosis initiated when BH3 ligands engage multiple Bcl-2 homologs, not Bax or Bak.* Science, 2007. **315**(5813): p. 856-9.
352. Kluck, R.M., et al., *The release of cytochrome c from mitochondria: a primary site for Bcl-2 regulation of apoptosis.* Science, 1997. **275**(5303): p. 1132-6.
353. Yang, J., et al., *Prevention of apoptosis by Bcl-2: release of cytochrome c from mitochondria blocked.* Science, 1997. **275**(5303): p. 1129-32.
354. Chipuk, J.E. and D.R. Green, *How do BCL-2 proteins induce mitochondrial outer membrane permeabilization?* Trends Cell Biol, 2008. **18**(4): p. 157-64.
355. Lindsten, T., et al., *The combined functions of proapoptotic Bcl-2 family members bak and bax are essential for normal development of multiple tissues.* Mol Cell, 2000. **6**(6): p. 1389-99.
356. Wei, M.C., et al., *Proapoptotic BAX and BAK: a requisite gateway to mitochondrial dysfunction and death.* Science, 2001. **292**(5517): p. 727-30.
357. Puthalakath, H., et al., *ER stress triggers apoptosis by activating BH3-only protein Bim.* Cell, 2007. **129**(7): p. 1337-49.
358. Hao, Z., et al., *Specific ablation of the apoptotic functions of cytochrome C reveals a differential requirement for cytochrome C and Apaf-1 in apoptosis.* Cell, 2005. **121**(4): p. 579-91.
359. Ho, A.T., et al., *Coupling of caspase-9 to Apaf1 in response to loss of pRb or cytotoxic drugs is cell-type-specific.* Embo J, 2004. **23**(2): p. 460-72.
360. Ho, A.T., et al., *XIAP activity dictates Apaf-1 dependency for caspase 9 activation.* Mol Cell Biol, 2007. **27**(16): p. 5673-85.
361. Lum, J.J., R.J. DeBerardinis, and C.B. Thompson, *Autophagy in metazoans: cell survival in the land of plenty.* Nat Rev Mol Cell Biol, 2005. **6**(6): p. 439-48.

362. Kim, I., S. Rodriguez-Enriquez, and J.J. Lemasters, *Selective degradation of mitochondria by mitophagy.* Arch Biochem Biophys, 2007. **462**(2): p. 245-53.
363. He, C. and D.J. Klionsky, *Regulation mechanisms and signaling pathways of autophagy.* Annu Rev Genet, 2009. **43**: p. 67-93.
364. Sattler, T. and A. Mayer, *Cell-free reconstitution of microautophagic vacuole invagination and vesicle formation.* J Cell Biol, 2000. **151**(3): p. 529-38.
365. Wang, C.-W. and D.J. Klionsky, *Microautophagy*, in *Autophagy*. 2003, Landes Bioscience: Georgetown, TX. p. 107-114.
366. Kunz, J.B., H. Schwarz, and A. Mayer, *Determination of four sequential stages during microautophagy in vitro.* J Biol Chem, 2004. **279**(11): p. 9987-96.
367. Chiang, H.L. and J.F. Dice, *Peptide sequences that target proteins for enhanced degradation during serum withdrawal.* J Biol Chem, 1988. **263**(14): p. 6797-805.
368. Dice, J.F., *Chaperone-mediated autophagy.* Autophagy, 2007. **3**(4): p. 295-9.
369. Chirico, W.J., M.G. Waters, and G. Blobel, *70K heat shock related proteins stimulate protein translocation into microsomes.* Nature, 1988. **332**(6167): p. 805-10.
370. Deshaies, R.J., et al., *A subfamily of stress proteins facilitates translocation of secretory and mitochondrial precursor polypeptides.* Nature, 1988. **332**(6167): p. 800-5.
371. Chiang, H.L., et al., *A role for a 70-kilodalton heat shock protein in lysosomal degradation of intracellular proteins.* Science, 1989. **246**(4928): p. 382-5.
372. Cuervo, A.M. and J.F. Dice, *A receptor for the selective uptake and degradation of proteins by lysosomes.* Science, 1996. **273**(5274): p. 501-3.
373. Liang, C. and J.U. Jung, *Autophagy genes as tumor suppressors.* Curr Opin Cell Biol, 2009.
374. Levine, B. and D.J. Klionsky, *Development by self-digestion: molecular mechanisms and biological functions of autophagy.* Dev Cell, 2004. **6**(4): p. 463-77.
375. Schmelzle, T. and M.N. Hall, *TOR, a central controller of cell growth.* Cell, 2000. **103**(2): p. 253-62.
376. Hay, N. and N. Sonenberg, *Upstream and downstream of mTOR.* Genes Dev, 2004. **18**(16): p. 1926-45.
377. Ravikumar, B., et al., *Inhibition of mTOR induces autophagy and reduces toxicity of polyglutamine expansions in fly and mouse models of Huntington disease.* Nat Genet, 2004. **36**(6): p. 585-95.
378. Hosokawa, N., et al., *Nutrient-dependent mTORC1 association with the ULK1-Atg13-FIP200 complex required for autophagy.* Mol Biol Cell, 2009. **20**(7): p. 1981-91.
379. Jung, C.H., et al., *ULK-Atg13-FIP200 complexes mediate mTOR signaling to the autophagy machinery.* Mol Biol Cell, 2009. **20**(7): p. 1992-2003.
380. Hara, T., et al., *FIP200, a ULK-interacting protein, is required for autophagosome formation in mammalian cells.* J Cell Biol, 2008. **181**(3): p. 497-510.
381. Mercer, C.A., A. Kaliappan, and P.B. Dennis, *A novel, human Atg13 binding protein, Atg101, interacts with ULK1 and is essential for macroautophagy.* Autophagy, 2009. **5**(5): p. 649-62.

382. Inoki, K., et al., *TSC2 integrates Wnt and energy signals via a coordinated phosphorylation by AMPK and GSK3 to regulate cell growth.* Cell, 2006. **126**(5): p. 955-68.
383. Shaw, R.J. and L.C. Cantley, *Ras, PI(3)K and mTOR signalling controls tumour cell growth.* Nature, 2006. **441**(7092): p. 424-30.
384. Inoki, K., T. Zhu, and K.L. Guan, *TSC2 mediates cellular energy response to control cell growth and survival.* Cell, 2003. **115**(5): p. 577-90.
385. Levine, A.J., et al., *Coordination and communication between the p53 and IGF-1-AKT-TOR signal transduction pathways.* Genes Dev, 2006. **20**(3): p. 267-75.
386. Carling, D., *Ampk.* Curr Biol, 2004. **14**(6): p. R220.
387. Hardie, D.G., *The AMP-activated protein kinase pathway--new players upstream and downstream.* J Cell Sci, 2004. **117**(Pt 23): p. 5479-87.
388. Bolster, D.R., et al., *AMP-activated protein kinase suppresses protein synthesis in rat skeletal muscle through down-regulated mammalian target of rapamycin (mTOR) signaling.* J Biol Chem, 2002. **277**(27): p. 23977-80.
389. Liang, J., et al., *The energy sensing LKB1-AMPK pathway regulates p27(kip1) phosphorylation mediating the decision to enter autophagy or apoptosis.* Nat Cell Biol, 2007. **9**(2): p. 218-24.
390. Sarkar, S., et al., *Trehalose, a novel mTOR-independent autophagy enhancer, accelerates the clearance of mutant huntingtin and alpha-synuclein.* J Biol Chem, 2007. **282**(8): p. 5641-52.
391. Sarkar, S., et al., *Lithium induces autophagy by inhibiting inositol monophosphatase.* J Cell Biol, 2005. **170**(7): p. 1101-11.
392. Mizushima, N., T. Yoshimori, and B. Levine, *Methods in mammalian autophagy research.* Cell. **140**(3): p. 313-26.
393. Sarkar, S., et al., *Small molecules enhance autophagy and reduce toxicity in Huntington's disease models.* Nat Chem Biol, 2007. **3**(6): p. 331-8.
394. Williams, A., et al., *Novel targets for Huntington's disease in an mTOR-independent autophagy pathway.* Nat Chem Biol, 2008. **4**(5): p. 295-305.
395. Berridge, M.J., *Inositol trisphosphate and calcium signalling.* Nature, 1993. **361**(6410): p. 315-25.
396. Mammucari, C., et al., *FoxO3 controls autophagy in skeletal muscle in vivo.* Cell Metab, 2007. **6**(6): p. 458-71.
397. Zhao, J., et al., *FoxO3 coordinately activates protein degradation by the autophagic/lysosomal and proteasomal pathways in atrophying muscle cells.* Cell Metab, 2007. **6**(6): p. 472-83.
398. Liang, X.H., et al., *Induction of autophagy and inhibition of tumorigenesis by beclin 1.* Nature, 1999. **402**(6762): p. 672-6.
399. Sun, Q., et al., *Identification of Barkor as a mammalian autophagy-specific factor for Beclin 1 and class III phosphatidylinositol 3-kinase.* Proc Natl Acad Sci U S A, 2008. **105**(49): p. 19211-6.
400. Pattingre, S., et al., *Bcl-2 antiapoptotic proteins inhibit Beclin 1-dependent autophagy.* Cell, 2005. **122**(6): p. 927-39.
401. Suzuki, K., et al., *Hierarchy of Atg proteins in pre-autophagosomal structure organization.* Genes Cells, 2007. **12**(2): p. 209-18.

402. Mizushima, N., et al., *Mouse Apg16L, a novel WD-repeat protein, targets to the autophagic isolation membrane with the Apg12-Apg5 conjugate.* J Cell Sci, 2003. **116**(Pt 9): p. 1679-88.
403. Kabeya, Y., et al., *LC3, a mammalian homologue of yeast Apg8p, is localized in autophagosome membranes after processing.* Embo J, 2000. **19**(21): p. 5720-8.
404. Mizushima, N., *Autophagy: process and function.* Genes Dev, 2007. **21**(22): p. 2861-73.
405. Klionsky, D.J., et al., *Guidelines for the use and interpretation of assays for monitoring autophagy in higher eukaryotes.* Autophagy, 2008. **4**(2): p. 151-75.
406. Mizushima, N. and T. Yoshimori, *How to interpret LC3 immunoblotting.* Autophagy, 2007. **3**(6): p. 542-5.
407. Kirisako, T., et al., *The reversible modification regulates the membrane-binding state of Apg8/Aut7 essential for autophagy and the cytoplasm to vacuole targeting pathway.* J Cell Biol, 2000. **151**(2): p. 263-76.
408. Seglen, P.O. and P.B. Gordon, *3-Methyladenine: specific inhibitor of autophagic/lysosomal protein degradation in isolated rat hepatocytes.* Proc Natl Acad Sci U S A, 1982. **79**(6): p. 1889-92.
409. Xue, L., V. Borutaite, and A.M. Tolkovsky, *Inhibition of mitochondrial permeability transition and release of cytochrome c by anti-apoptotic nucleoside analogues.* Biochem Pharmacol, 2002. **64**(3): p. 441-9.
410. Tanaka, Y., et al., *Accumulation of autophagic vacuoles and cardiomyopathy in LAMP-2-deficient mice.* Nature, 2000. **406**(6798): p. 902-6.
411. Jager, S., et al., *Role for Rab7 in maturation of late autophagic vacuoles.* J Cell Sci, 2004. **117**(Pt 20): p. 4837-48.
412. Iwai-Kanai, E., et al., *A method to measure cardiac autophagic flux in vivo.* Autophagy, 2008. **4**(3): p. 322-9.
413. Tanida, I., et al., *Lysosomal turnover, but not a cellular level, of endogenous LC3 is a marker for autophagy.* Autophagy, 2005. **1**(2): p. 84-91.
414. Tolkovsky, A.M., *Mitophagy.* Biochim Biophys Acta, 2009. **1793**(9): p. 1508-15.
415. Lemasters, J.J., *Selective mitochondrial autophagy, or mitophagy, as a targeted defense against oxidative stress, mitochondrial dysfunction, and aging.* Rejuvenation Res, 2005. **8**(1): p. 3-5.
416. Menzies, R.A. and P.H. Gold, *The turnover of mitochondria in a variety of tissues of young adult and aged rats.* J Biol Chem, 1971. **246**(8): p. 2425-9.
417. Sandoval, H., et al., *Essential role for Nix in autophagic maturation of erythroid cells.* Nature, 2008. **454**(7201): p. 232-5.
418. Boya, P., et al., *Inhibition of macroautophagy triggers apoptosis.* Mol Cell Biol, 2005. **25**(3): p. 1025-40.
419. Shimizu, S., et al., *Role of Bcl-2 family proteins in a non-apoptotic programmed cell death dependent on autophagy genes.* Nat Cell Biol, 2004. **6**(12): p. 1221-8.
420. Tolkovsky, A.M., et al., *Mitochondrial disappearance from cells: a clue to the role of autophagy in programmed cell death and disease?* Biochimie, 2002. **84**(2-3): p. 233-40.
421. Xue, L., G.C. Fletcher, and A.M. Tolkovsky, *Mitochondria are selectively eliminated from eukaryotic cells after blockade of caspases during apoptosis.* Curr Biol, 2001. **11**(5): p. 361-5.

422. Maiuri, M.C., et al., *Self-eating and self-killing: crosstalk between autophagy and apoptosis.* Nat Rev Mol Cell Biol, 2007. **8**(9): p. 741-52.
423. Degenhardt, K., et al., *Autophagy promotes tumor cell survival and restricts necrosis, inflammation, and tumorigenesis.* Cancer Cell, 2006. **10**(1): p. 51-64.
424. Lum, J.J., et al., *Growth factor regulation of autophagy and cell survival in the absence of apoptosis.* Cell, 2005. **120**(2): p. 237-48.
425. Kanki, T., et al., *Atg32 is a mitochondrial protein that confers selectivity during mitophagy.* Dev Cell, 2009. **17**(1): p. 98-109.
426. Okamoto, K., N. Kondo-Okamoto, and Y. Ohsumi, *Mitochondria-anchored receptor Atg32 mediates degradation of mitochondria via selective autophagy.* Dev Cell, 2009. **17**(1): p. 87-97.
427. Narendra, D., et al., *Parkin is recruited selectively to impaired mitochondria and promotes their autophagy.* J Cell Biol, 2008. **183**(5): p. 795-803.
428. Geisler, S., et al., *PINK1/Parkin-mediated mitophagy is dependent on VDAC1 and p62/SQSTM1.* Nat Cell Bio, 2010. **12**(2): p. 119-133.
429. Tracy, K., et al., *BNIP3 is an RB/E2F target gene required for hypoxia-induced autophagy.* Mol Cell Biol, 2007. **27**(17): p. 6229-42.
430. Polager, S., M. Ofir, and D. Ginsberg, *E2F1 regulates autophagy and the transcription of autophagy genes.* Oncogene, 2008. **27**(35): p. 4860-4.
431. Zhang, J. and P.A. Ney, *Role of BNIP3 and NIX in cell death, autophagy, and mitophagy.* Cell Death Differ, 2009. **16**(7): p. 939-46.
432. Vande Velde, C., et al., *BNIP3 and genetic control of necrosis-like cell death through the mitochondrial permeability transition pore.* Mol Cell Biol, 2000. **20**(15): p. 5454-68.
433. Daido, S., et al., *Pivotal role of the cell death factor BNIP3 in ceramide-induced autophagic cell death in malignant glioma cells.* Cancer Res, 2004. **64**(12): p. 4286-93.
434. Kanzawa, T., et al., *Arsenic trioxide induces autophagic cell death in malignant glioma cells by upregulation of mitochondrial cell death protein BNIP3.* Oncogene, 2005. **24**(6): p. 980-91.
435. Reef, S., et al., *A short mitochondrial form of p19ARF induces autophagy and caspase-independent cell death.* Mol Cell, 2006. **22**(4): p. 463-75.
436. Abida, W.M. and W. Gu, *p53-Dependent and p53-independent activation of autophagy by ARF.* Cancer Res, 2008. **68**(2): p. 352-7.
437. Humbey, O., et al., *The ARF tumor suppressor can promote the progression of some tumors.* Cancer Res, 2008. **68**(23): p. 9608-13.
438. Balaban, R.S., S. Nemoto, and T. Finkel, *Mitochondria, oxidants, and aging.* Cell, 2005. **120**(4): p. 483-95.
439. Carew, J.S. and P. Huang, *Mitochondrial defects in cancer.* Mol Cancer, 2002. **1**: p. 9.
440. Scheffler, I., *Mitochondria*. 1999.
441. Hock, M.B. and A. Kralli, *Transcriptional control of mitochondrial biogenesis and function.* Annu Rev Physiol, 2009. **71**: p. 177-203.
442. Kelly, D.P. and R.C. Scarpulla, *Transcriptional regulatory circuits controlling mitochondrial biogenesis and function.* Genes Dev, 2004. **18**(4): p. 357-68.

443. Anderson, S., et al., *Sequence and organization of the human mitochondrial genome.* Nature, 1981. **290**(5806): p. 457-65.
444. Pagliarini, D.J., et al., *A mitochondrial protein compendium elucidates complex I disease biology.* Cell, 2008. **134**(1): p. 112-23.
445. McDonald, T.G. and J.E. Van Eyk, *Mitochondrial proteomics. Undercover in the lipid bilayer.* Basic Res Cardiol, 2003. **98**(4): p. 219-27.
446. Garesse, R. and C.G. Vallejo, *Animal mitochondrial biogenesis and function: a regulatory cross-talk between two genomes.* Gene, 2001. **263**(1-2): p. 1-16.
447. Frey, T.G. and C.A. Mannella, *The internal structure of mitochondria.* Trends Biochem Sci, 2000. **25**(7): p. 319-24.
448. Chipuk, J.E., L. Bouchier-Hayes, and D.R. Green, *Mitochondrial outer membrane permeabilization during apoptosis: the innocent bystander scenario.* Cell Death Differ, 2006. **13**(8): p. 1396-402.
449. Rostovtseva, T.K. and S.M. Bezrukov, *VDAC regulation: role of cytosolic proteins and mitochondrial lipids.* J Bioenerg Biomembr, 2008. **40**(3): p. 163-70.
450. Lemasters, J.J. and E. Holmuhamedov, *Voltage-dependent anion channel (VDAC) as mitochondrial governator--thinking outside the box.* Biochim Biophys Acta, 2006. **1762**(2): p. 181-90.
451. Zhivotovsky, B., et al., *Adenine nucleotide translocase: a component of the phylogenetically conserved cell death machinery.* Cell Death Differ, 2009. **16**(11): p. 1419-25.
452. Halestrap, A.P., *What is the mitochondrial permeability transition pore?* J Mol Cell Cardiol, 2009. **46**(6): p. 821-31.
453. Zoratti, M., I. Szabo, and U. De Marchi, *Mitochondrial permeability transitions: how many doors to the house?* Biochim Biophys Acta, 2005. **1706**(1-2): p. 40-52.
454. Herrmann, J.M. and K. Hell, *Chopped, trapped or tacked--protein translocation into the IMS of mitochondria.* Trends Biochem Sci, 2005. **30**(4): p. 205-11.
455. Munoz-Pinedo, C., et al., *Different mitochondrial intermembrane space proteins are released during apoptosis in a manner that is coordinately initiated but can vary in duration.* Proc Natl Acad Sci U S A, 2006. **103**(31): p. 11573-8.
456. Scalettar, B.A., J.R. Abney, and C.R. Hackenbrock, *Dynamics, structure, and function are coupled in the mitochondrial matrix.* Proc Natl Acad Sci U S A, 1991. **88**(18): p. 8057-61.
457. Puigserver, P., et al., *A cold-inducible coactivator of nuclear receptors linked to adaptive thermogenesis.* Cell, 1998. **92**(6): p. 829-39.
458. Knutti, D., A. Kaul, and A. Kralli, *A tissue-specific coactivator of steroid receptors, identified in a functional genetic screen.* Mol Cell Biol, 2000. **20**(7): p. 2411-22.
459. Wu, Z., et al., *Mechanisms controlling mitochondrial biogenesis and respiration through the thermogenic coactivator PGC-1.* Cell, 1999. **98**(1): p. 115-24.
460. St-Pierre, J., et al., *Bioenergetic analysis of peroxisome proliferator-activated receptor gamma coactivators 1alpha and 1beta (PGC-1alpha and PGC-1beta) in muscle cells.* J Biol Chem, 2003. **278**(29): p. 26597-603.
461. Handschin, C., et al., *Skeletal muscle fiber-type switching, exercise intolerance, and myopathy in PGC-1alpha muscle-specific knock-out animals.* J Biol Chem, 2007. **282**(41): p. 30014-21.

462. Handschin, C., et al., *Abnormal glucose homeostasis in skeletal muscle-specific PGC-1alpha knockout mice reveals skeletal muscle-pancreatic beta cell crosstalk.* J Clin Invest, 2007. **117**(11): p. 3463-74.
463. van Raalte, D.H., et al., *Peroxisome proliferator-activated receptor (PPAR)-alpha: a pharmacological target with a promising future.* Pharm Res, 2004. **21**(9): p. 1531-8.
464. Berger, J. and D.E. Moller, *The mechanisms of action of PPARs.* Annu Rev Med, 2002. **53**: p. 409-35.
465. Sher, T., et al., *cDNA cloning, chromosomal mapping, and functional characterization of the human peroxisome proliferator activated receptor.* Biochemistry, 1993. **32**(21): p. 5598-604.
466. Greene, M.E., et al., *Isolation of the human peroxisome proliferator activated receptor gamma cDNA: expression in hematopoietic cells and chromosomal mapping.* Gene Expr, 1995. **4**(4-5): p. 281-99.
467. Schmidt, A., et al., *Identification of a new member of the steroid hormone receptor superfamily that is activated by a peroxisome proliferator and fatty acids.* Mol Endocrinol, 1992. **6**(10): p. 1634-41.
468. Kliewer, S.A., et al., *Differential expression and activation of a family of murine peroxisome proliferator-activated receptors.* Proc Natl Acad Sci U S A, 1994. **91**(15): p. 7355-9.
469. Dreyer, C., et al., *Control of the peroxisomal beta-oxidation pathway by a novel family of nuclear hormone receptors.* Cell, 1992. **68**(5): p. 879-87.
470. Lee, S.S., et al., *Targeted disruption of the alpha isoform of the peroxisome proliferator-activated receptor gene in mice results in abolishment of the pleiotropic effects of peroxisome proliferators.* Mol Cell Biol, 1995. **15**(6): p. 3012-22.
471. Rosen, E.D., et al., *C/EBPalpha induces adipogenesis through PPARgamma: a unified pathway.* Genes Dev, 2002. **16**(1): p. 22-6.
472. Braissant, O., et al., *Differential expression of peroxisome proliferator-activated receptors (PPARs): tissue distribution of PPAR-alpha, -beta, and -gamma in the adult rat.* Endocrinology, 1996. **137**(1): p. 354-66.
473. Wang, Y.X., et al., *Peroxisome-proliferator-activated receptor delta activates fat metabolism to prevent obesity.* Cell, 2003. **113**(2): p. 159-70.
474. Tanaka, T., et al., *Activation of peroxisome proliferator-activated receptor delta induces fatty acid beta-oxidation in skeletal muscle and attenuates metabolic syndrome.* Proc Natl Acad Sci U S A, 2003. **100**(26): p. 15924-9.
475. Wang, Y.X., et al., *Regulation of muscle fiber type and running endurance by PPARdelta.* PLoS Biol, 2004. **2**(10): p. e294.
476. Wenz, T., et al., *Activation of the PPAR/PGC-1alpha pathway prevents a bioenergetic deficit and effectively improves a mitochondrial myopathy phenotype.* Cell Metab, 2008. **8**(3): p. 249-56.
477. Hondares, E., et al., *PPARdelta, but not PPARalpha, activates PGC-1alpha gene transcription in muscle.* Biochem Biophys Res Commun, 2007. **354**(4): p. 1021-7.
478. Bastin, J., et al., *Activation of peroxisome proliferator-activated receptor pathway stimulates the mitochondrial respiratory chain and can correct deficiencies in*

patients' cells lacking its components. J Clin Endocrinol Metab, 2008. **93**(4): p. 1433-41.
479. Issemann, I. and S. Green, *Activation of a member of the steroid hormone receptor superfamily by peroxisome proliferators.* Nature, 1990. **347**(6294): p. 645-50.
480. Fothergill-Gilmore, L.A. and P.A. Michels, *Evolution of glycolysis.* Prog Biophys Mol Biol, 1993. **59**(2): p. 105-235.
481. Srere, P.A., *Complexes of sequential metabolic enzymes.* Annu Rev Biochem, 1987. **56**: p. 89-124.
482. Villar-Palasi, C. and J. Larner, *Glycogen metabolism and glycolytic enzymes.* Annu Rev Biochem, 1970. **39**: p. 639-72.
483. Nelson, D.L. and M.M. Cox, *Lehninger Principles of Biochemistry, 5th ed.* 2008, New York: W.H. Freeman.
484. Gatenby, R.A. and R.J. Gillies, *Why do cancers have high aerobic glycolysis?* Nat Rev Cancer, 2004. **4**(11): p. 891-9.
485. Hertz, L. and G.A. Dienel, *Lactate transport and transporters: general principles and functional roles in brain cells.* J Neurosci Res, 2005. **79**(1-2): p. 11-8.
486. Garrett, R. and G. Charles, *Biochemistry*. 4th ed. 2009.
487. Behal, R.H., et al., *Regulation of the pyruvate dehydrogenase multienzyme complex.* Annu Rev Nutr, 1993. **13**: p. 497-520.
488. van den Heuvel, L. and J. Smeitink, *The oxidative phosphorylation (OXPHOS) system: nuclear genes and human genetic diseases.* Bioessays, 2001. **23**(6): p. 518-25.
489. Hosler, J.P., S. Ferguson-Miller, and D.A. Mills, *Energy transduction: proton transfer through the respiratory complexes.* Annu Rev Biochem, 2006. **75**: p. 165-87.
490. Hatefi, Y., *The mitochondrial electron transport and oxidative phosphorylation system.* Annu Rev Biochem, 1985. **54**: p. 1015-69.
491. Pedersen, P.L., *Warburg, me and Hexokinase 2: Multiple discoveries of key molecular events underlying one of cancers' most common phenotypes, the "Warburg Effect", i.e., elevated glycolysis in the presence of oxygen.* J Bioenerg Biomembr, 2007. **39**(3): p. 211-22.
492. Warburg, O.H., *The metabolism of tumours*. 1931, New York, NY: R.R. Smith.
493. Semenza, G.L., et al., *'The metabolism of tumours': 70 years later.* Novartis Found Symp, 2001. **240**: p. 251-60; discussion 260-4.
494. Warburg, O., *On respiratory impairment in cancer cells.* Science, 1956. **124**(3215): p. 269-70.
495. Pelicano, H., et al., *Glycolysis inhibition for anticancer treatment.* Oncogene, 2006. **25**(34): p. 4633-46.
496. Kroemer, G. and J. Pouyssegur, *Tumor cell metabolism: cancer's Achilles' heel.* Cancer Cell, 2008. **13**(6): p. 472-82.
497. Hsu, P.P. and D.M. Sabatini, *Cancer cell metabolism: Warburg and beyond.* Cell, 2008. **134**(5): p. 703-7.
498. Kim, J.W. and C.V. Dang, *Cancer's molecular sweet tooth and the Warburg effect.* Cancer Res, 2006. **66**(18): p. 8927-30.

499. Tennant, D.A., R.V. Duran, and E. Gottlieb, *Targeting metabolic transformation for cancer therapy.* Nat Rev Cancer. **10**(4): p. 267-77.
500. Wang, G.L., et al., *Hypoxia-inducible factor 1 is a basic-helix-loop-helix-PAS heterodimer regulated by cellular O2 tension.* Proc Natl Acad Sci U S A, 1995. **92**(12): p. 5510-4.
501. Cockman, M.E., et al., *Hypoxia inducible factor-alpha binding and ubiquitylation by the von Hippel-Lindau tumor suppressor protein.* J Biol Chem, 2000. **275**(33): p. 25733-41.
502. Maxwell, P.H., et al., *The tumour suppressor protein VHL targets hypoxia-inducible factors for oxygen-dependent proteolysis.* Nature, 1999. **399**(6733): p. 271-5.
503. Ohh, M., et al., *Ubiquitination of hypoxia-inducible factor requires direct binding to the beta-domain of the von Hippel-Lindau protein.* Nat Cell Biol, 2000. **2**(7): p. 423-7.
504. Tanimoto, K., et al., *Mechanism of regulation of the hypoxia-inducible factor-1 alpha by the von Hippel-Lindau tumor suppressor protein.* Embo J, 2000. **19**(16): p. 4298-309.
505. Semenza, G.L., *Hypoxia-inducible factor 1 (HIF-1) pathway.* Sci STKE, 2007. **2007**(407): p. cm8.
506. Taylor, C.T. and J. Pouyssegur, *Oxygen, hypoxia, and stress.* Ann N Y Acad Sci, 2007. **1113**: p. 87-94.
507. Maxwell, P.H., et al., *Hypoxia-inducible factor-1 modulates gene expression in solid tumors and influences both angiogenesis and tumor growth.* Proc Natl Acad Sci U S A, 1997. **94**(15): p. 8104-9.
508. Chen, C., et al., *Regulation of glut1 mRNA by hypoxia-inducible factor-1. Interaction between H-ras and hypoxia.* J Biol Chem, 2001. **276**(12): p. 9519-25.
509. Ramanathan, A., C. Wang, and S.L. Schreiber, *Perturbational profiling of a cell-line model of tumorigenesis by using metabolic measurements.* Proc Natl Acad Sci U S A, 2005. **102**(17): p. 5992-7.
510. Elstrom, R.L., et al., *Akt stimulates aerobic glycolysis in cancer cells.* Cancer Res, 2004. **64**(11): p. 3892-9.
511. Li, F., et al., *Myc stimulates nuclearly encoded mitochondrial genes and mitochondrial biogenesis.* Mol Cell Biol, 2005. **25**(14): p. 6225-34.
512. Matoba, S., et al., *p53 regulates mitochondrial respiration.* Science, 2006. **312**(5780): p. 1650-3.
513. Bensaad, K., et al., *TIGAR, a p53-inducible regulator of glycolysis and apoptosis.* Cell, 2006. **126**(1): p. 107-20.
514. Osthus, R.C., et al., *Deregulation of glucose transporter 1 and glycolytic gene expression by c-Myc.* J Biol Chem, 2000. **275**(29): p. 21797-800.
515. Shim, H., et al., *c-Myc transactivation of LDH-A: implications for tumor metabolism and growth.* Proc Natl Acad Sci U S A, 1997. **94**(13): p. 6658-63.
516. Fantin, V.R., J. St-Pierre, and P. Leder, *Attenuation of LDH-A expression uncovers a link between glycolysis, mitochondrial physiology, and tumor maintenance.* Cancer Cell, 2006. **9**(6): p. 425-34.
517. Christofk, H.R., et al., *The M2 splice isoform of pyruvate kinase is important for cancer metabolism and tumour growth.* Nature, 2008. **452**(7184): p. 230-3.

518. Classon, M. and E. Harlow, *The retinoblastoma tumour suppressor in development and cancer.* Nat Rev Cancer, 2002. **2**(12): p. 910-7.
519. Burkhart, D.L. and J. Sage, *Cellular mechanisms of tumour suppression by the retinoblastoma gene.* Nat Rev Cancer, 2008. **8**(9): p. 671-82.
520. Bremner, R. and E. Zacksenhaus, *Cyclins, Cdks, E2f, Skp2, and more at the first international RB Tumor Suppressor Meeting.* Cancer Res, 2010. **70**(15): p. 6114-8.
521. Mantela, J., et al., *The retinoblastoma gene pathway regulates the postmitotic state of hair cells of the mouse inner ear.* Development, 2005. **132**(10): p. 2377-88.
522. Guo, Z., et al., *Inactivation of the retinoblastoma tumor suppressor induces Apaf-1 dependent and independent apoptotic pathways during embryogenesis.* Cancer Research, 2001. **61**: p. 8395-8400.
523. Morselli, E., et al., *Anti- and pro-tumor functions of autophagy.* Biochim Biophys Acta, 2009. **1793**(9): p. 1524-32.
524. Levine, B. and G. Kroemer, *Autophagy in the pathogenesis of disease.* Cell, 2008. **132**(1): p. 27-42.
525. Mizushima, N., *Physiological functions of autophagy.* Curr Top Microbiol Immunol, 2009. **335**: p. 71-84.
526. Bampton, E.T., et al., *The dynamics of autophagy visualized in live cells: from autophagosome formation to fusion with endo/lysosomes.* Autophagy, 2005. **1**(1): p. 23-36.
527. Mazure, N.M. and J. Pouyssegur, *Hypoxia-induced autophagy: cell death or cell survival?* Curr Opin Cell Biol, 2009.
528. Jiang, Z. and E. Zacksenhaus, *Activation of retinoblastoma protein in mammary gland leads to ductal growth suppression, precocious differentiation, and adenocarcinoma.* J Cell Biol, 2002. **156**(1): p. 185-98.
529. Amthor, H., et al., *Lack of myostatin results in excessive muscle growth but impaired force generation.* Proc Natl Acad Sci U S A, 2007. **104**(6): p. 1835-40.
530. Trincheri, N.F., et al., *Resveratrol-induced apoptosis depends on the lipid kinase activity of Vps34 and on the formation of autophagolysosomes.* Carcinogenesis, 2008. **29**(2): p. 381-9.
531. Chen, T.T. and J.Y. Wang, *Establishment of irreversible growth arrest in myogenic differentiation requires the RB LXCXE-binding function.* Mol Cell Biol, 2000. **20**(15): p. 5571-80.
532. Briaud, I., et al., *Insulin receptor substrate-2 proteasomal degradation mediated by a mammalian target of rapamycin (mTOR)-induced negative feedback down-regulates protein kinase B-mediated signaling pathway in beta-cells.* J Biol Chem, 2005. **280**(3): p. 2282-93.
533. Skurk, C., et al., *The FOXO3a transcription factor regulates cardiac myocyte size downstream of AKT signaling.* J Biol Chem, 2005. **280**(21): p. 20814-23.
534. Attaix, D. and D. Bechet, *FoxO3 controls dangerous proteolytic liaisons.* Cell Metab, 2007. **6**(6): p. 425-7.
535. Sankaran, V.G., S.H. Orkin, and C.R. Walkley, *Rb intrinsically promotes erythropoiesis by coupling cell cycle exit with mitochondrial biogenesis.* Genes Dev, 2008. **22**(4): p. 463-75.

536. Zhu, S., et al., *Minocycline inhibits cytochrome c release and delays progression of amyotrophic lateral sclerosis in mice.* Nature, 2002. **417**(6884): p. 74-8.
537. Leonard, K.C., et al., *XIAP protection of photoreceptors in animal models of retinitis pigmentosa.* PLoS One, 2007. **2**(3): p. e314.
538. Di Carlo, A., et al., *Hypoxia inhibits myogenic differentiation through accelerated MyoD degradation.* J Biol Chem, 2004. **279**(16): p. 16332-8.
539. Maynard, M.A. and M. Ohh, *The role of hypoxia-inducible factors in cancer.* Cell Mol Life Sci, 2007. **64**(16): p. 2170-80.
540. Sufan, R.I., et al., *Oxygen-independent degradation of HIF-alpha via bioengineered VHL tumour suppressor complex.* EMBO Mol Med, 2009. **1**(1): p. 66-78.
541. Vincent, K.A., et al., *Angiogenesis is induced in a rabbit model of hindlimb ischemia by naked DNA encoding an HIF-1alpha/VP16 hybrid transcription factor.* Circulation, 2000. **102**(18): p. 2255-61.
542. Ho, A.T.V., *Determination of Apaf1-independent apoptosis and differentiation functions of Rb pocket proteins in skeletal myogenesis*. 2006, University of Toronto: Thesis, Ph.D.
543. Dimova, D.K. and N.J. Dyson, *The E2F transcriptional network: old acquaintances with new faces.* Oncogene, 2005. **24**(17): p. 2810-26.
544. Skapek, S.X., Y.R. Pan, and E.Y. Lee, *Regulation of cell lineage specification by the retinoblastoma tumor suppressor.* Oncogene, 2006. **25**(38): p. 5268-76.
545. Scime, A., et al., *Oxidative status of muscle is determined by p107 regulation of PGC-1alpha.* J Cell Biol. **190**(4): p. 651-62.
546. Lee, E.Y.H.P., et al., *Mice deficient for Rb are nonviable and show defects in neurogenesis and haematopoiesis.* Nature, 1992. **359**(6393): p. 288-294.
547. Clarke, A.R., et al., *Requirement for a functional Rb-1 gene in murine development.* Nature, 1992. **359**(6393): p. 328-330.
548. Lee, E.Y.-H.P., et al., *Dual roles of the retinoblastoma protein in cell cycle regulation and neuron differentiation.* Genes & Dev, 1994. **8**: p. 2008-2021.
549. Mulligan, G. and T. Jacks, *The retinoblastoma gene family: cousins with overlapping interests.* Trends Genet, 1998. **14**: p. 223-229.
550. Macleod, K., *pRb and E2f-1 in mouse development and tumorigenesis.* Current Opinion In Genetics & Development, 1999. **9**: p. 31-39.
551. Takahashi, C., et al., *Rb and N-ras function together to control differentiation in the mouse.* Mol Cell Biol, 2003. **23**(15): p. 5256-68.
552. Ciavarra, G. and E. Zacksenhaus, *Rescue of myogenic defects in Rb-deficient cells by inhibition of autophagy or by hypoxia-induced glycolytic shift.* Journal of Cell Biology, **In Press**, 2010.
553. Castano, E., Y. Kleyner, and B.D. Dynlacht, *Dual cyclin-binding domains are required for p107 to function as a kinase inhibitor.* Mol Cell Biol, 1998. **18**(9): p. 5380-91.
554. Bruce, J.L., et al., *Requirements for cell cycle arrest by p16INK4a.* Mol Cell, 2000. **6**(3): p. 737-42.
555. Chicas, A., et al., *Dissecting the unique role of the retinoblastoma tumor suppressor during cellular senescence.* Cancer Cell. **17**(4): p. 376-87.

556. Ullah, Z., C.Y. Lee, and M.L. Depamphilis, *Cip/Kip cyclin-dependent protein kinase inhibitors and the road to polyploidy.* Cell Div, 2009. **4**: p. 10.
557. Zhu, L., E. Xie, and L.S. Chang, *Differential roles of two tandem E2F sites in repression of the human p107 promoter by retinoblastoma and p107 proteins.* Mol Cell Biol, 1995. **15**(7): p. 3552-62.
558. Pattingre, S. and B. Levine, *Bcl-2 inhibition of autophagy: a new route to cancer?* Cancer Res, 2006. **66**(6): p. 2885-8.
559. Huang, H. and X. He, *Wnt/beta-catenin signaling: new (and old) players and new insights.* Curr Opin Cell Biol, 2008. **20**(2): p. 119-25.
560. Stambolic, V., L. Ruel, and J.R. Woodgett, *Lithium inhibits glycogen synthase kinase-3 activity and mimics wingless signalling in intact cells.* Curr Biol, 1996. **6**(12): p. 1664-8.
561. Haq, S., et al., *Stabilization of beta-catenin by a Wnt-independent mechanism regulates cardiomyocyte growth.* Proc Natl Acad Sci U S A, 2003. **100**(8): p. 4610-5.
562. Marino, S., et al., *Induction of medulloblastomas in p53-null mutant mice by somatic inactivation of Rb in the external granular layer cells of the cerebellum.* Genes Dev, 2000. **14**(8): p. 994-1004.
563. Shen, X., et al., *Genome-wide examination of myoblast cell cycle withdrawal during differentiation.* Dev Dyn, 2003. **226**(1): p. 128-38.
564. Cobrinik, D., *Pocket proteins and cell cycle control.* Oncogene, 2005. **24**(17): p. 2796-809.
565. Liu, H., et al., *New roles for the RB tumor suppressor protein.* Curr Opin Genet Dev, 2004. **14**(1): p. 55-64.
566. Morgenbesser, S.D., et al., *p53-dependent apoptosis produced by Rb-deficiency in the developing mouse lens.* Nature, 1994. **371**(6492): p. 72-4.
567. Hong, F.D., et al., *Structure of the human retinoblastoma gene.* Proc Natl Acad Sci U S A, 1989. **86**(14): p. 5502-6.
568. Strausberg, R.L., et al., *Generation and initial analysis of more than 15,000 full-length human and mouse cDNA sequences.* Proc Natl Acad Sci U S A, 2002. **99**(26): p. 16899-903.
569. Maandag, E.C., et al., *Developmental rescue of an embryonic-lethal mutation in the retinoblastoma gene in chimeric mice.* Embo J, 1994. **13**(18): p. 4260-8.
570. Williams, B.O., et al., *Extensive contribution of Rb-deficient cells to adult chimeric mice with limited histopathological consequences.* Embo J, 1994. **13**(18): p. 4251-9.
571. Hansen, J.B., et al., *Activation of peroxisome proliferator-activated receptor gamma bypasses the function of the retinoblastoma protein in adipocyte differentiation.* J Biol Chem, 1999. **274**(4): p. 2386-93.
572. Scime, A., et al., *Rb and p107 regulate preadipocyte differentiation into white versus brown fat through repression of PGC-1alpha.* Cell Metab, 2005. **2**(5): p. 283-95.
573. Haas-Kogan, D.A., et al., *Inhibition of apoptosis by the retinoblastoma gene product.* Embo J, 1995. **14**(3): p. 461-72.
574. Bremner, R. and E. Zacksenhaus, *Cyclins, Cdks, E2f, Skp2, and more at the first international RB Tumor Suppressor Meeting.* Cancer Res. **70**(15): p. 6114-8.

575. Elliott, S., et al., *Proof of differentiative mode of action of all-trans retinoic acid in acute promyelocytic leukemia using X-linked clonal analysis.* Blood, 1992. **79**(8): p. 1916-9.
576. Tallman, M.S., et al., *All-trans-retinoic acid in acute promyelocytic leukemia.* N Engl J Med, 1997. **337**(15): p. 1021-8.
577. Levine, B., S. Sinha, and G. Kroemer, *Bcl-2 family members: dual regulators of apoptosis and autophagy.* Autophagy, 2008. **4**(5): p. 600-6.
578. Yu, L., et al., *Regulation of an ATG7-beclin 1 program of autophagic cell death by caspase-8.* Science, 2004. **304**(5676): p. 1500-2.
579. Ray, R., et al., *BNIP3 heterodimerizes with Bcl-2/Bcl-X(L) and induces cell death independent of a Bcl-2 homology 3 (BH3) domain at both mitochondrial and nonmitochondrial sites.* J Biol Chem, 2000. **275**(2): p. 1439-48.
580. Quinsay, M.N., et al., *Bnip3 mediates permeabilization of mitochondria and release of cytochrome c via a novel mechanism.* J Mol Cell Cardiol, 2009.
581. Kubli, D.A., J.E. Ycaza, and A.B. Gustafsson, *Bnip3 mediates mitochondrial dysfunction and cell death through Bax and Bak.* Biochem J, 2007. **405**(3): p. 407-15.
582. Crompton, M., *The mitochondrial permeability transition pore and its role in cell death.* Biochem J, 1999. **341 (Pt 2)**: p. 233-49.
583. Bellot, G., et al., *Hypoxia-induced autophagy is mediated through hypoxia-inducible factor induction of BNIP3 and BNIP3L via their BH3 domains.* Mol Cell Biol, 2009. **29**(10): p. 2570-81.
584. Lemasters, J.J., et al., *The mitochondrial permeability transition in cell death: a common mechanism in necrosis, apoptosis and autophagy.* Biochim Biophys Acta, 1998. **1366**(1-2): p. 177-96.
585. Xue, L., G.C. Fletcher, and A.M. Tolkovsky, *Autophagy is activated by apoptotic signalling in sympathetic neurons: an alternative mechanism of death execution.* Mol Cell Neurosci, 1999. **14**(3): p. 180-98.
586. Potts, P.R., et al., *Critical function of endogenous XIAP in regulating caspase activation during sympathetic neuronal apoptosis.* J Cell Biol, 2003. **163**(4): p. 789-99.
587. Chan, D.C., *Mitochondrial fusion and fission in mammals.* Annu Rev Cell Dev Biol, 2006. **22**: p. 79-99.
588. Chen, H., et al., *Mitofusins Mfn1 and Mfn2 coordinately regulate mitochondrial fusion and are essential for embryonic development.* J Cell Biol, 2003. **160**(2): p. 189-200.
589. Chen, H., J.M. McCaffery, and D.C. Chan, *Mitochondrial fusion protects against neurodegeneration in the cerebellum.* Cell, 2007. **130**(3): p. 548-62.
590. Chen, H., A. Chomyn, and D.C. Chan, *Disruption of fusion results in mitochondrial heterogeneity and dysfunction.* J Biol Chem, 2005. **280**(28): p. 26185-92.
591. Chen, H., et al., *Mitochondrial fusion is required for mtDNA stability in skeletal muscle and tolerance of mtDNA mutations.* Cell. **141**(2): p. 280-9.
592. Jackman, R.W. and S.C. Kandarian, *The molecular basis of skeletal muscle atrophy.* Am J Physiol Cell Physiol, 2004. **287**(4): p. C834-43.

593. Zhao, J., et al., *Coordinate activation of autophagy and the proteasome pathway by FoxO transcription factor.* Autophagy, 2008. **4**(3): p. 378-80.
594. Pugh, C.W. and P.J. Ratcliffe, *Regulation of angiogenesis by hypoxia: role of the HIF system.* Nat Med, 2003. **9**(6): p. 677-84.
595. Ikeda, E., et al., *Hypoxia-induced transcriptional activation and increased mRNA stability of vascular endothelial growth factor in C6 glioma cells.* J Biol Chem, 1995. **270**(34): p. 19761-6.
596. Mandriota, S.J. and M.S. Pepper, *Regulation of angiopoietin-2 mRNA levels in bovine microvascular endothelial cells by cytokines and hypoxia.* Circ Res, 1998. **83**(8): p. 852-9.
597. Esteban, M.A., et al., *Regulation of E-cadherin expression by VHL and hypoxia-inducible factor.* Cancer Res, 2006. **66**(7): p. 3567-75.
598. Pouyssegur, J., F. Dayan, and N.M. Mazure, *Hypoxia signalling in cancer and approaches to enforce tumour regression.* Nature, 2006. **441**(7092): p. 437-43.
599. Budde, A., et al., *Retinoblastoma susceptibility gene product pRB activates hypoxia-inducible factor-1 (HIF-1).* Oncogene, 2005. **24**(10): p. 1802-8.
600. Boutrid, H., et al., *Targeting hypoxia, a novel treatment for advanced retinoblastoma.* Invest Ophthalmol Vis Sci, 2008. **49**(7): p. 2799-805.
601. Fernandez de Mattos, S., E.W. Lam, and A. Tauler, *An E2F-binding site mediates the activation of the proliferative isoform of 6-phosphofructo-2-kinase/fructose-2,6-bisphosphatase by phosphatidylinositol 3-kinase.* Biochem J, 2002. **368**(Pt 1): p. 283-91.
602. Culmsee, C. and M.P. Mattson, *p53 in neuronal apoptosis.* Biochem Biophys Res Commun, 2005. **331**(3): p. 761-77.
603. Kondoh, H., et al., *Glycolytic enzymes can modulate cellular life span.* Cancer Res, 2005. **65**(1): p. 177-85.
604. Zhang, H., et al., *HIF-1 inhibits mitochondrial biogenesis and cellular respiration in VHL-deficient renal cell carcinoma by repression of C-MYC activity.* Cancer Cell, 2007. **11**(5): p. 407-20.
605. Dang, C.V., et al., *The interplay between MYC and HIF in cancer.* Nat Rev Cancer, 2008. **8**(1): p. 51-6.
606. Kim, J.W., et al., *Hypoxia-inducible factor 1 and dysregulated c-Myc cooperatively induce vascular endothelial growth factor and metabolic switches hexokinase 2 and pyruvate dehydrogenase kinase 1.* Mol Cell Biol, 2007. **27**(21): p. 7381-93.
607. Sarkar, S., et al., *A rational mechanism for combination treatment of Huntington's disease using lithium and rapamycin.* Hum Mol Genet, 2008. **17**(2): p. 170-8.
608. van Harn, T., et al., *Loss of Rb proteins causes genomic instability in the absence of mitogenic signaling.* Genes Dev. **24**(13): p. 1377-88.
609. Garcia-Cao, M., et al., *A role for the Rb family of proteins in controlling telomere length.* Nat Genet, 2002. **32**(3): p. 415-9.
610. Blais, A., et al., *Retinoblastoma tumor suppressor protein-dependent methylation of histone H3 lysine 27 is associated with irreversible cell cycle exit.* J Cell Biol, 2007. **179**(7): p. 1399-412.
611. Calo, E., et al., *Rb regulates fate choice and lineage commitment in vivo.* Nature. **466**(7310): p. 1110-4.

612. Buckingham, M. and S.D. Vincent, *Distinct and dynamic myogenic populations in the vertebrate embryo.* Curr Opin Genet Dev, 2009. **19**(5): p. 444-53.
613. Viatour, P., et al., *Hematopoietic stem cell quiescence is maintained by compound contributions of the retinoblastoma gene family.* Cell Stem Cell, 2008. **3**(4): p. 416-28.
614. Ajioka, I., et al., *Differentiated horizontal interneurons clonally expand to form metastatic retinoblastoma in mice.* Cell, 2007. **131**(2): p. 378-90.
615. Chong, J.L., et al., *E2f3a and E2f3b contribute to the control of cell proliferation and mouse development.* Mol Cell Biol, 2009. **29**(2): p. 414-24.
616. Kuma, A., et al., *The role of autophagy during the early neonatal starvation period.* Nature, 2004. **432**(7020): p. 1032-6.
617. Mulligan, H.D. and M.J. Tisdale, *Effect of the lipid-lowering agent bezafibrate on tumour growth rate in vivo.* Br J Cancer, 1991. **64**(6): p. 1035-8.
618. Diwan, A., et al., *Inhibition of ischemic cardiomyocyte apoptosis through targeted ablation of Bnip3 restrains postinfarction remodeling in mice.* J Clin Invest, 2007. **117**(10): p. 2825-33.
619. Santel, A., et al., *Mitofusin-1 protein is a generally expressed mediator of mitochondrial fusion in mammalian cells.* J Cell Sci, 2003. **116**(Pt 13): p. 2763-74.